LA-2327(Prelim.)

C7.2

LOS ALAMOS SCIENTIFIC LABORATORY
OF THE UNIVERSITY OF CALIFORNIA ○ LOS ALAMOS NEW MEXICO

LOS ALAMOS MOLTEN PLUTONIUM REACTOR
EXPERIMENT (LAMPRE) HAZARD REPORT

LEGAL NOTICE

LOS ALAMOS SCIENTIFIC LABORATORY
OF THE UNIVERSITY OF CALIFORNIA   LOS ALAMOS   NEW MEXICO

LOS ALAMOS MOLTEN PLUTONIUM REACTOR
EXPERIMENT (LAMPRE) HAZARD REPORT

Compiled by

E. O. Swickard

Contributors

H. G. Barkmann, M. E. Battat, R. I. Brasier, J. A. Bridge,
W. Bruce, C. C. Burwell, B. M. Carmichael, W. H. Cooper,
R. L. Cubitt, D. M. Holm, J. E. Kemme, R. N. Kennedy,
R. M. Kiehn, J. L. Lundgren, R. E. Peterson, G. L. Ragan,
A. E. Wilson

- 1 -

NOTE

This report has been duplicated and given limited distribution in preliminary, unedited form in order to meet the requirement for prompt reporting of the information.

Although the substance of the report will not be affected, further reviews will be made, and this document will be reissued and distributed as a formal Los Alamos report under the same number, LA-2327. It is requested that all copies of the preliminary document be destroyed upon receipt of the final report.

CONTENTS

TABLES

ILLUSTRATIONS

1. INTRODUCTION, SUMMARY, AND CONCLUSIONS

1.1 Introduction

The Los Alamos Scientific Laboratory is investigating plutonium-fueled reactors for possible application to fast breeder systems. The fuels presently being considered are molten alloys of plutonium which offer the possibility of high burnup and in-place reprocessing.

The first reactor in this program is called the Los Alamos Molten Plutonium Reactor Experiment Number One (LAMPRE I). This reactor will use a molten plutonium-iron alloy contained in tantalum capsules, cooled with liquid sodium. The design power of the reactor is 1 Mw, which will result in an average specific power of 40 w/g of fuel. This reactor is intended to serve a vital function in providing a facility to test materials under operating conditions.

The reactor is presently being installed in an existing underground cell located at Site TA-35 of the Los Alamos Scientific Laboratory. The same cell was used previously for operation of LAPRE I.

1.2 Summary

The possible hazards associated with the startup and operation of LAMPRE I have been analyzed with consideration of the effect of various temperature coefficients of reactivity, fuel element bowing, and rupture of the coolant system or of fuel capsules. Attention has also been given

to the effect of failure of various components, to the consequences of
large positive reactivity insertions, and to establishing safe handling
techniques for the fuel.

1.3 Conclusions

Analysis of hazards potentially present in the LAMPRE I system
leads to the conclusion that the large negative prompt temperature co-
efficient resulting from the thermal expansion of the liquid fuel makes
this reactor unusually safe. The maximum credible malfunctions of the
system are estimated to lead to reactivity insertions of the order of
several hundred dollars per second, an order of magnitude less than that
required for formation of an explosive shock. Operational procedures
and sequencing of operations have been designed to minimize to the point
of impossibility any power excursion of sufficient magnitude to vaporize
the sodium coolant or to melt the core container. As with any system
using high-temperature sodium, sodium fire represents one of the prin-
cipal dangers to the experiment. A sodium fire might terminate the
experiment, but release of radioactive smoke to the atmosphere is pre-
vented so that personnel will not be endangered. There are provisions
for alpha particle containment in various phases of the fuel handling
equipment in order to guard against any hazard resulting from rupture
of a fuel element.

2. DESCRIPTION OF THE REACTOR

2.1 Type and Purpose

LAMPRE I is to be an experimental test reactor using a molten plutonium alloy fuel operating with a fast neutron spectrum. The reactor will be used to investigate (a) the feasibility of using molten alloys of plutonium as reactor fuels, (b) the satisfactory containment of such fuels, (c) fission gas disengagement from the molten fuel, and (d) the suitability of this type of reactor concept for future power breeder reactors using similar fuels.

Figures 2.1 and 2.2 are plan and elevation layouts respectively of the reactor installation. The location of the reactor is the same as that used for LAPRE I.

2.2 Core Configuration

The core of the reactor is made up of an array of tantalum capsules containing plutonium-iron alloy fuel. There are locations for a total of 199 capsules, some of which will be used for unfueled reflector pins. Figure 2.3 is a cutaway view of the core region. Coolant sodium enters the reactor vessel and flows downward through an annulus to the bottom of the vessel. From the bottom the sodium flows up through the bottom reflector into a plenum, then through the capsule locator plate into the core. After flowing past and receiving heat from the capsules, the sodium passes
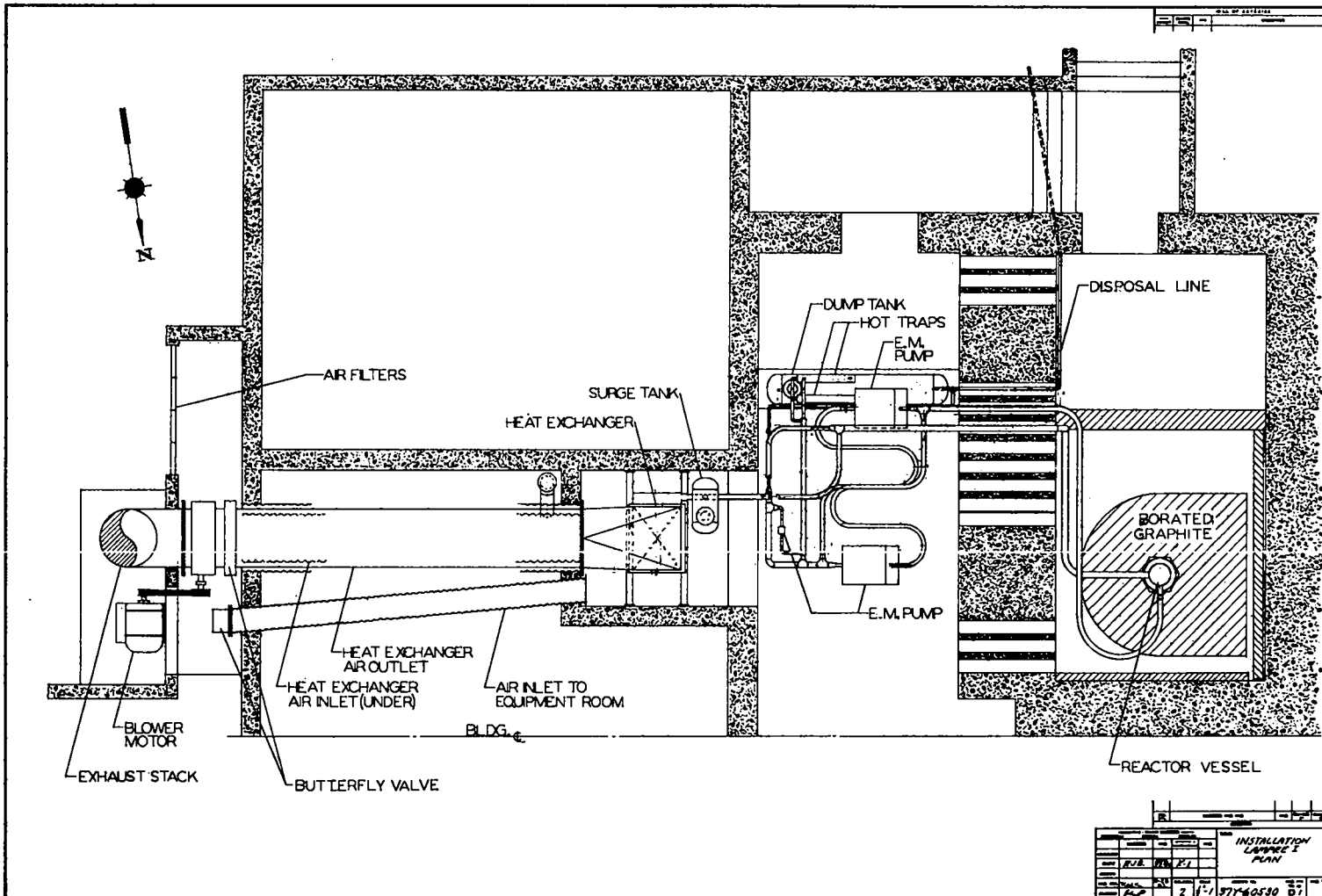
Fig. 2.1 Plan view of reactor installation.
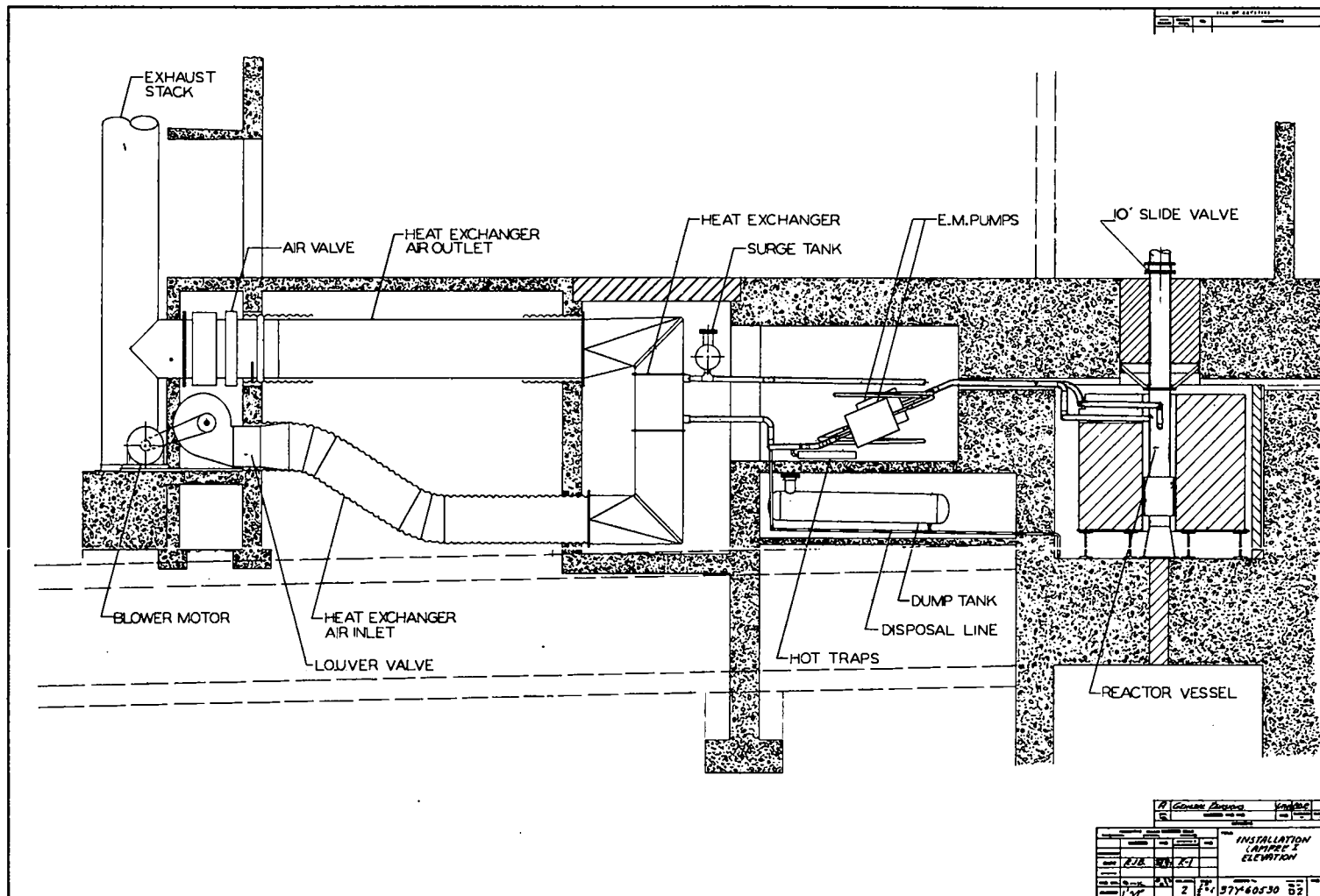
Fig. 2.2 Elevation view of reactor installation.

OUTER VESSEL

GRAPHITE SHIELDING

COOLANT INLET

COOLANT OUTLET

UPPER REFLECTOR

SHIM

CORE

CONTROL ROD

LOWER REFLECTOR

INNER VESSEL

SUPPORT PLATE
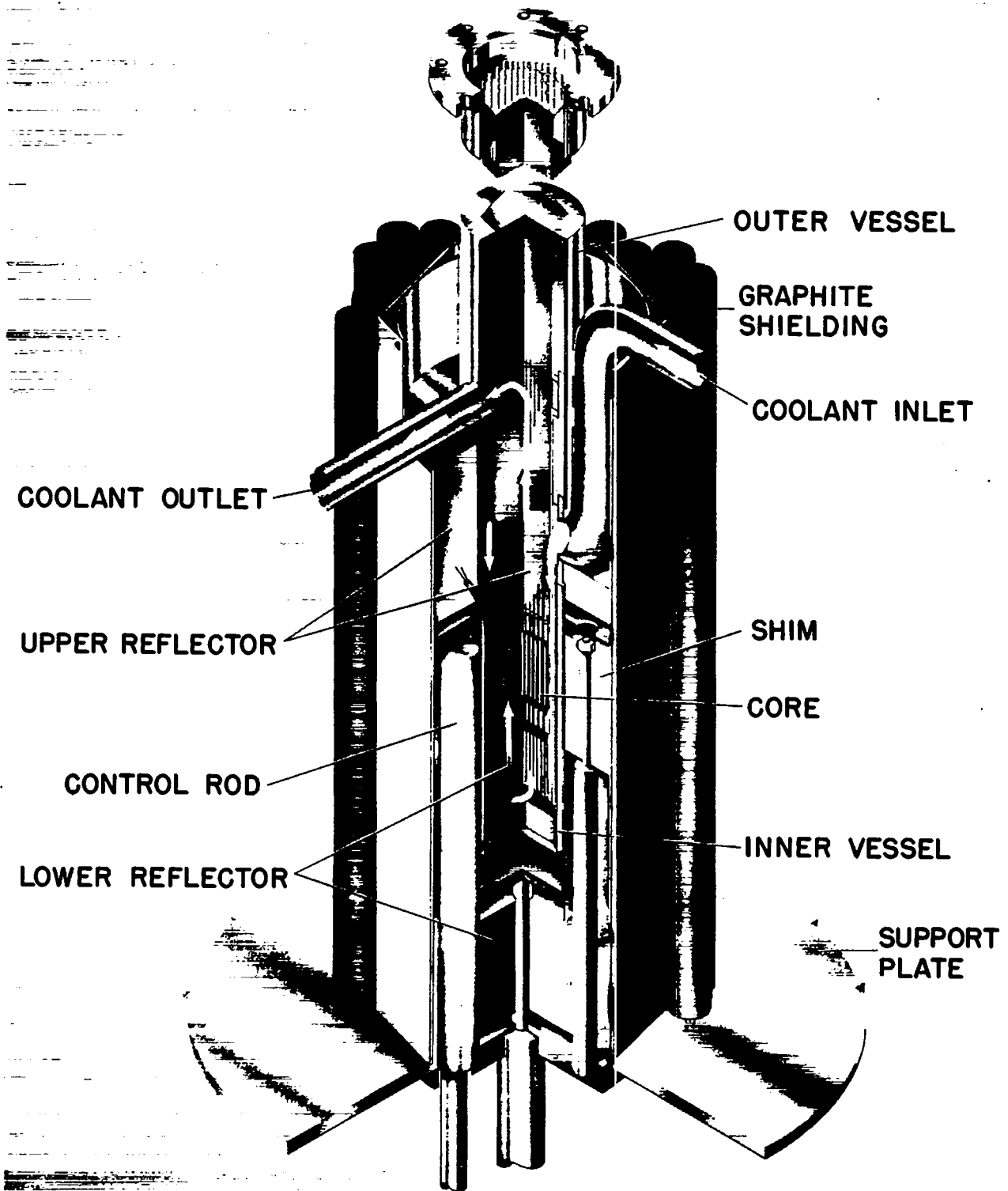
Fig. 2.3 Cutaway view of vessel region.

into the upper reflector region and out of the vessel. A tantalum catchpot, for containing fuel in the event of a capsule rupture, is located just below the turn-around plenum. Within the catchpot a diluent plug of Armco iron is provided, with holes drilled so that there is about a 35% void. The plug serves to dilute fuel in the catchpot to a subcritical concentration, and also serves to alloy with and "dry up" the fuel by raising its melting point.

The bottom reflector is also made of Armco iron drilled for sodium passage. The cross sectional area for sodium flow of the reflector is about 17%. The capsule locator plate is 1-3/4 in. thick stainless steel, the top of which has been faced with a 1/4 in. thick sheet of tantalum. Sockets are drilled in the tantalum plate on a 0.497 in. triangular pitch to locate the conical capsule bottom. The purpose of the tantalum face on the locator plate is to prevent soldering of the capsule tip to the stainless steel plate in the event leaking plutonium enters the socket.

The lower part of the reactor vessel is double-walled, with no pipes entering in the region. The core cannot be drained of coolant accidentally unless there is a leak in both walls of the double containment. A small line extends from the bottom of the catchpot through the sodium inlet pipe by which the vessel may be drained should it become necessary.

Capsule handles, described below, constitute the upper reflector and also part of the radiation shield. Above the vessel sodium outlet the capsule handles have an hexagonal cross section and extend to the top of the vessel. The top of the vessel is fitted with a 10 in. slide vacuum valve which will be closed when the reactor is operating.

An annular shim moving outside the sodium vessel furnishes coarse reactivity control. Vernier reactivity control is provided by four separately actuated control rods which are portions of the shim. Above and below the shim are stationary steel shields. Surrounding these two shields and the shim is the flue which aids in cooling the boron impregnated graphite immediately outside the flue. Figure 2.4 shows a horizontal cross section through the core. Figures 2.5, 2.6, 2.7, and 2.8 show the bottom

SHIM

INLET SODIUM

COOLING AIR

4 CONTROL RODS

ELECTRICAL
HEATERS

PRIMARY VESSEL

SECONDARY VESSEL

199 FUEL CAPSULE
LOCATIONS

FLOW DIVIDER

FLUE
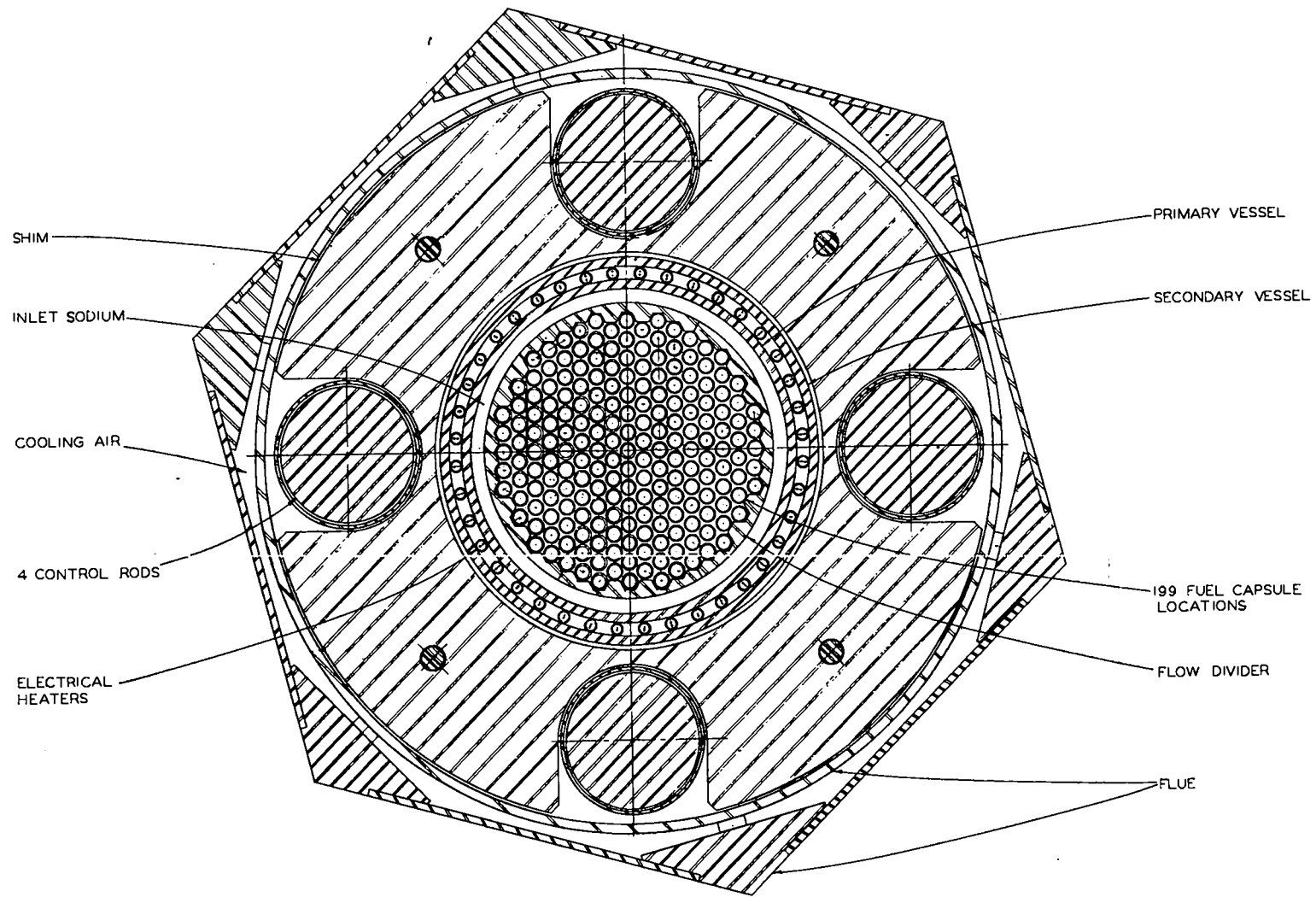
Fig. 2.4   Horizontal cross section through reactor core.
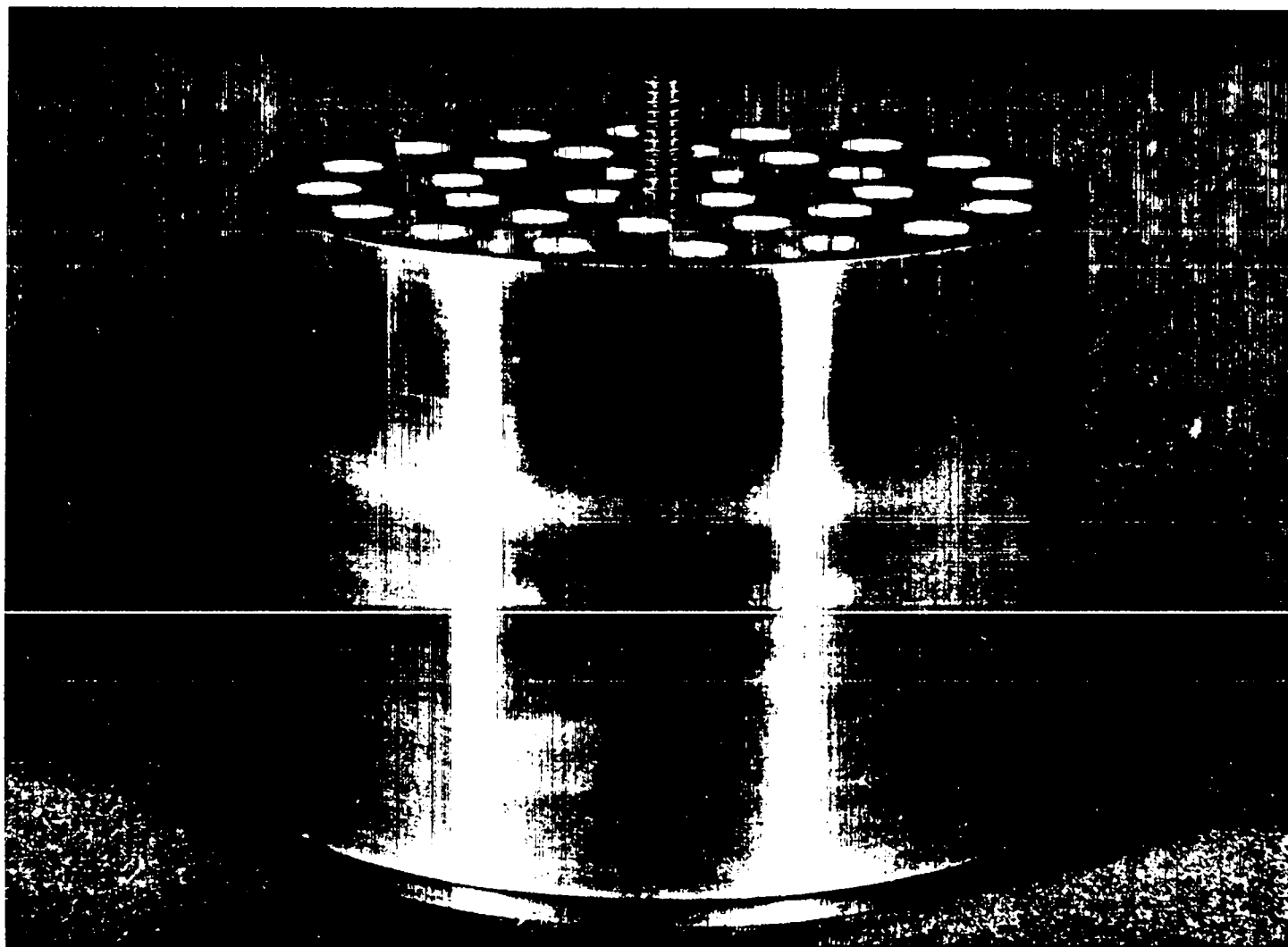
Fig. 2.5   Bottom reflector.
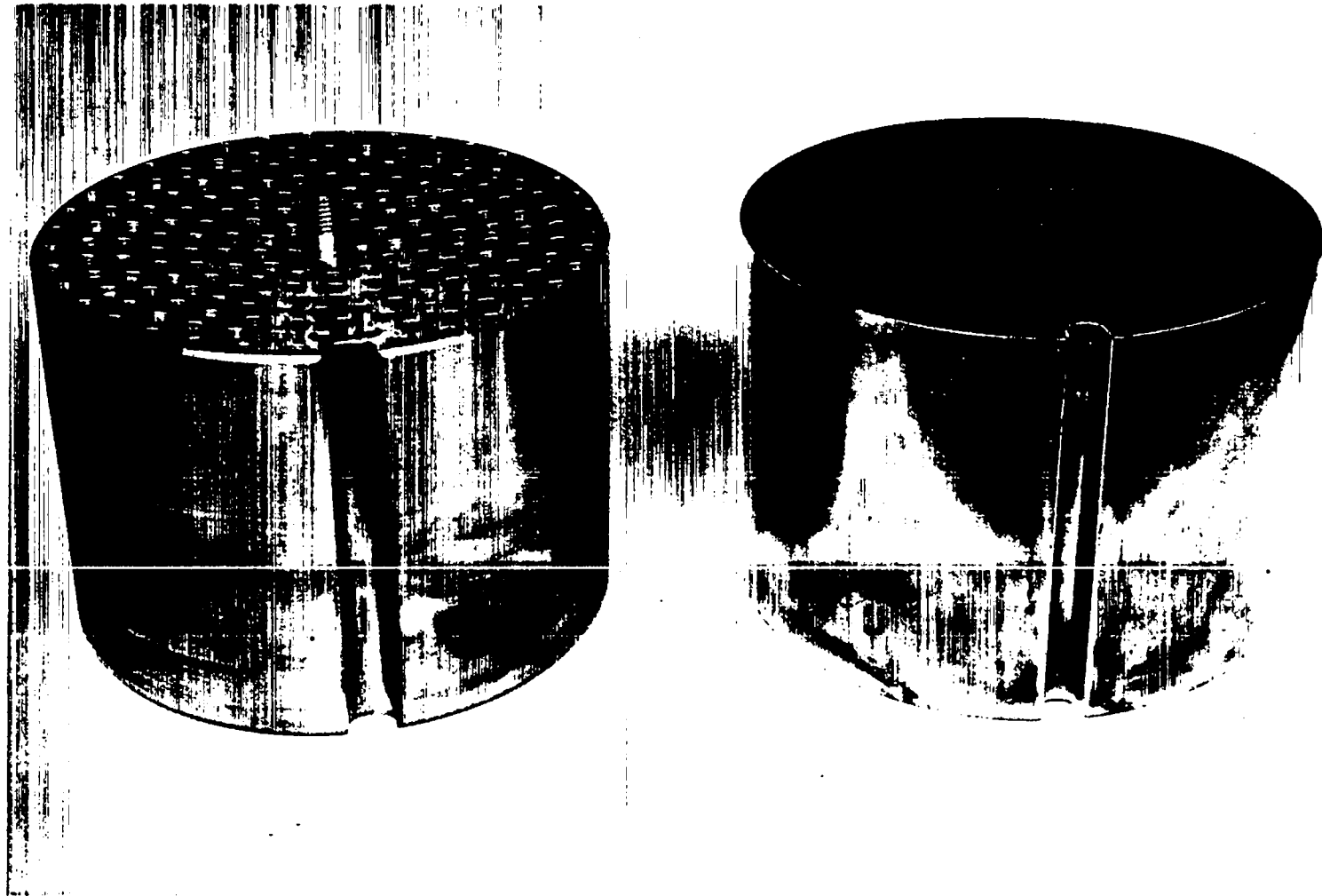
Fig. 2.6 Catchpot and diluent plug.
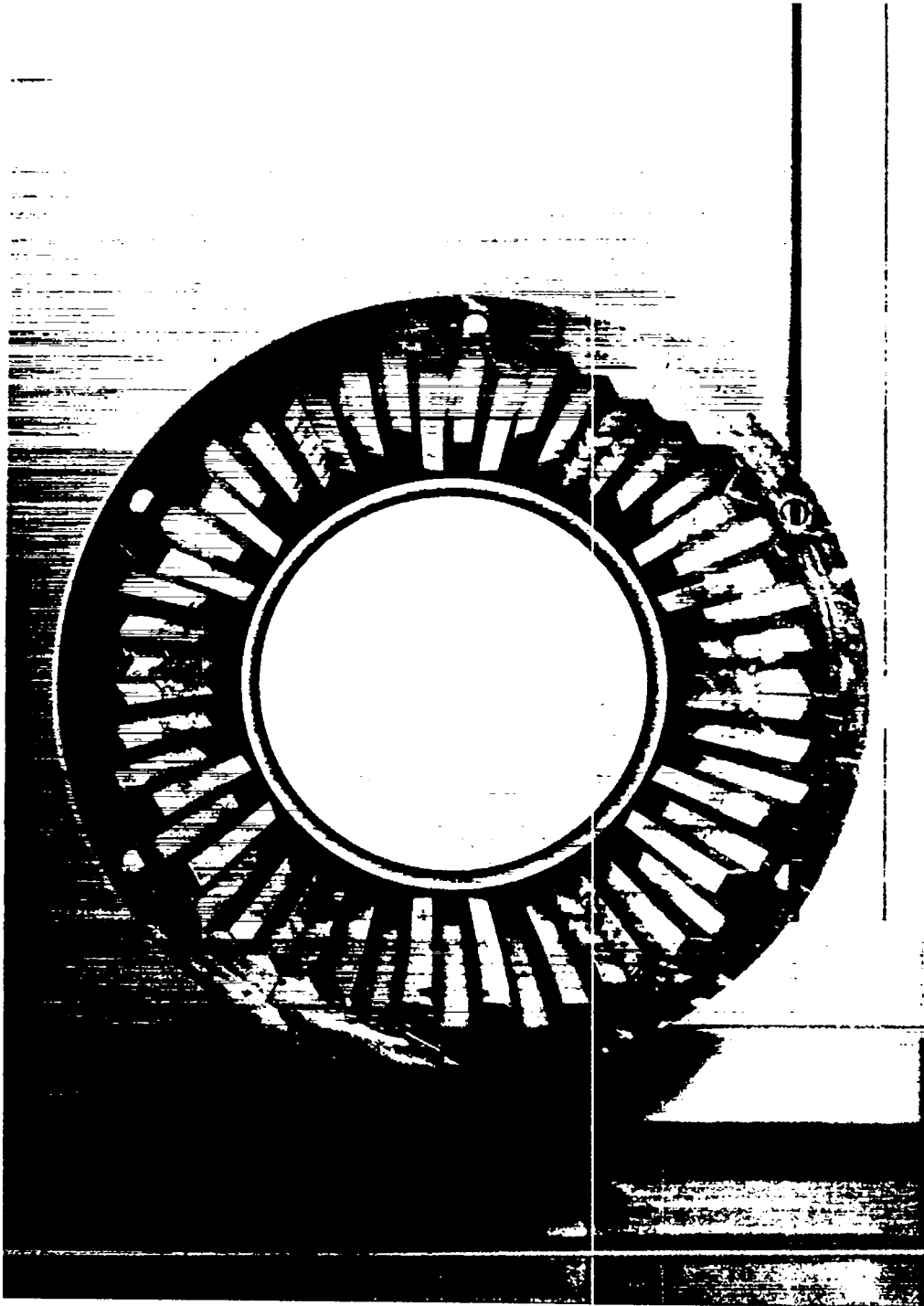
Fig. 2.7 Flow divider.
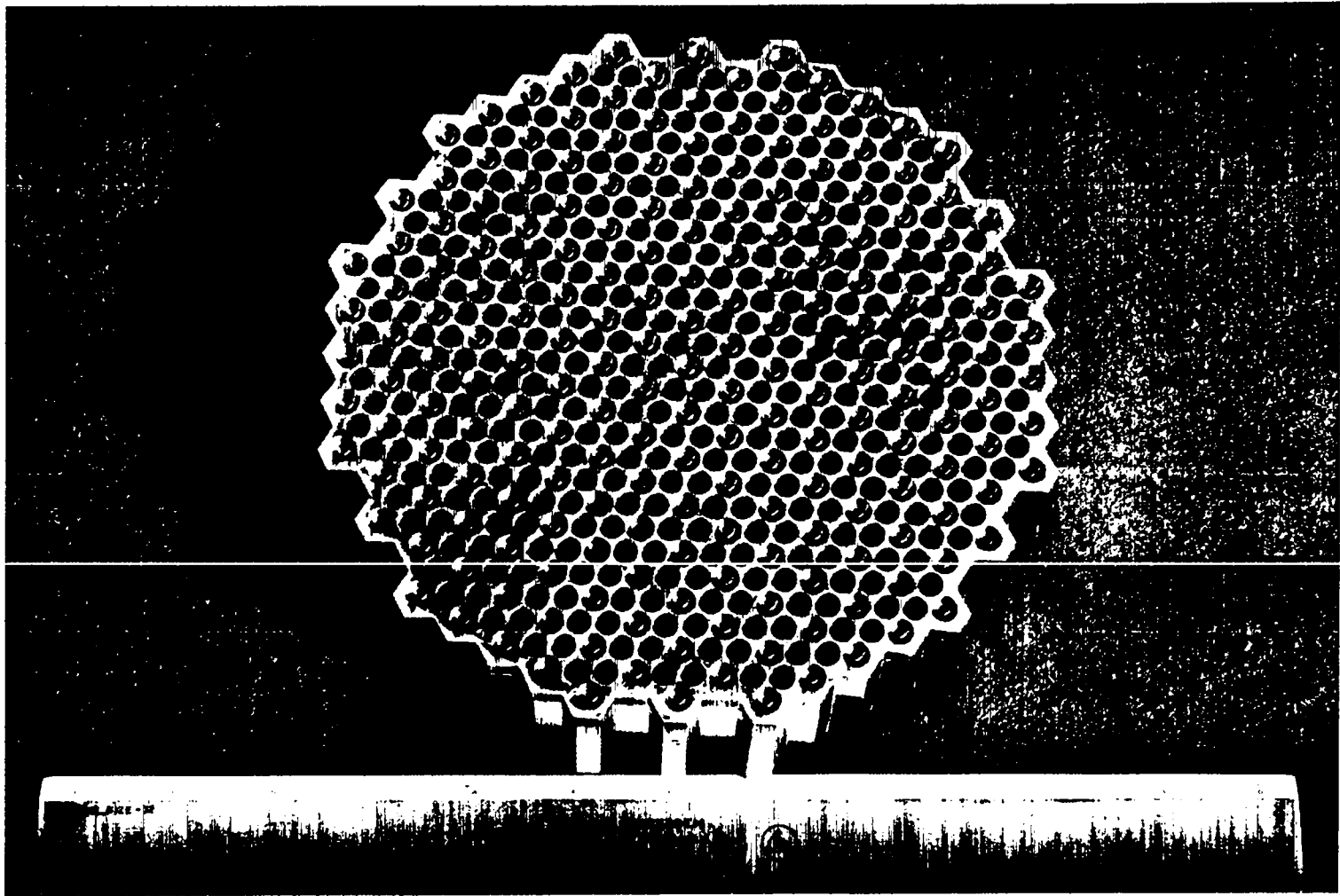
Fig. 2.8 Capsule locator plate.

reflector, catchpot and diluent plug, flow divider and locator plate respectively. Figure 2.9 is a photograph of the vessel.

2.3 Fuel Element Design

Figures 2.10 and 2.11 show details of the fuel capsule; Figs. 2.12 and 2.13 show the complete element. In Fig. 2.13 a fuel element is suspended outside the vessel but at the same elevation relative to the vessel that it would have if the capsule were in the core. The fuel capsule is deep drawn from high purity tantalum. It has an inside diameter of 0.375 in. and a 0.026 in. wall. The bottom six inches of the capsule will contain fuel and fission product gases will accumulate in the remaining top two inches of the capsule. A tantalum closure plug is welded into the capsule top and has pinned to it a stainless steel adapter with a male thread which screws into the handle. Just above the point where the capsule is screwed to the handle is a locator section which positions the capsule tops. Sodium flows through this locator section in six splines and then into the top reflector region. The handle in the top reflector has a diameter of 0.420 in. In the outlet plenum region the handle has a diameter of 0.375 in. The remainder of the handle length has a hexagonal cross section of 0.483 in. across flats except for the handling and locking details at the upper end. Capsule locations in the core not used for fuel-filled capsules will be occupied by reflector pins. The reflector pin is a solid stainless steel cylinder having a conical tip and screwing into the handle in the same fashion as a fuel capsule. Pin diameter is 0.485 in. Three grooves in the pin allow passage through the wrench which unscrews the handle.

Specifications for the plutonium alloy fuel are listed in Table 2.1 Corrosion tests of tantalum by this fuel have been made using rocking bomb furnaces with a temperature differential of 150°C over several temperature ranges. With a high temperature of 700°C, corrosion is less than 1 mil/yr. Tests show that a trace amount of carbon in the fuel inhibits solution attack of the tantalum, but that very low level of interstitial

Fig. 2.9 Reactor vessel.

.065 RAD. 61°   .025
                                                         .376 DIA

8.312

TANTALUM NRC TEMESCAL
ELECTRON BEAM VACUUM
MELTED

$\frac{5}{8}$
$\frac{1}{32}$ DRILL

.378 DIA   .251   .428 DIA
                  .DIA
1.90°
             $\frac{1}{4}$
$\frac{1}{8}$ .040 $\frac{1}{8}$

TANTALUM NRC COMMERCIAL
GRADE ROD

LENGTH TO BE DETERMINED
BY WEIGHT SPECIFICATION
                                         .350 DIA

PU-FE ALLOY
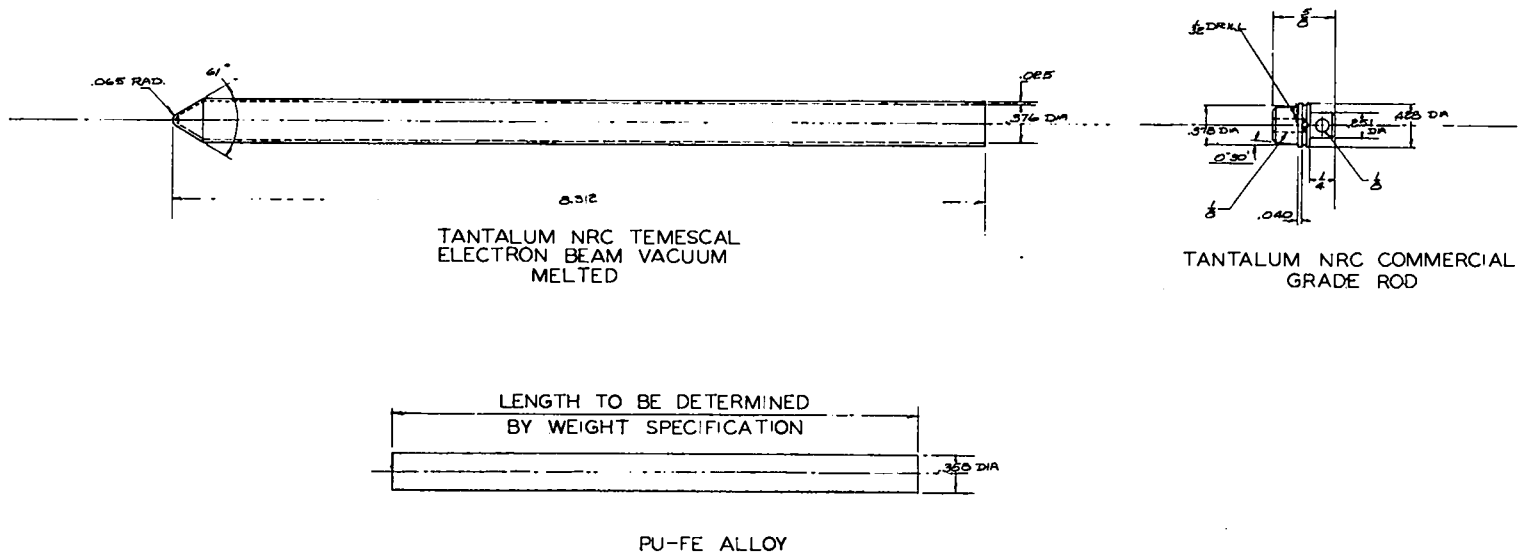
Fig. 2.10 Fuel capsule.
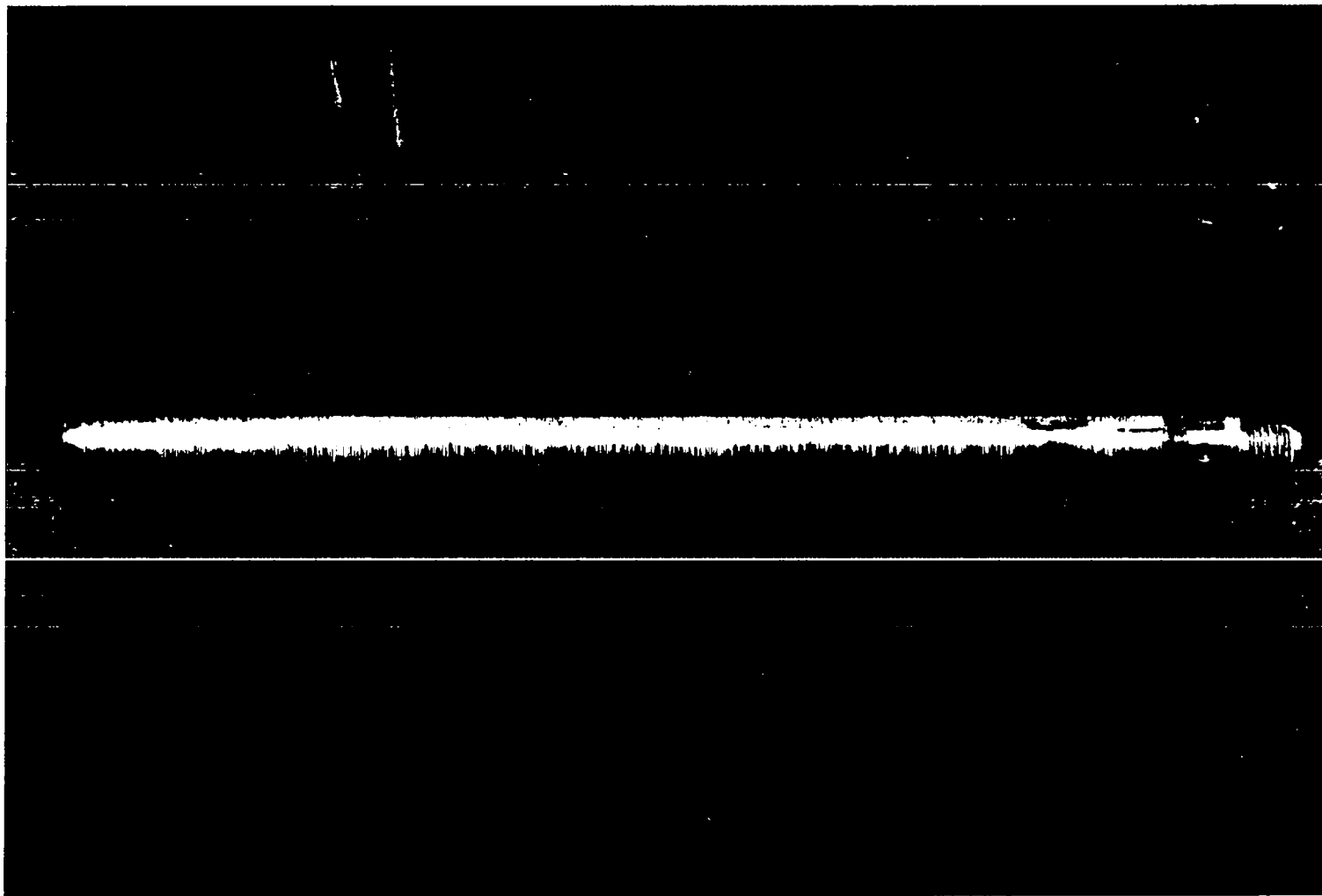
Fig. 2.11   Fuel capsule.
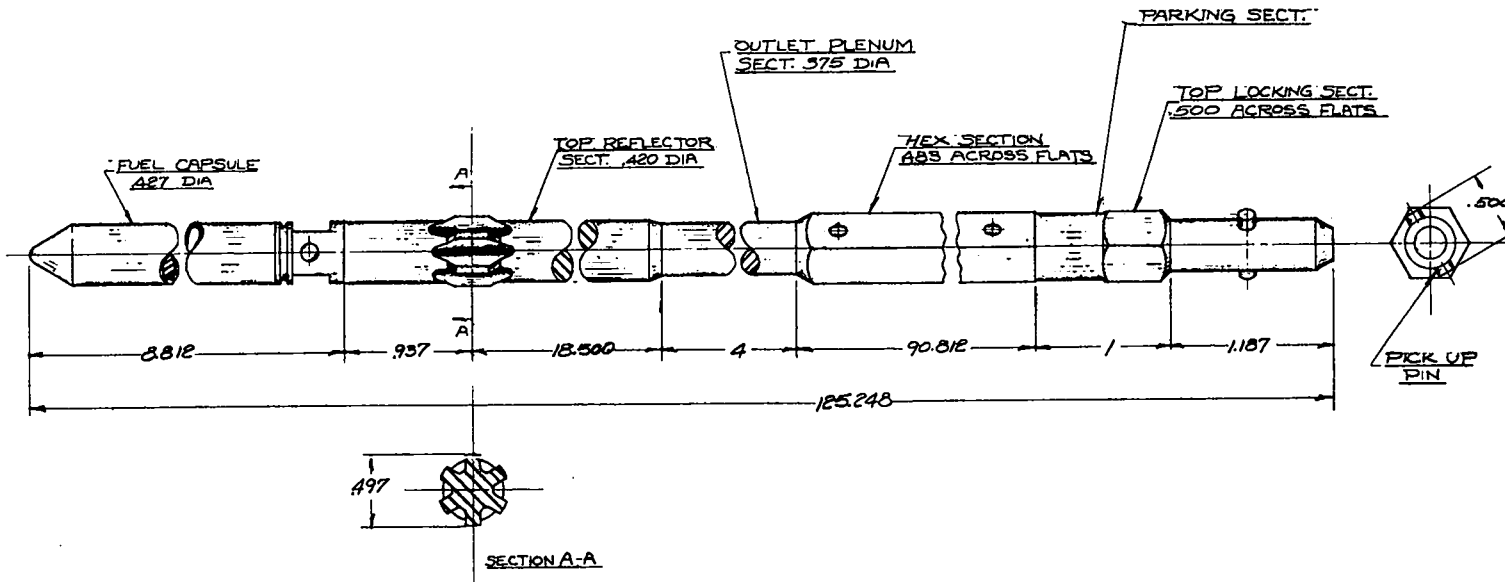
Fig. 2.12 Fuel element.
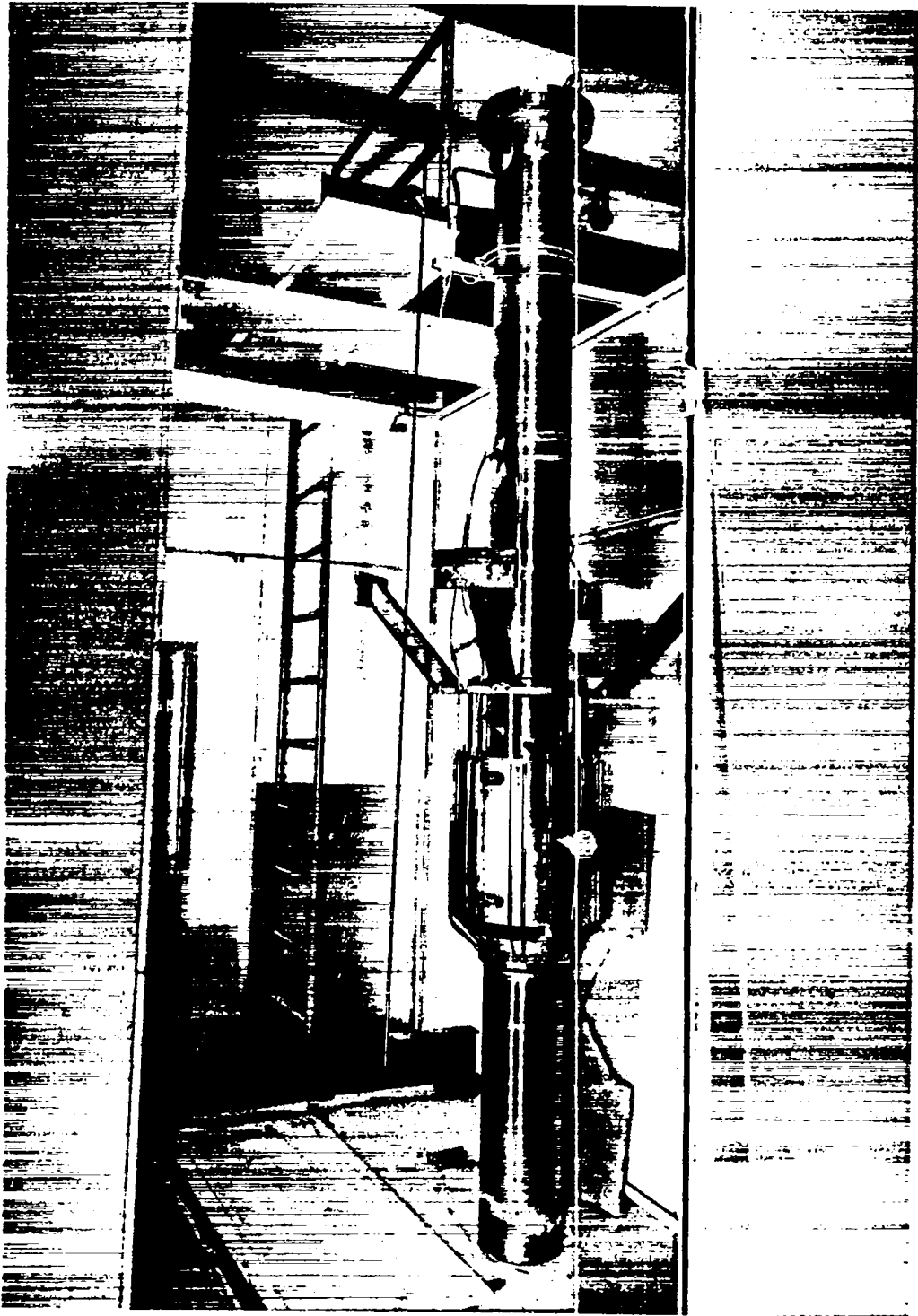
Fig. 2.13 Fuel element.

Table 2.1

FUEL SPECIFICATIONS

a. This specification defines the fuel composition, impurity limits and analytical results for acceptance of LAMPRE I fuel slugs.

b. A melt analysis will be accomplished and submitted to K Division before final machining of the fuel slug. The following defines the impurity limits of certain elements.

Element	Concentration (ppm)
O	< 50
C	> 4 x the O_2 content
P	Reported

c. The iron content will be within 9.5 to 10.5 a/o based on 100% plutonium-iron material.

d. The source of the iron will be cast iron powder as was used in melts 3280 and 3466.

e. Fuel production techniques are to be similar to those of melts 3280 and 3466.

f. The Pu^{240} content will be reported on the basis of the production history of the plutonium used.

g. The weight of each fuel slug will be 175 ± 2 g.

h. As a result of the preceding fuel requirements a typical chemical analysis on an acceptable fuel lot should be as follows:

Element	Concentration (ppm)	Element	Concentration (ppm)
Li	< 0.2	La	< 10
Be	< 0.2	Si	400-800
Na	< 10	Pb	< 20
Mg	< 40	Cu	$< 10-50$
Ca	< 5	Mn	100-500
Al	< 35	Sn	< 20
Bi	< 20	Cr	30-70
Ag	< 10	Ni	100-900
Zn	< 100	C	> 150
Co	$< 10-50$	O	40
B	< 5	H	< 15
F	< 5	N	< 20

i. Deviations from the above specifications will be reviewed by K Division and will be subject to waiver.

impurities in the metal are essential to prevent intergranular attack. The heat affected zone of a fusion weld is more subject to intergranular attack than other regions; for this reason the capsule is deep drawn and the fusion weld at the cap is made in the gas region which is out of contact with fuel.

The plutonium-iron phase diagram is shcwn by Fig. 2.14. Thermal expansion properties of the fuel are given in Fig. 2.15. The thermal conductivity of molten fuel alloy is about the same as that of stainless steel. The measured value is 0.20 ± 0.01 w/cm $^\circ$C at 500°C.

2.4 Core Physics

The calculational methods employed in estimating some of the basic nuclear parameters of the LAMPRE I core are based upon the S_4 transport scheme for spherical systems.* Empirical methods were used to convert spherical system results to the corresponding values for cylindrical systems. The values of some LAMPRE I parameters were experimentally determined from studies made with a critical assembly. The program carried out with the assembly designated LAMPRE Critical Experiment Number Two, or LCX II, is described briefly in Appendix A.

The following steps were involved in the calculations and conversions:

a. Spherical S_4 core calculations were performed for constant, specified, thicknesses of reflector materials, using, in turn, the reflector thicknesses taken from LAMPRE design in three different directions: top, side, and bottom.

b. From the above calculations, the infinite media buckling and reflector savings were obtained for the spherical systems. The material buckling for the cylinder is computed from the average of the spherical system bucklings (reduced by 2% to account for inherent systematic errors). To obtain the reflector savings for the cylindrical system, the spherical

---

*Kiehn, R. M., "Some Applications of the S_n Method," Nuclear Sci. and Eng. 4 166-179 (1958).
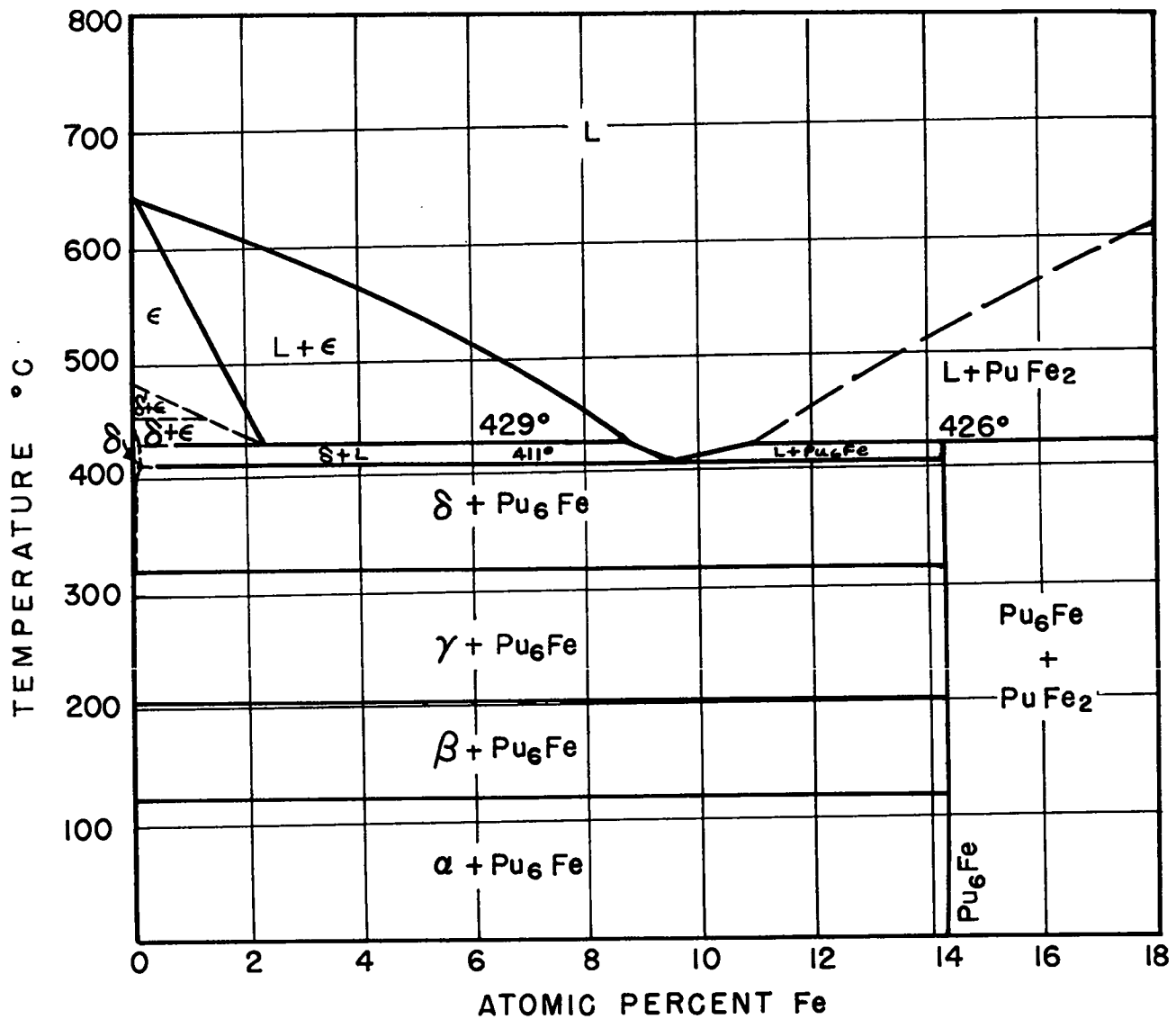
Fig. 2.14 Pu-Fe phase diagram.
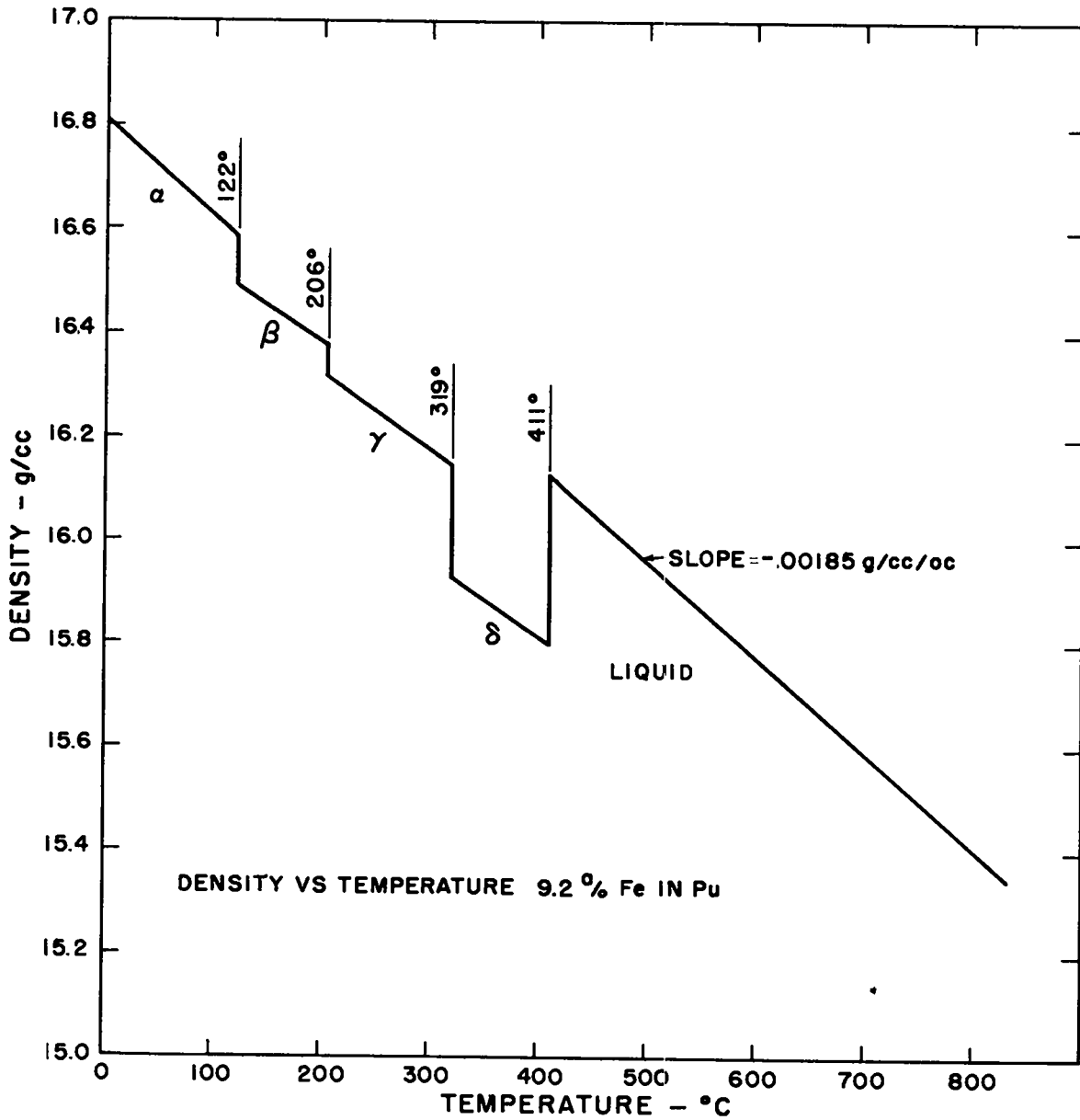
Fig. 2.15 Pu-Fe fuel expansion drawing.

reflector savings were multiplied by empirical factors 0.866 for the ends of the cylinder and 0.937 for the sides.

c. The cylindrical mass was then computed from the formula

$$B^2 = \left(\frac{\pi}{H + \delta_T + \delta_B}\right)^2 + \left(\frac{J_0}{R + \delta_r}\right)^2$$

The core volume fractions used in the computations were:

Fuel alloy   0.5001 (ρ = 16.051 g/cm^3 at 550°C)

Tantalum   0.15403

Sodium   0.34587.

Slightly different constants will apply to the as-built core.

The thicknesses and compositions of the side and end reflectors used in the computations are those listed in Table 2.2. For each of the three cases in the table, core composition remained the same. The results of these calculations indicate that for the hot (1 Mw) LAMPRE I configuration the important nuclear parameters have the following values:

Core buckling	B^2 = 0.048549 cm^{-2}
Side reflector savings	δ_r = 5.374 cm
Top reflector savings	δ_r = 4.312 cm
Bottom reflector savings	δ_B = 5.080 cm
Cylindrical radius	R = 7.758 cm
Cylindrical height	H = 16.249 cm
Fuel alloy mass	m = 24.99 kg alloy
Core volume	V_c = 3.06 liters
K_∞ core	$(\nu\Sigma_r)/(\Sigma_a)$ = 2.62
K_{eff}	Adjusted to 1.00 by shim
Central median fission energy	$\bar{E}_f$ ~ 1 Mev
Prompt neutron lifetime	$\ell^* = \nu\Sigma_f\bar{V}$ = 8.9 x 10^{-9} sec.

The system temperature coefficients were determined by a series of mass calculations in which the material densities were varied in a suitable manner. The expansion coefficients used in obtaining the temperature coefficients were:

Table 2.2

MATERIALS AND THEIR THICKNESSES USED FOR S_4 CALCULATIONS

Material or Region	Thickness (cm)	Composition
SIDE REFLECTOR		
Reflector pins	1.27	0.34587 Na, 0.65413 S.S. (430)
Flow divider	0.635	S.S. (304)
Na (inlet flow region)	0.9525	Na
Inner containment vessel	0.635	S.S. (304)
Heaters	0.9525	0.15 S.S. (304)
Outer containment vessel	0.635	S.S. (304)
Air gap	0.3175	Air
Shim	11.7475	0.98 S.S. (430)
Air gap	0.15875	Air
Circular flue wall	0.635	S.S. (430)
Air gap	1.27	Air
Hexagonal flue wall	0.635	Carbon steel
Shield	50.8	0.9108 B^{10} + C (0.4 w/o boron)
TOP REFLECTOR		
Gas space in fuel capsules	5.08	0.15403 Ta, 0.34587 Na, 0.5001 air
Capsule fuel capsule plugs	1.27	Ta
Capsule handles	50.8	0.61518 S.S. (430), 0.38482 Na
BOTTOM REFLECTOR		
Locator plate facing	0.508	Ta
Locator plate	4.572	0.23795 Na, 0.76205 S.S. (304)
Locator plate plenum	1.905	Na
Bottom reflector	12.70	0.1422 Na, 0.8578 Armco Fe
Turn-around plenum	1.905	Na
Catchpot	15.24	0.47 Na, 0.53 Armco Fe
Inner containment vessel	1.905	S.S. (304)
Air gap	6.35	Air
Bottom vessel shield	11.43	S.S. (304)

$$\left(\frac{\Delta\rho}{\rho}\right)_{fuel} = -89 \times 10^{-6}/^{\circ}C$$

$$\left(\frac{\Delta\rho}{\rho}\right)_{Ta} = -19.5 \times 10^{-6}/^{\circ}C$$

$$\left(\frac{\Delta\rho}{\rho}\right)_{S.S.\ (304)} = -36 \times 10^{-6}/^{\circ}C$$

$$\left(\frac{\Delta\rho}{\rho}\right)_{Na} = -300 \times 10^{-6}/^{\circ}C$$

The results of the computations are expressed in terms of changes in critical mass of fuel alloy per unit change in the temperature of the appropriate material. These derived constants are listed below:

Change in critical mass due to fuel temperature variation in an otherwise isothermal system:

$$\left(\frac{\partial m}{\partial \theta}\right)_{fuel\ (prompt)} = -2.72\ g/^{\circ}C$$

This may also be expressed as a function of fuel density:

$$\left(\frac{\partial m}{\partial \rho}\right)_{fuel} = -1.91 \times 10^{3}\ g/(g/cm^{3})$$

Change in critical mass due to variation in the temperature (isothermal distribution) of all core materials:

$$\left(\frac{\partial m}{\partial \theta}\right)_{all\ core\ materials} = -4.27\ g/^{\circ}C$$

Critical mass change associated with a space independent sodium coolant temperature variation in an otherwise isothermal system:

$$\left(\frac{\partial m}{\partial \theta}\right)_{Na} = -0.80\ g/^{\circ}C$$

If the locating splines on the fuel pin assemblies (see Fig. 2.12) are assumed to be in contact, there is an additional temperature co-efficient. This is produced by the outward displacement of fuel pins as the temperature increases. The displacement is different at the top and the bottom of the core, however, since the bottom ends of the fuel pins are spaced by the tantalum locator plate, which expands at a different

rate than the stainless steel parts (splines) which position the fuel elements at the top end. An average expansion coefficient

$$\Delta \ell / \ell = 9.5 \times 10^6/^\circ C$$

was assumed to be applicable to the effective radial expansion of the core. The temperature coefficient of reactivity produced by the resulting variation in average fuel density was found to be, for an isothermal temperature distribution,

$$\left(\frac{\partial m}{\partial \theta} \right)_{\text{location geometry}} = -0.57 \text{ g}/^\circ C$$

These estimated mass relationships may be converted to temperature coefficients of reactivity by using the experimentally determined value (see Appendix A).

$$\frac{\Delta k}{\Delta M} = 1.18 \text{ ¢/g fuel} \; \cdot$$

In summary, the zero power, isothermal reactor system is characterized by these coefficients:

$$\left(\frac{\partial k}{\partial \theta} \right)_{\text{fuel (prompt)}} = -3.21 \text{ ¢/}^\circ C$$

$$\left(\frac{\partial k}{\partial \theta} \right)_{\text{Na}} = -0.94 \text{ ¢/}^\circ C$$

$$\left(\frac{\partial k}{\partial \theta} \right)_{\text{location geometry}} = -0.67 \text{ ¢/}^\circ C$$

$$\left(\frac{\partial k}{\partial \theta} \right)_{\text{reflector}} = -0.88 \text{ ¢/}^\circ C$$

The power coefficient of the system may be estimated from the above reactivity coefficients. It is necessary only to sum the effects of the listed coefficients, taking proper account of the fact that the temperatures of the fuel, the coolant, and the reflector structure increase by different amounts as operating power is raised. (For instance, it is calculated that for full coolant flow the average fuel temperature increases about three times as fast as the average sodium temperature when power demand is increased.) The total power coefficient is, on this basis, found to be

$$\left(-\frac{\partial k}{\partial P}\right) \cong -0.69 \ \text{¢/kw}$$

or

$$\left(-\frac{\partial k}{\partial \theta}\right) \cong -12.3 \ \text{¢/°C rise in Na temperature}$$

Approximately three-fourths of the power coefficient results from the temperature rise in the fuel and is therefore a prompt effect. If there is a significant amount of convective circulation of fuel in the capsules, the average temperature of the fuel will be lower (relative to the coolant temperature at a given power), and the absolute value of the power coefficient would be smaller than the estimated value given here. Mechanical clearances in the core structure, not considered in the above power coefficient estimates, could produce a similar effect through their relation to core distortion (capsule bowing) as a function of power.

Since the LAMPRE I fuel is molten under operating conditions, a radial temperature gradient across the core does not produce strong bowing effects in the fuel capsules. Some bowing may occur, however, since the radial temperature variation will tend to introduce bowing forces in the tantalum fuel capsules themselves, and in the fuel capsule handles. The amount of bowing which can take place is a complicated function of assembly clearance on the fuel element assemblies and of the actual temperature distribution in the reactor. These variables, and their effects on the overall power coefficient, are considered in Appendix B which may be summarized briefly as follows:

a. In the bowing calculation it was assumed that assembly clearances between fuel capsule handles are uniformly distributed, and that initially there is no contact between adjacent fuel capsules at the spline sections of the handles. If, as will almost certainly be the case, a few percent of the fuel capsules are initially constrained by contact between adjacent spline sections, the effect of bowing is markedly reduced.

- 33 -

b. With the uniform clearance assumption, both capsule and handle bowing make positive contributions to the power coefficient up to about 10% of full power. At higher power levels only capsule bowing persists and it produces only a small reactivity effect.

c. On the basis of the pessimistic distribution of mechanical clearances assumed, the overall power coefficient, including the bowing contribution, is calculated to be positive up to a power level of 100 kw, with a value of about 0.025 ¢/kw. Above the 100 kw power level, bowing is of little consequence, and the overall power coefficient becomes ~ -0.7 ¢/kw.

d. The prompt component of the power coefficient is negative over the entire power range, with a value of about -0.55 ¢/kw.

There is one other recognized source of a small positive component of the overall power coefficient. Relative motion between the reactor core and the control elements occurs as the average sodium temperature changes with variation in power. The motion is such as to increase reactivity as power, and hence the average sodium temperature, increases. A design feature which has to a large measure eliminated this effect is described in Section 2.7. It is estimated, however, that a positive component of the power coefficient of $\leq$ 0.015 ¢/kw still remains due to this thermally induced, relative motion between the reactor core and the control elements.

Calculations indicate that with the reactor at operating temperature, but at low power, withdrawing the shim and control rods reduces reactivity by an amount equivalent to about 6000 g of fuel, or by roughly $70. While the relative effectiveness of the control rods and the control shim is not known precisely for LAMPRE I, it appears that about $60 of the above shutdown control is produced by the shim.

It has been also estimated that if the reactor is shut down from full power operating conditions by withdrawing the shim and the control rods, the reactor will be subcritical at room temperature by an amount equivalent to 2.8 kg of fuel, or by ~ $33.

The dry (no sodium) cold critical loading of the reactor is calculated to be 25.48 kg of fuel with the rods and shim inserted. The corresponding value with all control elements withdrawn is 31.68 kg.

Reactivity worth of the sodium coolant (including that in the inlet and outlet plenums) is listed below, expressed in terms of the equivalent change in critical mass:

$$Na \text{ worth at } 20^\circ C, \text{ shim and rods in} \cong 3.1 \text{ kg}$$
$$Na \text{ worth at } 20^\circ C, \text{ shim and rods out} \cong 3.9 \text{ kg}$$
$$Na \text{ worth at } 550^\circ C, \text{ shim and rods in} \cong 2.6 \text{ kg}$$
$$Na \text{ worth at } 550^\circ C, \text{ shim and rods out} \cong 4.1 \text{ kg.}$$

2.5 Operating Conditions

General

LAMPRE I startup and approach to operation at full power will be carried out in four major steps. First, a set of cold critical experiments will serve to determine critical mass and control element worth for comparison with calculated estimates based on LCX II observations. During this period no sodium coolant will be present in the reactor, and the entire system will be at room temperature. Second, after the conclusion of the cold critical measurements, all the fuel will be removed from the reactor, and the fuel capsules will be replaced by stainless steel dummies; the reactor system will then be filled with sodium and operated at an appropriate temperature, and for a suitable length of time, to clean up all system components. Third, the dummy elements will be replaced one by one with fueled elements, and a determination of the hot, wet critical mass and the control element worth will be made at a reactor system temperature in the range of 450°C to 500°C, and at "zero" nuclear power. The fuel in each capsule will melt as it is inserted into the core. The value of the negative temperature coefficient will also be measured under these

conditions. Finally, the reactor power will be raised stepwise and at each power level reactor stability will be investigated by a series of reactor oscillator experiments.

Table 2.3 gives values of some core parameters.

Reactor Startup and Approach to Full-power Operation

Cold Critical

The design of the mechanized fuel element handling system, or capsule charger, is such that it cannot load fuel into an empty reactor core. Therefore, an initial loading of dummy elements must be made manually before the capsule charger is attached to the reactor during the final stages of system assembly. At the start of the cold critical measurements, the reactor will therefore be completely filled with dummy fuel elements and reflector pins. Dummy capsules will be replaced manually, one at a time, by fuel capsules until a multiplication of 10 (with shim and rods down) is achieved. At this point the capsule charger will be installed and further replacement will be accomplished using the charger. Rules governing personnel access to reactor areas will be applied during the cold critical phase of operations. Protective instrumentation and interlocks described in a subsequent portion of this section of the report will be connected if they are related to nuclear safety considerations. Startup detectors will consist of at least three B^{10} lined proportional counters. A startup neutron source of sufficient intensity is provided by Pu^{240} in the fuel itself.

The actual charger manipulations involved in replacing the dummy fuel elements with fuel-filled capsules are as follows: The vertical lift mechanism is lowered to engage a fuel element handle; the handle with its dummy element is lifted into the charger housing and the element then unscrewed from the handle. The dummy element is transferred out of the housing through a port, and a real fuel element inserted into the housing

Table 2.3

VALUES OF CORE PARAMETERS

Capsule material	National Research Corporation high-purity Ta refined by Temescal electron beam melting
Capsule size	0.375 in. i.d. x 0.26 in. wall
Core capacity	199 capsules in hexagonal array
Number of capsules for criticality	143 (calculated)
Capsule spacing	0.497 in. triangular pitch
v/o fuel	51.5
v/o Na	33.5
v/o Ta	15.0
Fuel height	6 in.
Fission gas volume height	2 in.
Design power	1 Mw
Average fuel temperature	637°C
Maximum fuel temperature	870°C
Na inlet temperature	450°C
Na outlet temperature	563°C
Na flow rate	133 gpm
Central to edge power ratio	1.8
Axial power ratio	1.8

	Average	Maximum	Minimum
Specific power (w/g)	40	61	19
Heat flux (w/cm^2)	145	220	68
(Btu/hr/ft^2)	460,000	700,000	214,000
Na outlet temperature (°C)	563	597	531
ΔT in fuel (°C)	200	307	93
ΔT in Ta (°C)	17	24	8
Ta thermal stress (psi)	2800	4300	1300

and attached to the handle by the reverse process. The element is then lowered into the reactor vessel and is positioned in the space formerly occupied by the dummy.

All fuel additions are to be made with the control elements (shim and rods) in their least reactive, or down position. When about two-thirds of the estimated 25.48 kg critical mass has been loaded, the shim and rods will be inserted, and the neutron level observed. This procedure will be repeated at appropriate intervals during the rest of the fuel loading operation, until sufficient data are available to estimate satisfactorily the actual critical mass with shim and rods fully inserted. The final approach to delayed critical will be made by control rod manipulation.

Critical mass at partial shim insertions may be determined in an exactly similar fashion after making the appropriate adjustments to the mechanical stop which limits available range of shim travel. An extrapolation of the data to the shim-down case will determine the worth of the shim; for the cold critical case, its value has been estimated to be equivalent to 6.2 kg of fuel, or about 39 elements.

Fuel inventory records kept during these, and subsequent, loading procedures will list the identifying number of each element inserted into the reactor, together with its position in the core. The total loaded fuel inventory may be physically checked against the number of dummy elements removed from the core during loading operations.

Sodium System Cleanup

When the cold critical experiments have been finished, the fuel will be removed and replaced by the dummy capsules, element by element. The reactor system will by this time be ready to charge with sodium. Test operation, with electrical heating to about 500°C, will then begin, and continue until satisfactory performance of all coolant loop components has been demonstrated, and until the desired degree of sodium

purity has been obtained through the use of cold and hot traps. The fuel capsule charger will be tested while the reactor system is at operating temperature, and the various sodium system malfunction detectors checked out, insofar as possible, under actual operating conditions. Satisfactory mechanical functioning of the reactor control elements at elevated temperature will also be ensured.

Zero Power Hot Critical

When the coolant system cleanup and checkout program has been completed, the core may be loaded with fuel and the zero power, hot critical mass determined. During this operation, the reactor system will be held at a temperature of $450^{\circ}C$ to $500^{\circ}C$ by the use of electrical heaters. Zero power, or isothermal, operation above $500^{\circ}C$ is not advisable, since the sodium pumps (in the reactor inlet leg of the coolant loop) are not designed for temperatures in excess of $500^{\circ}C$. There will be no air flow through the sodium-to-air heat exchanger, but in other respects, the coolant system will be fully operative.

The insertion of fuel into the core will be accomplished in the same fashion as during the cold critical determination; i.e., a dummy capsule will be removed by the capsule charger, and a fuel capsule put in its place. It is expected that the fuel in a capsule will become fully molten during the time interval between its insertion and the loading of the succeeding fuel element.

A shim in, all rods in, critical configuration will first be determined. It will then be desirable to increase the fuel loading, one capsule at a time, to obtain a preliminary calibration of rod worth. A similar preliminary value of the temperature coefficient of reactivity will then be obtained by varying the electrical power input to the system and noting the configuration changes necessary to maintain criticality. Finally, critical mass as a function of shim insertion will be determined in the same fashion as during the cold critical

tests, and intercalibration of the shim and the control rods will be carried out.

The final fuel loading will be adjusted to such a value that, at full power, a critical configuration should be reached with the shim and two rods fully inserted, and the third rod partially inserted.

Approach to Full Power

The following basic plan will be followed in achieving full power operation. With the shim fully inserted, (corresponding to a slightly subcritical configuration at the 450°C, isothermal condition) the reactor will be made critical and coolant outlet temperature will be raised in small increments by inserting rods. A constant coolant inlet temperature will be maintained by decreasing the electrical heating power as nuclear power is increased.

The present estimate of overall power coefficient for LAMPRE I is 0.7 ¢/kw. Therefore, $7 of reactivity control must be available in the rods to reach the nominal 1 Mw design power. The estimated value of the total worth of three control rods is very ~ $10. It appears, therefore, that sufficient reactivity control is available to reach design power without shim adjustment. However, the power coefficient depends strongly on the actual value of parameters such as the thermal conductivity of the fuel, which is not accurately known at present; also the power coefficient of the reactor will be influenced by the amount of natural convection of the molten fuel within the capsules.

Protective Instrumentation

General Description of Safety Circuits

The safety instrumentation of the LAMPRE I system may be grouped into four classes: scram channels, rundown channels, annunciator channels, and interlocks.

- 40 -

Scram channel signals will produce reactor shutdown by causing the control shim to drop to its least reactive, or down, position. Rundown channel signals initiate automatic rod withdrawal with an attendant reduction in reactor power. Annunciator channel signals operate visible and audible alarms which indicate to operating personnel the existence of abnormal values of system parameters. Corrective action must be initiated by the reactor operator. Interlocks provide sequencing of certain operations affecting reactor criticality; they also regulate coolant system startup procedures and provide for ventilation system control in the event of fission product and sodium smoke release in certain areas.

Scram Channel Signals

The sources of scram signals are:

a. Reactor period less than preselected value
b. Neutron level above preselected value (two independent channels)
c. Reduction of coolant flow to ~ 1% of full flow
d. Excessive temperature indication from thermocouple located in heat exchanger air outlet duct
e. Slide valve at top of reactor vessel open
f. Manual scram switch
g. Electrical power failure in control element drive system.

The period signal is obtained in a conventional manner from a log amplifier circuit containing appropriate differentiation. The amplifier input signal originates in a neutron sensitive ion chamber. The differentiated amplifier output signal is fed into a fail safe electrical switching circuit; i.e., a Schmidt trigger employing a normally open plate relay whose contacts are connected in series with the scram buss.

Neutron level signals are obtained from ion chambers feeding linear amplifiers with trigger circuits similar to those noted above. Coolant flow signals are obtained from a permanent magnet flowmeter whose output is recorded on a line-drawing, strip chart recorder. A low limit switch on the recorder triggers the scram.

A gross leak in the heat exchanger would result in a sodium fire which would raise the air outlet temperature well above normal operating values. A thermocouple will trip a scram channel when the temperature in this region is about 100°C above the maximum expected normal temperature.

It is considered undesirable to operate the reactor unless the slide valve which isolates the fuel charger from the reactor is closed. An electrical interlock will prevent control shim operation if this valve is open. The reactor operator may shut down the reactor at his discretion by means of the console scram switch. Electrical power failure in the shim actuating hydraulic system will automatically produce a shim drop by de-energizing a normally open solenoid-operated valve.

Tests have indicated that 0.015 sec after the scram signal has reached the scram solenoid valve the shim will have begun to drop. An additional delay of not more than 0.050 sec is introduced by the relay circuits associated with scram channels a and b above. Short delays in the transmission of scram signals from sources c, d, and e are of no consequence, since these scram demands do not originate as a consequence of the nuclear behavior of the reactor.

Rundown Channel Signals

Certain malfunctions, or variations in reactor system operating parameters, make it desirable to reduce the reactor power until the source of the trouble can be recognized, evaluated, and removed. The occurrences which have been selected to initiate automatically a reduction in reactor power are tabulated below:

    a. Reduction of Na flow below a desired level

    b. Reactor coolant outlet temperature higher than a preselected value

    c. Stoppage of air flow through heat exchanger air ducts

    d. Excessive radiation level in heat exchanger air outlet duct

e. Presence of smoke in heat exchanger air outlet duct, in the Na equipment room, or in the reactor cell

f. Temperature of Na at heat dump outlet plenum higher than a preselected value.

Signals indicating that any of the above conditions exist will initiate automatic sequenced withdrawal of control rods. The withdrawal will continue until all rods are out unless the operator has been able to reset the rundown channel circuits. He can do this only if the system has returned to a normal condition. Any additional corrective measures must be chosen and initiated by operating personnel.

Annunciator Channel Signals

The annunciator channels which warn operating personnel (via visible and audible signals) of low urgency, off normal conditions in the reactor system are:

a. Leak in coolant piping system (signal comes from detection system which traces the piping); this method of leak detection is separate from the smoke detectors which can initiate a rundown

b. High gamma radiation levels at selected (seven) locations in reactor area

c. Na temperature at heat exchanger outlet below preselected value

d. Graphite shield temperature above preselected value

e. Leakage of Na from inner reactor vessel

f. Door between control room and reactor cell open

g. Temperature of main loop heating transformer above preselected value

h. Poor vacuum in gas disposal system holding tank

i. Na level in surge tank too high

j. Na level in surge tank too low

k. Cover gas pressure too high

l. Cover gas pressure too low

m. Improper voltages on neutron level detectors

n. Improper voltages in remote area gamma radiation monitoring system

o. Instrument air supply pressure too low

p. Pressure in shim drive hydraulic accumulator too low

q. Loss of cell blower power.

Interlocks

Electrical interlocks in the LAMPRE I instrumentation and control systems automatically enforce certain restrictions on operational procedures. These interlocks may be grouped in the following fashion with functions as indicated.

Shim and Control Rod Sequencing Interlocks. These interlocks provide five operational restrictions:

    a. All rods must be down before shim can be raised

    b. Shim must be up before any rod can be raised

    c. Rods can be raised only one at a time and then only in a pre-determined order

    d. Only one rod (at a time) can be held in a position between up and down and then only if the preceding rods in the sequence are up

    e. Automatic rod rundown is initiated in case of a scram signal.

Vessel Slide Valve Interlock. This is an interlock between the shim drive and the 10 in. slide valve which isolates the reactor vessel from the capsule charger. The shim cannot be up, i.e., reactor cannot be operating, unless the gate valve is closed. Therefore, the capsule charger cannot insert fuel into the core unless the reactor has been shut down to a scrammed configuration. This interlock is also listed in the scram channel tabulation, since opening the valve will produce a scram if the reactor is operating.

Cell Ventilation System Interlock. An abnormally high gamma radiation level in the reactor cell, assumed to be evidence of a reactor leak with subsequent escape of sodium and/or fission products, will stop the cell exhaust blower.

FRACTION OF FULL POWER

RANGES OF NEUTRON DETECTORS

10^{-11} 10^{-10} 10^{-9} 10^{-8} 10^{-7} 10^{-6} 10^{-5} 10^{-4} 10^{-3} 10^{-2} 10^{-1} 10^{0} 10^{1}

FULL POWER

B^{10} COUNTER

B^{10} COUNTER (START UP)

B^{10} COUNTER

B^{10} COUNTER (START UP)

LINEAR LEVEL RECORDER

CURRENT CHAMBER

CURRENT CHAMBER

LEVEL SCRAM

CURRENT CHAMBER

LEVEL SCRAM

CURRENT CHAMBER

LOG LEVEL RECORDER & PERIOD SCRAM

CURRENT CHAMBER
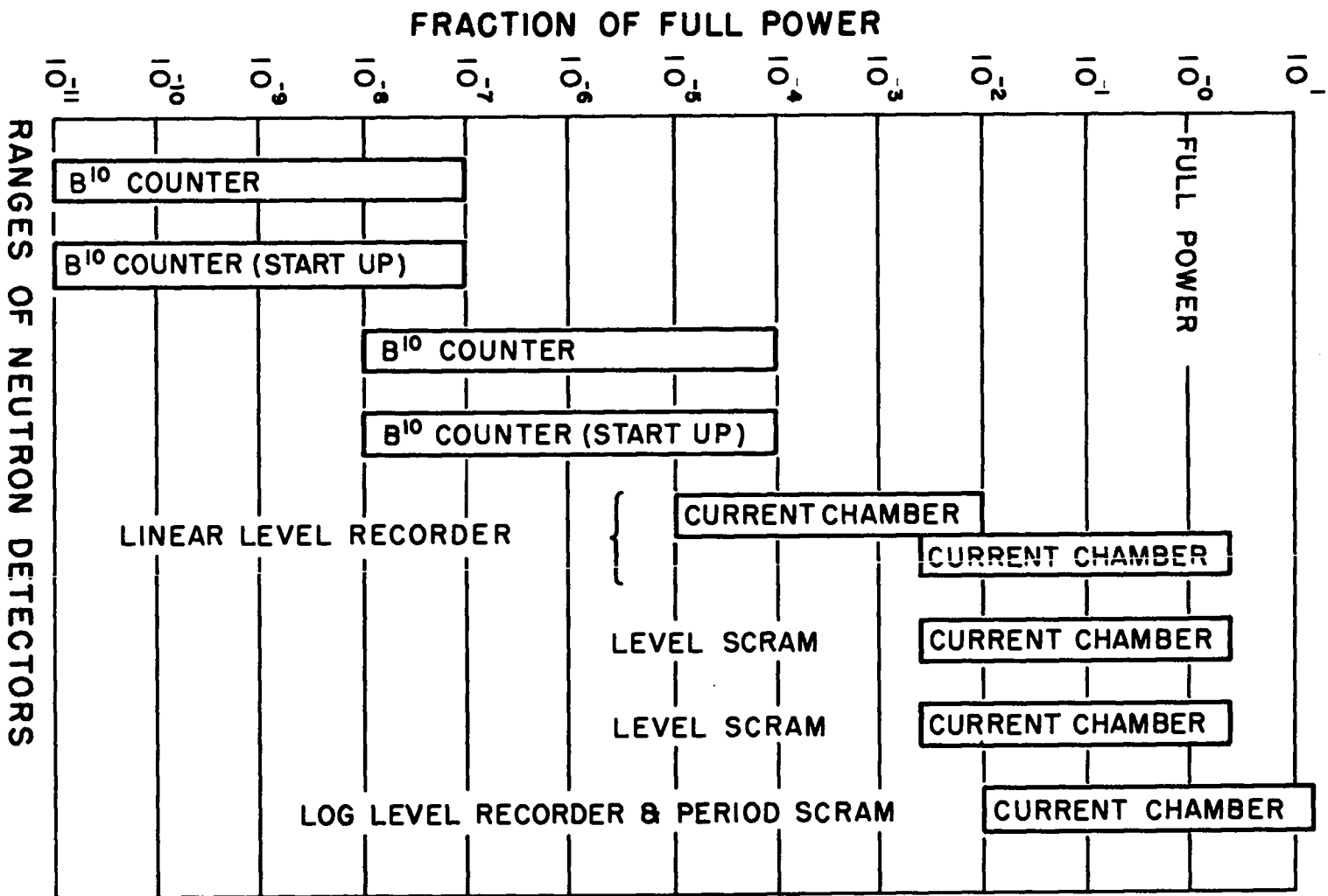
Fig. 2.16 Ranges of neutron detectors.

2.6 Coolant System

Components

The system which contains the sodium coolant is, in general, fabricated from Type 316 ELC stainless steel. Figure 2.17 is a schematic of the system and Figs. 2.18 and 2.19 show the coolant system layout. Components will be described individually.

Piping. Sodium piping is 2 and 3 in. Schedule 40, Type 316 ELC stainless steel. All weldments are made with an inert arc root pass followed by coated rod filler passes. Root passes are checked by the dye penetrant method and the completed weld both by dye penetrant and radiograph. The loop is suspended from spring hangers except at anchor points indicated in Figs. 2.18 and 2.19. All welds are leak tested using a helium mass spectrometer leak detector.

Pumps. Coolant pumping is done by two ac electromagnetic conduction pumps in parallel, each rated at 100 gpm at 20 psi head. Power to the pumps is controlled by motor-driven adjustable auto transformers. Check valves of the flapper type in the outlet of each pump prevent bypass flow.

Heat Exchanger. The heat exchanger, built by Griscom-Russell, is made up of finned sections which transfer heat from sodium to air which is exhausted up a stack outside the building. Airflow through the unit will be controlled by sodium temperature at the outlet from the exchanger. The temperature will be sensed by a thermocouple connected to a self-balancing potentiometer which in turn controls a pneumatic operator which positions a louver-type damper at the blower inlet.

Flowmeters. There will be a total of three electromagnetic flowmeters in the loop; one in each of the two 2 in. pump outlets and one in the 3 in. piping between the vessel and surge tank. The 3 in. pump meter was supplied and calibrated by Atomics International.

Dump Tank. The primary coolant system is filled from or drained to a tank which is located at the lowest part of the system. Sodium is pushed
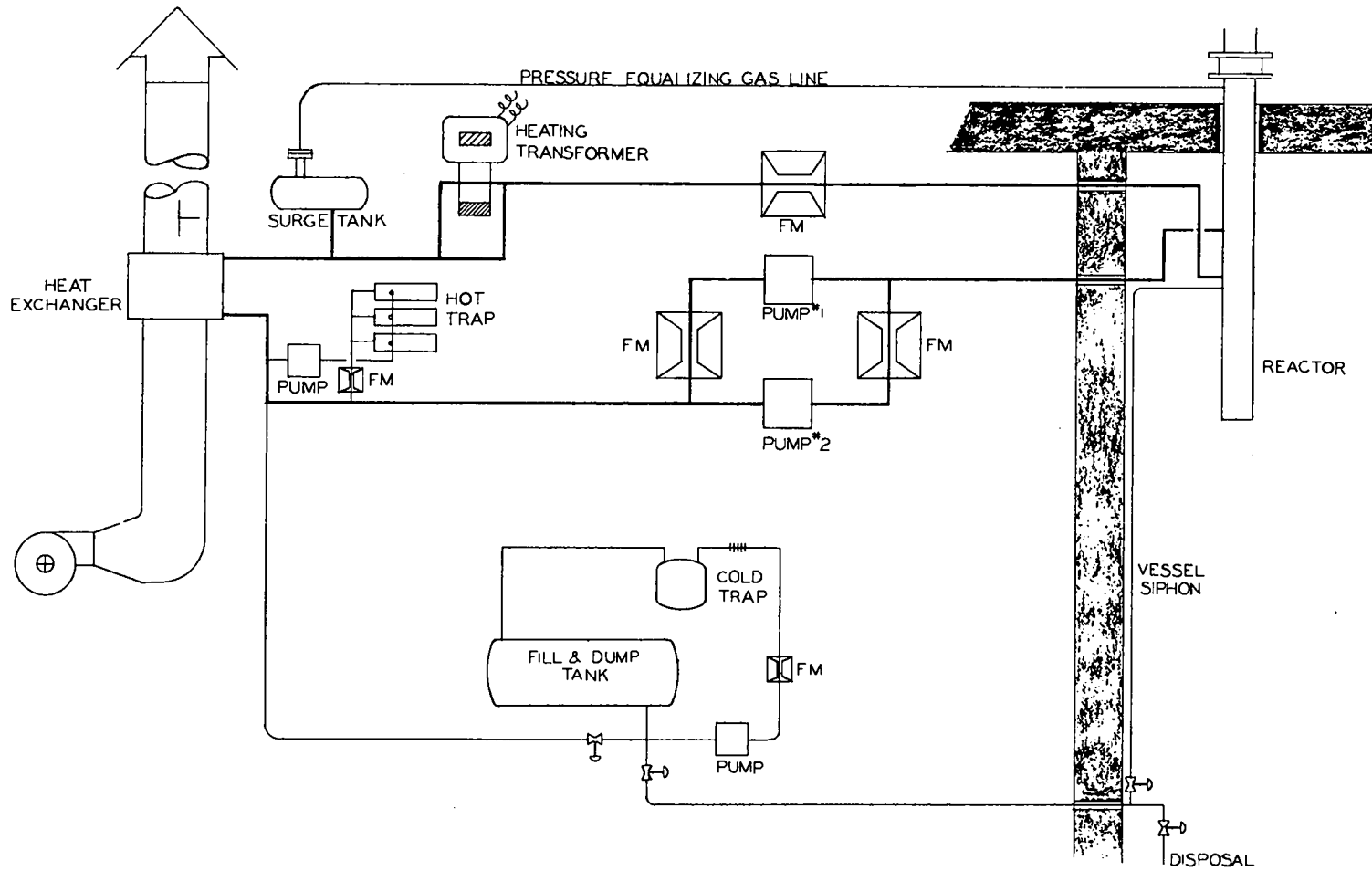
Fig. 2.17   Schematic of sodium system.
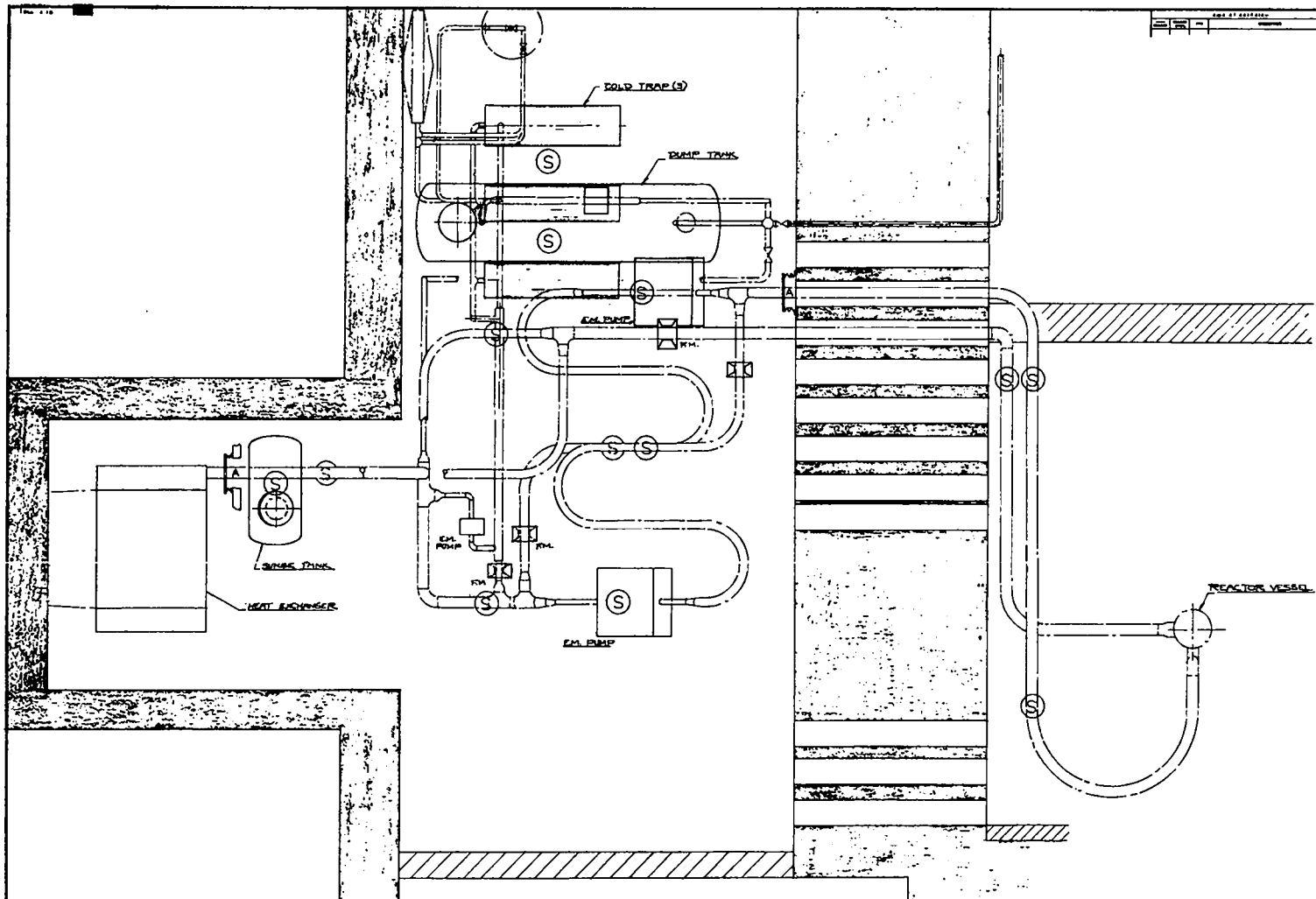
Fig. 2.18 Plan view of sodium system showing main components, support and anchor points.
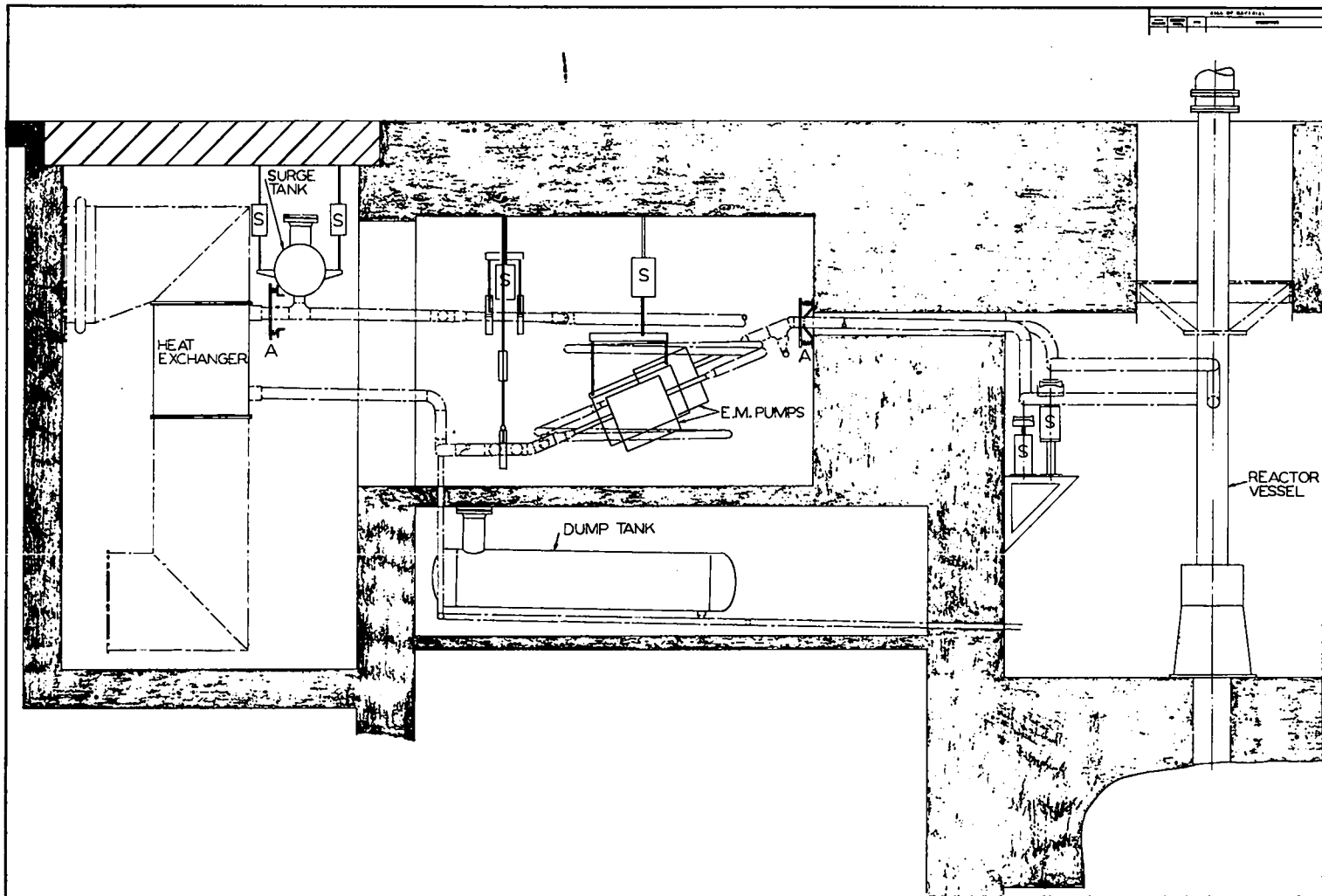
Fig. 2.19 Elevation of sodium system showing as above.

from the tank to the system by gas pressure. Dumping will normally be accomplished by gravity although gas pressure can be used to speed up the operation. A variable reluctance sodium level indicator has been developed and will be installed in the tank. Isolation of the dump tank from the main system is accomplished by a bellows sealed valve in the drain line.

Surge Tank. A combination surge and expansion tank will be installed just upstream of the heat exchanger inlet. A variable reluctance type of level indicator will be installed in this tank. Connecting the surge tank and the vessel gas volume is a 1 in. pressure equalization line. The sodium level in these two volumes will be different only by the friction drop in the 3 in. line connecting vessel and surge tank.

Cold Trap. A cold trap and plugging indicator is installed in a side loop on the dump tank. It is planned to circulate sodium in the primary coolant system, then return it to the dump tank for cold trapping and, in this way, accomplish cold trapping of the main system without having the cold trap attached to it. During reactor operation the cold trap, as well as the dump tank, will be valved off from the primary system. By means of the plugging indicator it will be possible to measure Na_2O content down to about 15 ppm.

Hot Trap. Three heated metal getter hot traps will be installed in a 1 in. bypass loop on the primary system. The three traps are connected in parallel and have a heater control for each trap. It is planned to use only one trap at a time. Bypass flow through the two unheated traps will be prevented by allowing the sodium in them to freeze. The metal used for gettering will be zirconium foil operated at $700^\circ C$. The hot trap loop will have its own electromagnetic pump and flowmeter. By use of hot traps it is expected to reduce the Na_2O content in the sodium coolant to 1 or 2 ppm. Capacity of the hot traps is estimated to be 10-fold greater than necessary. Hot trap bypass flow is about 5% of full power coolant flow.

Heating. Heat can be supplied to the loop by either or both of two methods. All piping and components are traced with electrical tubular heaters which will be used for warming up the system prior to sodium charging.

A second system will be used for supplying heat to maintain the entire coolant loop and vessel at a minimum of 450°C. The second heating system employs a transformer and part of the Na loop constructed so as to be a one-turn secondary on the transformer. There will be the capability of adding about 40 kw of heat in this fashion. It is, of course, necessary that there be some sodium flow during the period when transformer heating is used in order to prevent overheating of the one-turn secondary.

Corrosion of Component Materials in Sodium

Tests of materials which are in contact with the sodium coolant have been conducted at the Los Alamos Scientific Laboratory and elsewhere. Based on work by the Argonne National Laboratory and the Knolls Atomic Power Laboratory, there is confidence that stainless steels are satisfactory for use in sodium systems at LAMPRE I operating temperatures.

The use of tantalum capsules has required that the corrosion rate of tantalum in sodium be investigated. Figure 2.20 shows the corrosion rate of tantalum for both the hot and cold trapped cases.

Instrumentation

The coolant system instrumentation is conventional in most respects. In addition to thermocouples on the 2 and 3 in. piping, there will be thermocouples in the core region measuring core inlet, outlet and radial distribution temperatures. Remote indicating transmitters will measure pressures at the surge tank, pump inlet, pump outlet, and dump tank. Flow measurement will be made by the three electromagnetic flowmeters discussed above. There will be no orifice or flow tube differential pressure measurement. A sodium leak detector system, which consists of a glass insulated thermocouple pair tracing the bottom of sodium piping, will be installed. Figures 2.21 and 2.22 indicate locations of instrumentation.
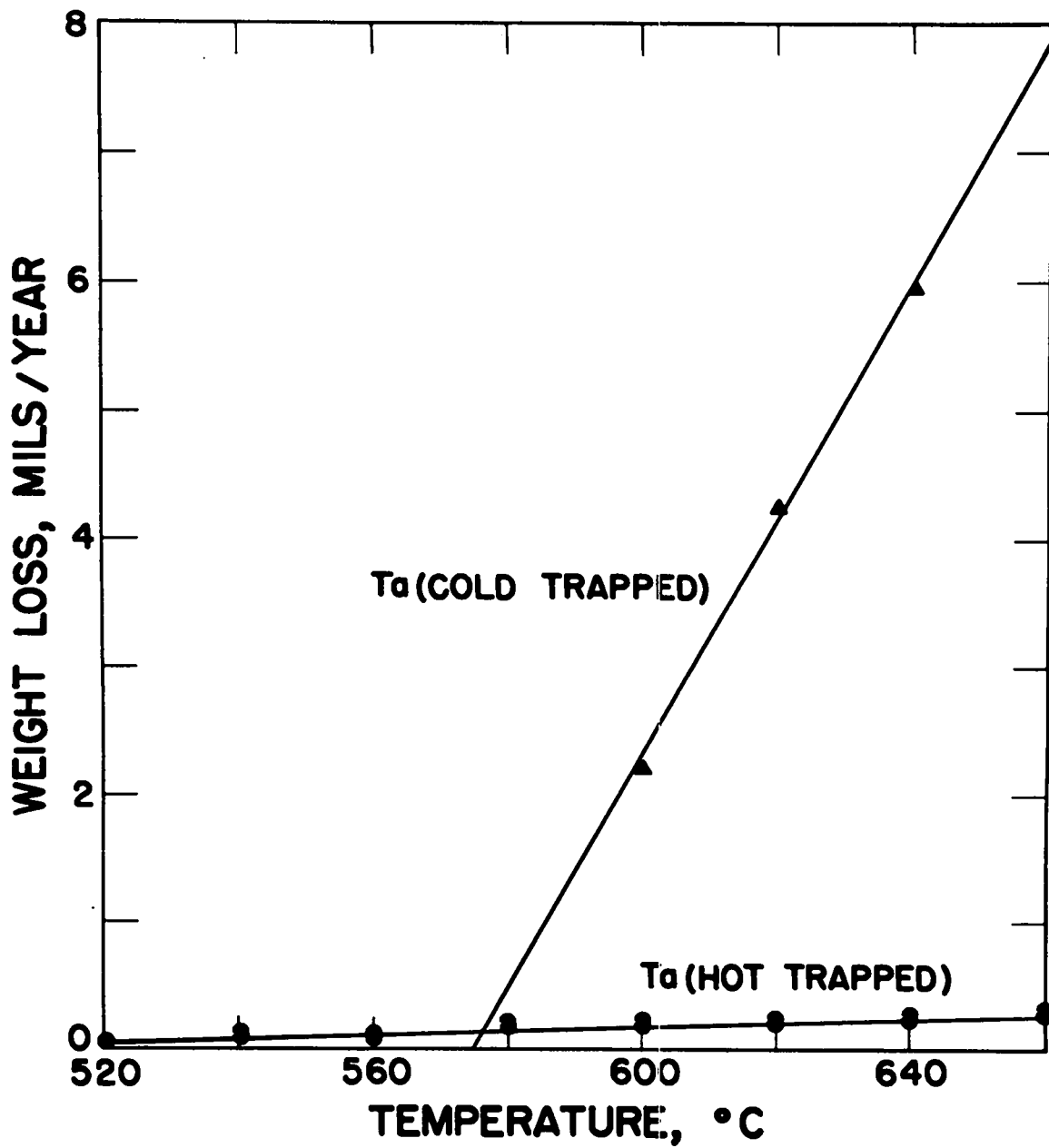
Fig. 2.20 Corrosion rate of tantalum in sodium vs temperature.
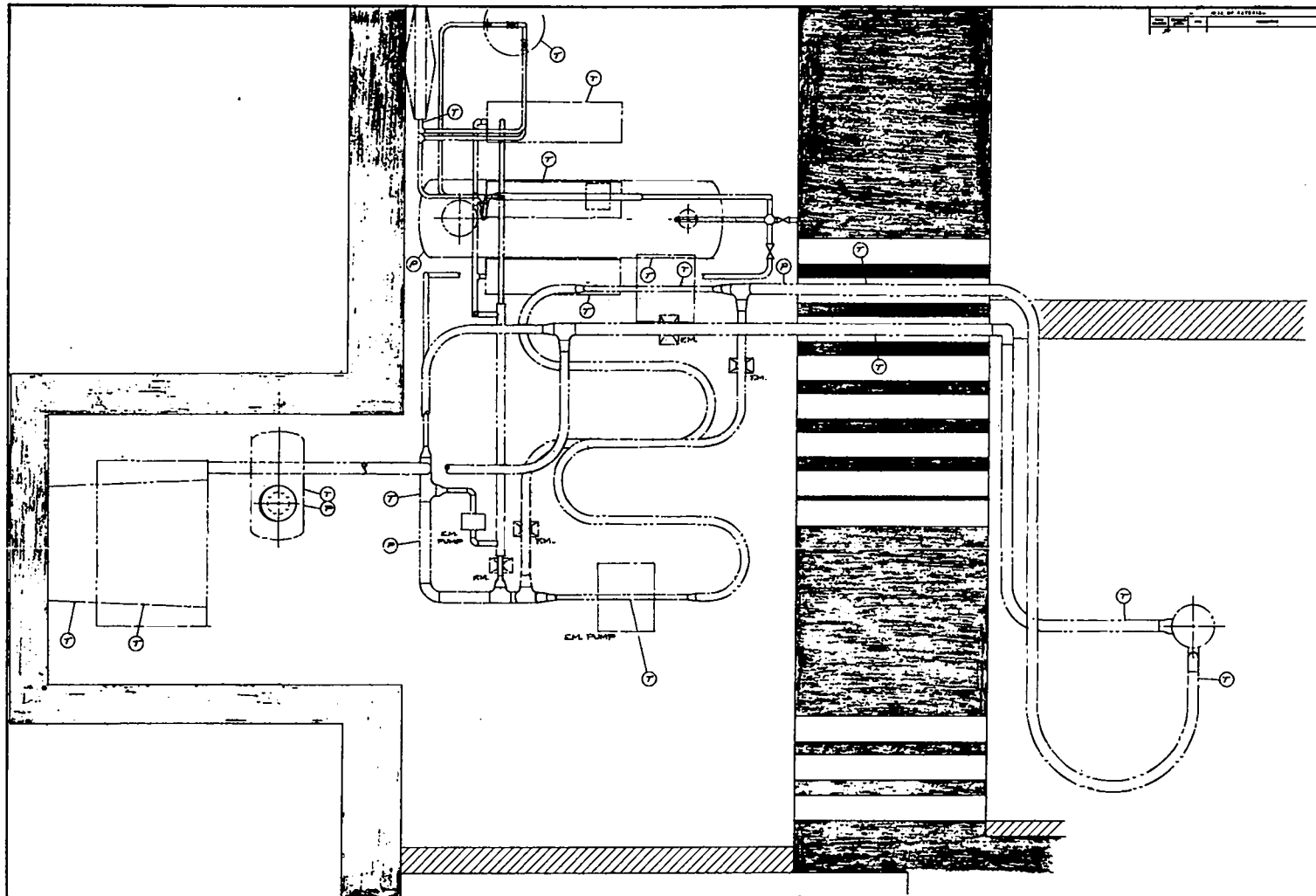
Fig. 2.21 Plan view of sodium system showing instrumentation.
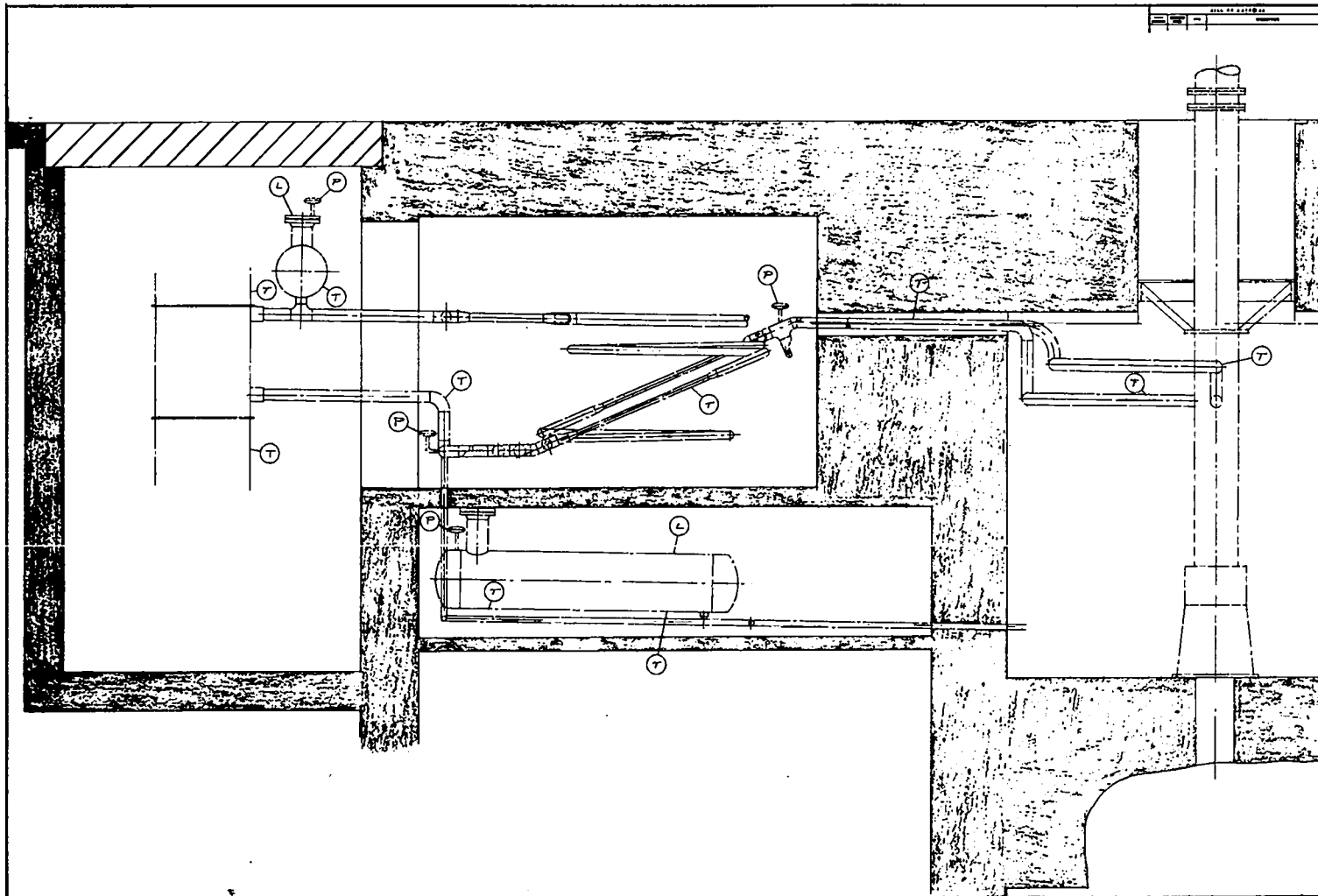
Fig. 2.22 Elevation of sodium system showing instrumentation.

Mockup Loop Operation

In order to gain experience in construction and operation prior to reactor installation, the reactor coolant loop was fabricated and tested using actual system components with the exception of the vessel. The heat exchanger, although welded into the system, was insulated and the loop was operated isothermally. Allowable pump temperatures limited operation to 550°C. Tests were concluded by running for 100 hr at 500°C. The items that were investigated and the results are:

a. Soundness of the containment: no sodium leaks existed or developed.

b. Pump performance: flow vs pump power was satisfactory up to 550°C inlet temperature. Pump inlet pressures as low as 5 psig did not result in cavitation.

c. Heating transformer performance: this method of heating performed quite well. As a result of this test, capacitors will be installed to improve the observed 0.3 power factor.

d. Tubular electrical heater performance: the installed tubular heaters operated adequately with no burn-outs.

e. Sodium level detector performance: the prototype detector was found to be accurate and reliable and will be incorporated into the reactor loop.

f. Thermocouple behavior: thermocouples functioned properly, but those installed in wells read 30°C to 50°C higher than those held against the pipe outer surface by spring pressure. As a result, more wells are being added to the reactor loop.

g. Filling and dumping techniques: the planned procedure for filling and dumping were found to be satisfactory.

h. Insulation effectiveness: as a result of mockup loop operation, the 3 in. Superex insulation is being replaced with a 2 in. inner layer of Superex on the outside of which is a 1-1/2 in. layer of 85% magnesia.

2.7 Control System

Reactivity adjustment of the reactor is accomplished by means of control elements consisting of movable reflector sections. The control shim is the largest of the movable reflector sections, and it serves as a shutdown or scram device. It has the form of an annular cylinder, concentric with the reactor vessel. It is made of Type 430 stainless steel 20 in. o.d., 10-3/4 in. i.d., and 16 in. long. It may be raised to a position such that it surrounds the core, or lowered to a position where its effectiveness as a reflector for neutrons escaping from the core is negligible. The differential worth of the shim over the range of its 16 in. travel is about $60. The shim is shown in Fig. 2.23. It is estimated, on the basis of LCX II data, that the maximum slope of the reactivity vs shim position curve is $6/in.

Adjustments to reactor criticality finer than those effected by shim motion are made by moving four control rods; these consist of nickel cylinders 3.8 in. diam x 16 in. long which move vertically in appropriate channels provided in the shim. The range of travel of these control rods is 16 in. The worth of the rods is not known precisely, but is estimated to be $2.50 to $3.50 for each rod.

The entire control element assembly, together with the lower vessel shield, is supported below the reactor by the floor shield plug. Figure 2.24 is a cross section through the complete control assembly. Drive mechanisms for the control elements are located in the subbasement below the reactor cell and are attached to the bottom of the shield plug. All parts of the drive mechanisms are accessible in the subbasement. Figure 2.25 shows the shim assembly with the shim at mid-position.

The lower vessel shield, which is rigidly attached to the floor shield plug, locates laterally the bottom of the reactor vessel. Alignment of the shim with the reactor vessel is accomplished by the shim actuating members which pass through the lower vessel shield and the floor shield plug. These actuating rods connect the shim to its drive unit.

Fig. 2.23 Control shim.
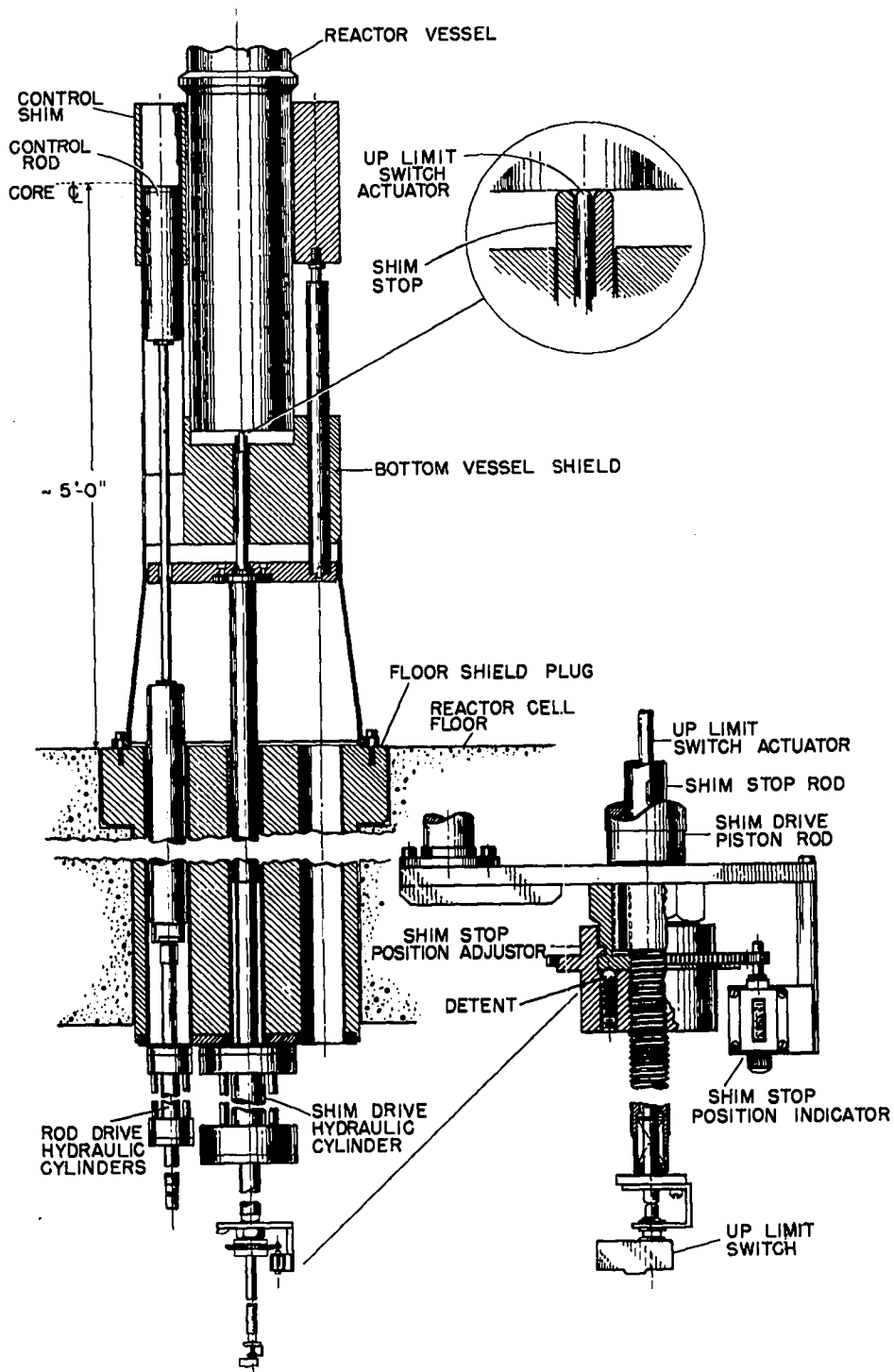
Fig. 2.24 Section through control assembly.
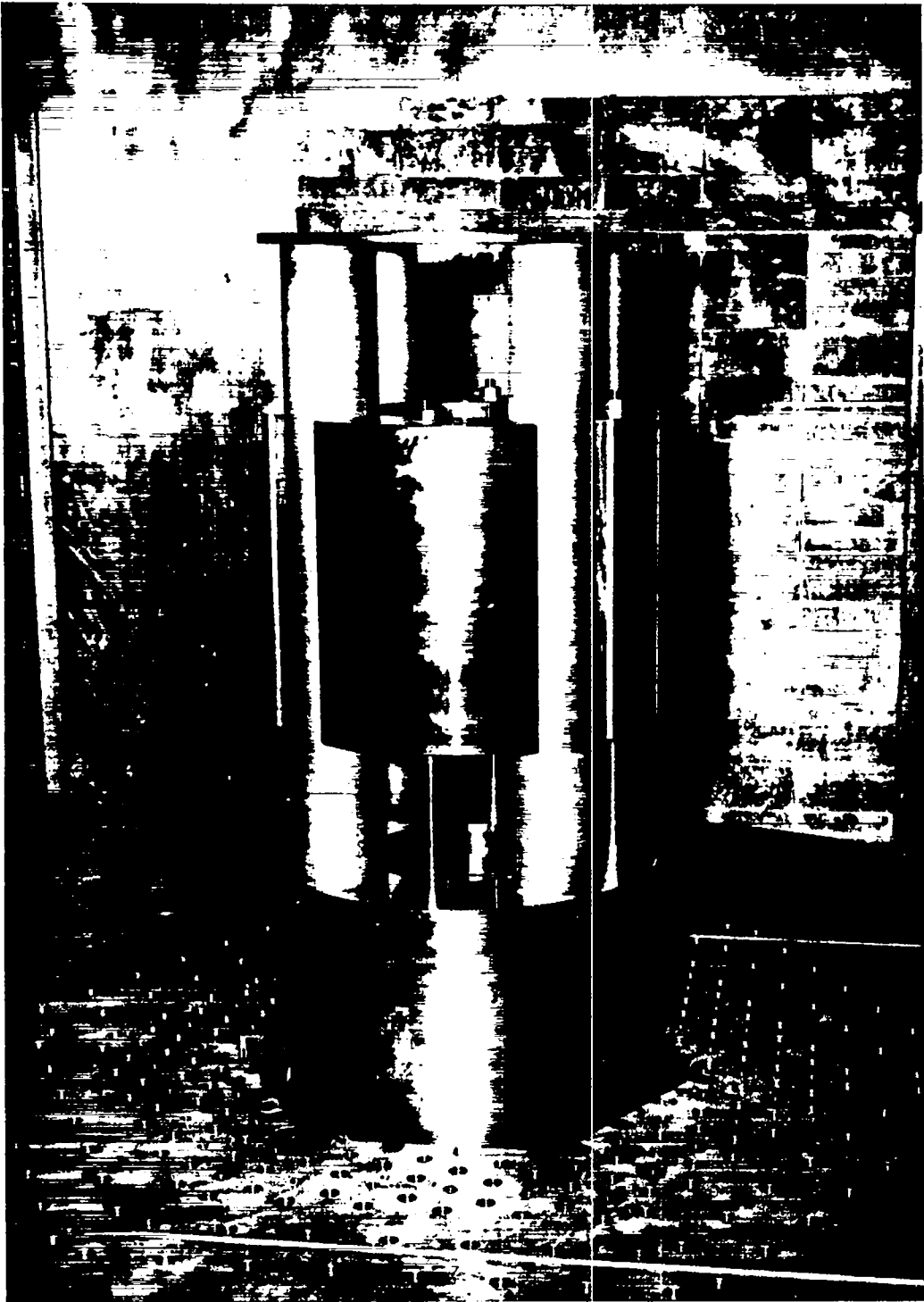
Fig. 2.25   Shim assembly.

Vertical sections of 4 in. i.d. stainless steel tube, rigidly attached to the bottom vessel shield, pass through the four channels in the shim. The control rods move inside these tubes and are guided by them.

Drive units for the shim and the control rods are double-ended hydraulic cylinders actuated by suitable hydraulic systems. The use of double-ended cylinders (with piston rods extending out both ends of the cylinders) permits gauging the position of the control elements by means of indicator mechanisms attached directly to the lower end of the piston rods.

Two separate, low pressure hydraulic systems are used; each has its own pump. One system supplies oil to the shim drive cylinder, the other supplies oil to all control rod actuating cylinders. Both pump systems are fitted with 250 psi rupture discs in the pump output lines. These prevent dangerous overpressuring of the drive units in the event of pressure regulator failure.

The hydraulic system for the shim is indicated schematically in Fig. 2.26. Figure 2.27 shows the corresponding circuit for a control rod.

Shim Drive System

The shim drive system is operated by reactor personnel from the main console. Console switches control relays for energizing the necessary valves, the pump, and the interlock circuits. All relays are located in a restricted access area. Relay power is supplied through a locked switch on the reactor console. The key may be removed from the lock only if the switch is off.

All valves operable from the console are of the solenoid-controlled, pilot-actuated type. Both normally open and normally closed valves are required in order to make the hydraulic system fail safe in the sense that power failure can result only in a shim motion which reduces reactor criticality. In no case will valve leakage result in addition of reactivity.

The reactor operator controls the shim through a four-way valve which admits oil (from the continuously operating supply pump) to the bottom or

DIAGRAM SHOWN FOR SCRAM CONDITION
ie - ALL SOLENOID VALVES
DE-ENERGIZED

NOTE
THE "4 WAY" VALVE MUST BE
ENERGIZED TO ALLOW UPWARD
MOTION OF THE SHIM

SHIM SCRAM VALVE

UP SLOW / UP FAST / DOWN FAST / DOWN SLOW

SHIM	POSITION OF VALVE				
OPERATION	#1	#2	#3	#4	#5
SLOW UP	CLOSED	CLOSED	CLOSED	CLOSED	ENERGIZED
FAST UP	CLOSED	CLOSED	OPEN	CLOSED	ENERGIZED
OFF	CLOSED	CLOSED	CLOSED	CLOSED	DE-ENERGIZED
SLOW DOWN	CLOSED	OPEN	CLOSED	CLOSED	DE-ENERGIZED
FAST DOWN	OPEN	OPEN	OPEN	CLOSED	DE-ENERGIZED
SCRAM	OPEN	OPEN	OPEN	OPEN	DE-ENERGIZED

ITEM	DESCRIPTION	REQ'D
1	PILOT OPERATED SOLENOID VALVE N.O. (OPEN WHEN DE-ENERGIZED)	1
2	" " " " " "	1
3	" " " " " "	1
4	" " " " " "	1
5	4 WAY SOLENOID VALVE	1
6	CHECK VALVE REPUBLIC NO. 483	3
7	VERNIER METERING VALVE HOKE #2PY281 & 4PY 281	4
8	RUPTURE DISC 300 PSI	1
9	HYD. PUMP UNIT GEAROTOR MOD 9101-B - 10 GAL TANK	1
10	RELIEF VALVE SET AT 150 PSI	1
11	ACCUMULATOR GREER NO 30A-5A	1
12	PRESSURE GAUGE 0-300 P.S.I.	1
13	FLOW CONTROL VALVE GATE 1" NPT	1
14	HYDRAULIC CYLINDER - HANNIFIN SPEC. 5" BORE 17" STROKE	1

JLL
PLM
JLL
V.P

TITLE
HYDRAULIC SCHEMATIC
LAMPRE I
SHIM CONTROL

37-60688   C2

Fig. 2.26   Schematic of shim hydraulic system.
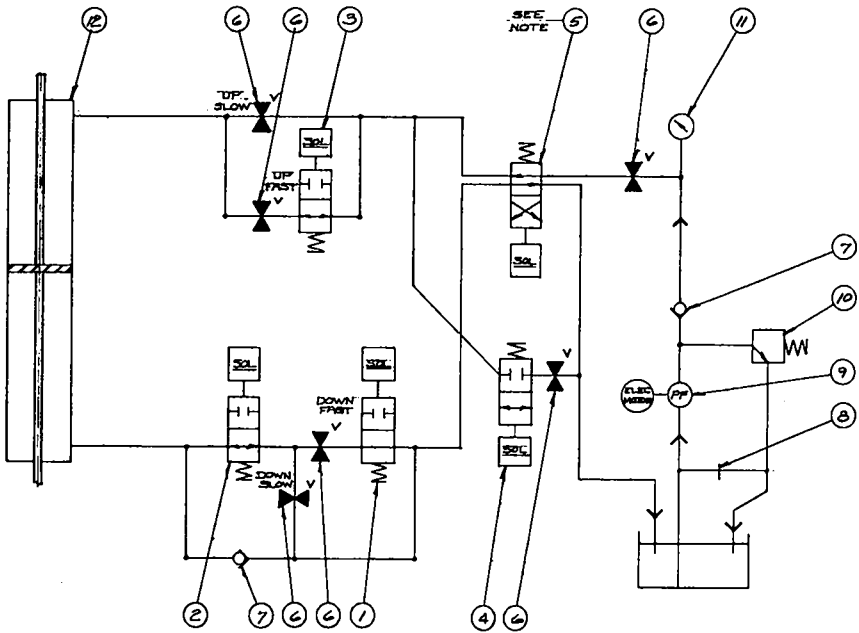
DIAGRAM - SHOWN FOR SCRAM POSITION
I.e. - ALL SOLENOID VALVES DE-ENERGIZED

NOTE
THE 4 WAY VALVE MUST BE ENERGIZED TO ALLOW UPWARD MOTION OF THE CONTROL ROD

CONTROL ROD	POSITION OF VALVE				
OPERATION	#1	#2	#3	#4	#5
SLOW UP	CLOSED	CLOSED	CLOSED	OPEN	ENERGIZED
FAST UP	CLOSED	CLOSED	OPEN	OPEN	ENERGIZED
OFF	CLOSED	CLOSED	CLOSED	OPEN	DE-ENERGIZED
SLOW DOWN	CLOSED	OPEN	CLOSED	OPEN	DE-ENERGIZED
FAST DOWN	OPEN	OPEN	OPEN	CLOSED	DE-ENERGIZED
SCRAM	OPEN	OPEN	OPEN	CLOSED	DE-ENERGIZED

PART	DESCRIPTION	REQ'D
1	PILOT OPERATED SOLENOID VALVE N.O. (OPEN WHEN DE-ENERGIZED)	1
2	" " " " " " " "	1
3	" " " " " " " "	1
4	PILOT OPERATED SOLENOID VALVE N.C. (CLOSED WHEN DE-ENERGIZED)	1
5	4 WAY SOLENOID VALVE	1
6	VERNIER METERING VALVE HOKE # 2PY281 & 4PY281	6
7	CHECK VALVE REPUBLIC No. 483	2
8	RUPTURE DISC 300 PSI	1
9	HYD PUMP UNIT - GEAROTOR MOD. 9101-B-10 GAL TANK	1
10	RELIEF VALVE SET AT 150 P.S.I.	1
11	PRESSURE GAUGE 0-300 P.S.I.	1
12	HYDRAULIC CYLINDER - HANNIFIN SPEC. 3 1/4 BORE 17" STROKE	1

HYDRAULIC SCHEMATIC
LAMPRE I
CONTROL ROD

37Y-60688

Fig. 2.27 Schematic of control rod hydraulic system.

the top of the shim drive cylinder to produce upward or downward motion of the shim. Shim position may be changed in increments as small as 0.020 in.

The shim may be moved at either of two speeds. The operator selects the desired speed by appropriate manipulation of the console shim control switch. Speed control is accomplished by regulating oil flow to the cylinders through two parallel lines. Each of the lines is fitted with an adjustable throttling valve and a solenoid controlled flow shutoff valve. If a slow rate of shim motion is desired, the slow speed channel is opened; the flow of oil in it occurs at a rate fixed by the setting of the throttling valve. When the fast rate of motion is required, both oil channels are opened; the total flow rate is then dependent on the setting of both throttling valves. The throttling valves are preset to give flow rates compatible with the desired maximum rate of reactivity addition. These rates cannot readily be altered by the reactor operator, since the valves are located in a locked area remote from the control room.

Shim position is indicated on a console-mounted digital register reading to 0.01 in. The register is driven through synchros by a gear train actuated by the shim cylinder piston rod. Electrical power for the synchro system is independent of main control console power, and is left on continuously whether the reactor is operating or not. The occurrence of power failure (no voltage) in the synchro system is indicated on the control room annunciator panel.

In its up position, the shim is in contact with a mechanical stop. When contact is made with the stop, a limit switch is actuated and pump pressure is continuously applied to the shim drive cylinder to hold the shim up against the mechanical stop. Should the shim be lowered by as little as 0.020 in. (either by the operator or through system malfunction) the limit switch is deactivated. The shim then cannot be reinserted except in accordance with the normal sequenced startup procedure.

The shim stop was designed so that variations in reactor temperature would not significantly affect the relative position of the shim and the reactor core. This was accomplished by limiting the upward shim motion with

a stop which abuts directly on the bottom of the reactor vessel (Fig. 2.24). As the reactor vessel temperature increases, for instance, the core, and the bottom of the vessel, move downward because of the vessel's thermal expansion; because of the shim stop mechanism, the shim is pushed down (against the hydraulic system pump pressure) by nearly the same amount as the change in core position. With the compensation provided by this shim stop design, the change in reactivity which can be produced by temperature variations in the reactor vessel should not exceed 0.1 $\not{c}/^{o}$C. The precise value of this positive contribution to the overall temperature coefficient of reactivity cannot be predicted until reactivity as a function of shim position has been measured during the initial critical experiments.

The position of the shim stop is adjustable in increments of 0.025 in. over an 8 in. range. This range of settings for the up position of the shim will be used to accommodate variations in core loading, and also during intercalibration of the shim with the control rods. Adjustment of the stop is performed in the restricted access subbasement under the reactor cell. Design of the assembly is such that changing the shim stop setting automatically repositions the up limit switch (Fig. 2.24).

The reactor is scrammed by rapidly lowering the shim. This is accomplished by opening the scram valve located in a line connecting the top and bottom ends of the shim drive cylinder. When the valve is opened, the differential pressure across the piston is reduced to approximately zero, and the weight of the shim and its supporting members ($\sim$ 1100 lb) forces the piston down. Shim position as a function of time after the scram signal appears at the valve solenoid is shown in Fig. 2.28. Since the scram valve is a normally open type, electrical power failure in the control circuits automatically lowers the shim. An electrical power failure (or a scram signal) results in a valve configuration such that oil can escape from the bottom of the cylinder and return to the oil storage reservoir. This mechanism
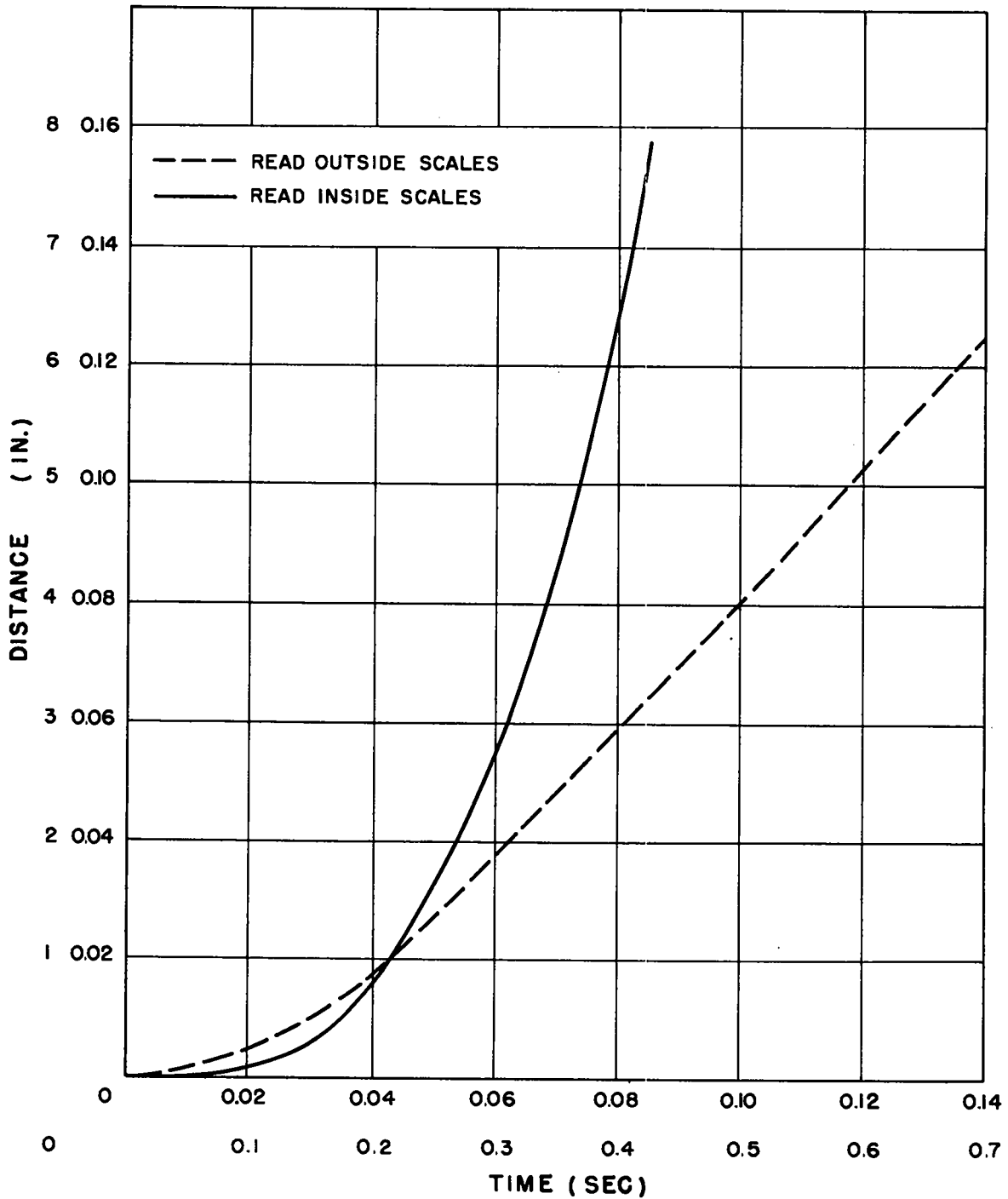
Fig. 2.28   Shim position vs time after scram signal.

contributes slightly to the rate of shim drop which follows a power failure or a scram signal, but oil flow through the scram valve is by far the more important factor determining shim drop time.

A gas-ballasted accumulator is fitted to the shim drive hydraulic system; the oil in this chamber is held at pump pressure so long as the pump is operating. Should the scram valve ever fail to open in case of power failure or receipt of a scram signal, or should the shim fail to drop freely during a scram, full accumulator pressure builds up above the shim drive piston. The resultant force tending to lower the shim will then be about twice that due to the weight of the shim assembly. If the scram valve sticks in the closed position, this extra force on the piston will be sufficient to lower the shim at a rate about equal to that normally obtainable by turning the console shim control switch to "fast down."

Control Rod Drive System

The drive system for the control rods is similar to that used for the shim except for the differences listed below:

a. There is no provision for scramming the control rods. Power failure does, nevertheless, result in the rods being withdrawn as oil is forced from the drive cylinders by the weight of the rod assemblies.

b. No accumulator is fitted to the pump system which supplies oil to the four rod drives.

c. The stops which determine the up positions of the rods are not adjustable.

d. There is no provision for temperature-compensated stops of the type used for the shim since the control rods reactivity worth is much less than that of the shim.

e. A rod fully inserted to the up position is held there by continuously supplied hydraulic system pressure, just as in the case of the shim. However, at partial insertion a rod is held up by the closing of a "lockup" valve in the oil line leading from the bottom

end of the hydraulic cylinder. The position of other control valves in the system is such that should the lockup valve leak, the control rod will be withdrawn, rather than inserted.

    f. Rates of rod motion will be adjusted so that reactivity insertion rates will be 5 $\cancel{c}$/sec and o.5 $\cancel{c}$/sec, respectively, for fast and slow rod speeds.

    g. Control rod position is displayed on a digital register reading to 0.001 in.

Control System Sequencing Interlocks

    Electrical interlocks permit control element movement only in a specified sequence. If the reactor operator deviates from the proper sequence, control elements either will not move or will be withdrawn.

    Restrictions imposed by the interlocks are listed in Section 2.5.

2.8 Capsule Charger

    Fuel capsules are loaded into or removed from the reactor by the capsule charger. The charger is bolted to the top of the 10 in. vessel closure valve and consists of a vertical lift unit, horizontal transfer unit and vertical transfer unit. The three units are contained in a housing which is gas tight and filled with helium. The housing is necessary to maintain cover gas purity when the closure valve is open and also to contain alpha contamination that would result from handling a ruptured capsule. Figure 2.29 is a pictorial representation of the charger; Fig. 2.30 a photograph of the housing.

    The sequence of removing a capsule begins by equalizing cover gas and housing pressures after which the closure valve is opened. The "grabber" of the vertical lift unit is capable of motion in a cylindrical coordinate system and is positioned by changing its r, θ and z location. It is moved so as to engage its bayonet socket with the
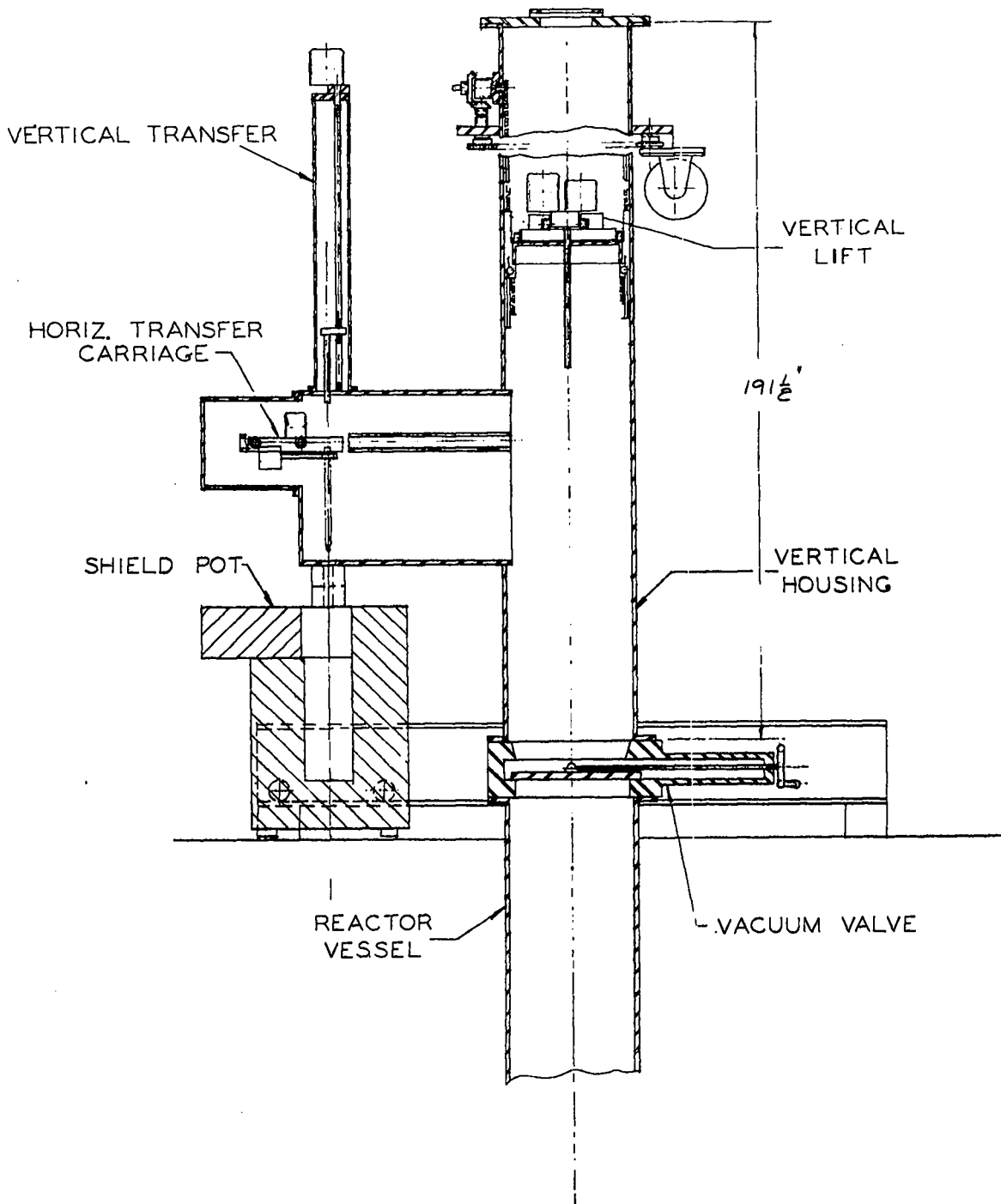
Fig. 2.29 Capsule charger schematic.
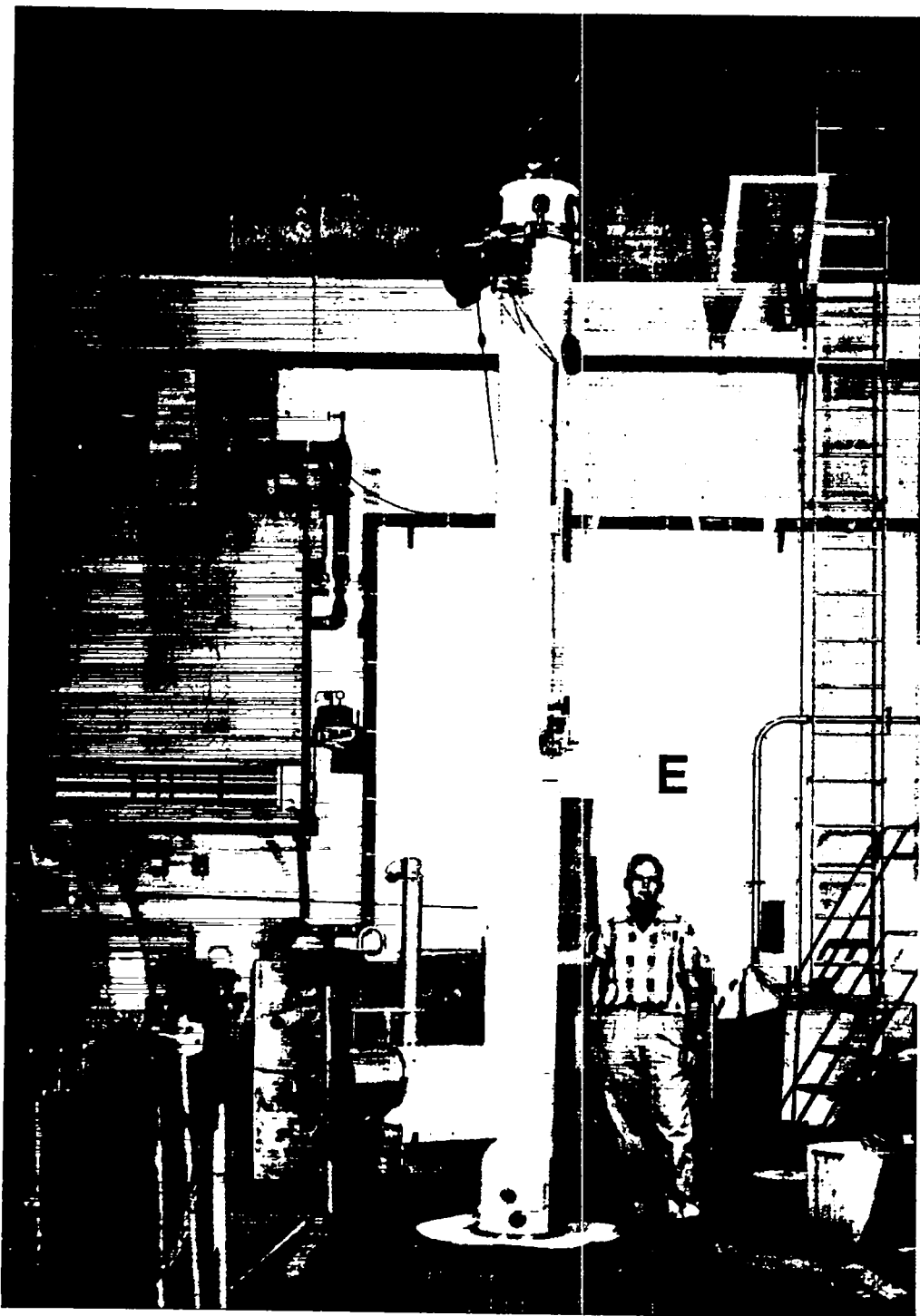
Fig. 2.30 Capsule charger housing.

mating end of the desired capsule handle. Alignment for engagement is accomplished visually by means of two periscopes which extend from windows in the housing through the lead shield.

After engagement of the bayonet socket, the vertical lift unit raises the fuel element to a station where the capsule is unscrewed from the handle. The splined locator section on the handle is rotated by a motor on the horizontal transfer unit while a flat on the capsule top is restrained by a stationary wrench. When the capsule is free of the handle, the horizontal transfer unit moves it to a position above a shield pot which is sealed to the transfer port. At this point the vertical transfer unit is engaged, the horizontal transfer unit disengaged and the capsule lowered into the shield pot. Port valves are closed and the shield pot disconnected from the port. Loading is done by reversing the sequence of events.

Power for vertical motion of the vertical lift unit is supplied by a hydraulic motor. Hydraulic pressure to the motor is adjustable and, during normal operation, will be only high enough for the unit to exert a force of about 30 lb on a handle. The components are designed, however, to withstand forces required to exert a 1000 lb pull in case a sticking handle makes it necessary. An 8 in. lead shield surrounds the bottom of the housing and will reduce the maximum dose rate outside the shield to at least 50 mr/hr. There is enough clearance between shield and housing to accommodate housing movement arising from thermal expansion of the vessel. The expansion is expected to be less than 1/2 in. A balcony about 11 ft above the transfer area floor permits viewing of charger components through housing windows at that level. Maintenance of external parts of the vertical lift mechanism can be performed from the balcony.

2.9 Helium and Gas Disposal System

The sodium cover gas is high purity helium. A NaK bubbler is used to remove water vapor and oxygen from helium before it is admitted to the cover gas volume. After purification, the helium contains less than 10 ppm impurities. Figure 2.31 is a schematic of the helium and gas disposal system.

If a capsule ruptures, fission gas escapes into the sodium coolant and will collect in the cover gas either in the vessel or surge tank. The gas disposal system permits transferring this radioactive gas to a holdup tank for decay and controlled release to the atmosphere. The holdup tank, with a capacity of 140 ft^3, is kept evacuated by a small vacuum pump. Fission gas activity in the cover gas volume can be reduced further by evacuating the volume with a mechanical vacuum pump and flushing with helium. A radiation alarm having a detector on the pressure-equalizing line will warn personnel of radiation coming from cover gas. All operations necessary for gas disposal can be performed from the control room.

As a part of the helium system there is a vacuum diffusion pump for evacuating and flushing cover gas and charger volumes. Undesirable gases coming from components within the capsule charger housing could diffuse into the vessel cover gas during periods when the closure valve is open and, although these components are being selected so as to constitute a minimum source of gas impurity, it may be necessary to flush the housing just prior to charger operation. Charger gas will be analyzed after the helium system and charger have been completed and the necessary measures for maintaining charger gas purity will be determined.

VALVE

CHECK VALVE

DPI DIFFERENTIAL PRESSURE
INDICATOR

PVG PRESSURE-VACUUM
GAUGE

VG VACUUM GAUGE

RELIEF VALVE(25) SET
PRESSURE

PTD PRESSURE TRANSDUCER

VS VACUUM SWITCH

REMOTE OPEPATED VALVE

DPI

CAPSULE CHARGER
HOUSING

CAPSULE
CHARGING
VG PORT

VG

GATE
VALVE

INNER
LINER

CORE

HELIUM 10 PSIG

PVG 45 VENT TO
CELL

HELIUM 15 PSIG

25

PVG

PVG

VAC PUMP

PVG

PVG

PVG

VAC
PUMP

PTD

SODIUM
SURGE
TANK

PRESSURE EQUILIZATION
LINE

PTD

SODIUM
DUMP
TANK

AIR FROM CELL

TO SGUBBER
AND FILTERS

TO SCRUBBER
AND FILTERS

VAC PUMP

VS

TRAP

PVG PTD

V-1

PHASE
SEPERATOR

V-3

PHASE
SEPERATOR

AIR FROM HOODS
IN LAB "A"

T-7

UNDERGROUND GAS
HOLDING TANK

Fig. 2.31 Schematic of helium and gas disposal system.

2.10 Shielding

Shielding requirements were arrived at by calculation of the radiation dose at selected points in the vicinity of the reactor for specified operating and/or shutdown conditions. Calculations were also made to determine the dose rates, due to induced Na^{24} activity, in areas adjacent to the sodium loop. Before proceeding to a detailed discussion of the reactor shielding the following should be noted. Since the reactor is situated in close proximity to some areas where personnel will be normally working, it is required that the shielding provided afford adequate radiation protection to personnel in these areas. Examples of such areas are the control room and the room above the reactor cell (see Figs. 2.32, 2.33, and 2.34). Therefore, during initial low power tests, a radiation survey of these areas will be made; from the survey results the adequacy of the shielding at 1 Mw power operation will be evaluated. Additional shielding will be installed where required before operation of the reactor at full power.

Radial Shield Towards Control Room

In the radial direction, the shielding between the reactor and control room consists of 3-1/2 ft of borated graphite plus 8 in. lead plus 5-1/2 ft of ordinary concrete. The borated graphite shield is made up of graphite cylinders 3-5/8 in. o.d. by 72 in. long containing an average of 0.4% by weight natural boron. Forced air cooling is provided to remove the 25 kw of heat which, it is estimated, will be deposited in the shield at 1 Mw operation. The graphite in the high flux region will be maintained at 150°C to 200°C to minimize radiation damage.

Calculations indicate that the neutron flux at the outer radius of the borated graphite shield will be ~ 10^9 neutrons/cm² sec with an average energy of 0.3 Mev. The lead and concrete shields will reduce

8' LEAD WALL

REACTOR VESSEL

DECONTAMINATION
PIT

8" LEAD WALL

CONTROL ROOM

RACKS

SODIUM EQUIP.
ROOM

CONSOLE

12" LEAD
WALL

RACKS

HEAT EXCHANGER
PIT

DUMP TANK
PIT

8" LEAD WALL

ELEC. EQUIP.
ROOM

EARTH
FILL

BORATED GRAPHITE
SHIELD

REMOVABLE NEUTRON
SHIELD

0 3 6
SCALE IN FEET
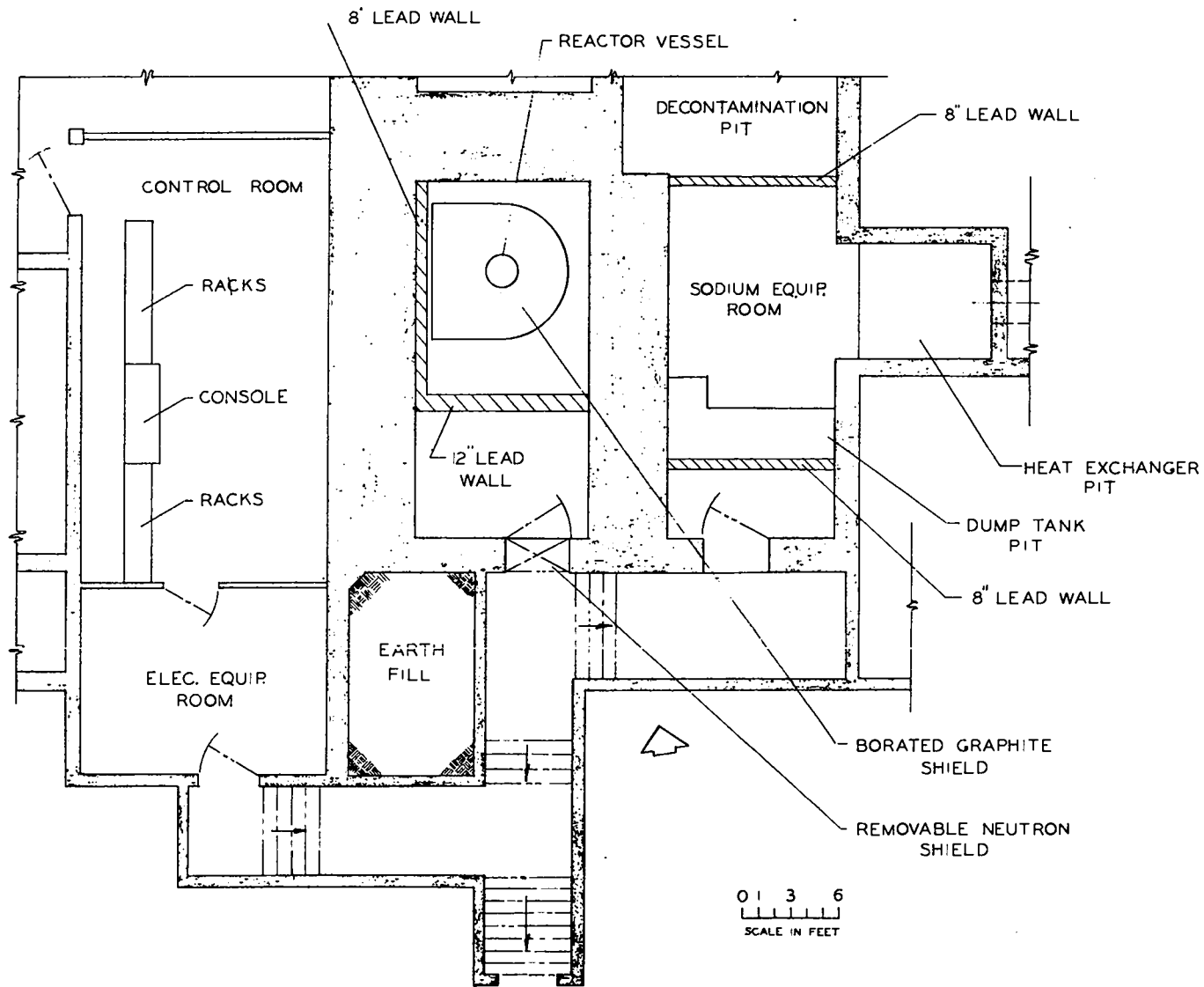
Fig. 2.32 Horizontal cross section showing reactor shielding.
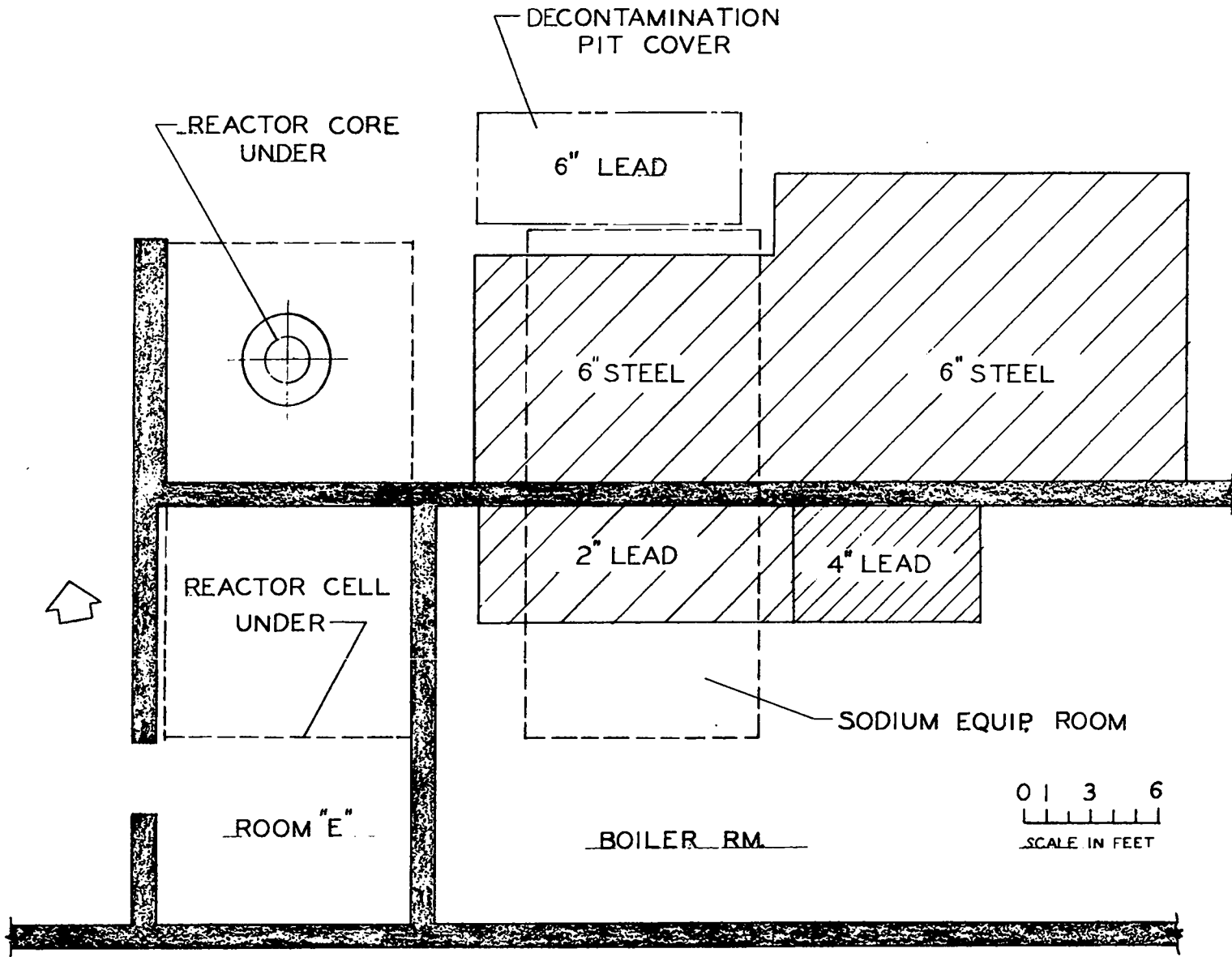
Fig. 2.33 Plan view of shielding on floor in area above reactor.

SODIUM EQUIP. ROOM

CEILING SHIELD PLUG

14" STEEL COVER

6" STEEL

CENTER OF
REACTOR CORE

BORATED
GRAPHITE

HEAT EXCHANGER PIT

6" LEAD

FLOOR SHIELD PLUG

SUB-BASEMENT

PLATFORM

0 1   3   6

SCALE IN FEET
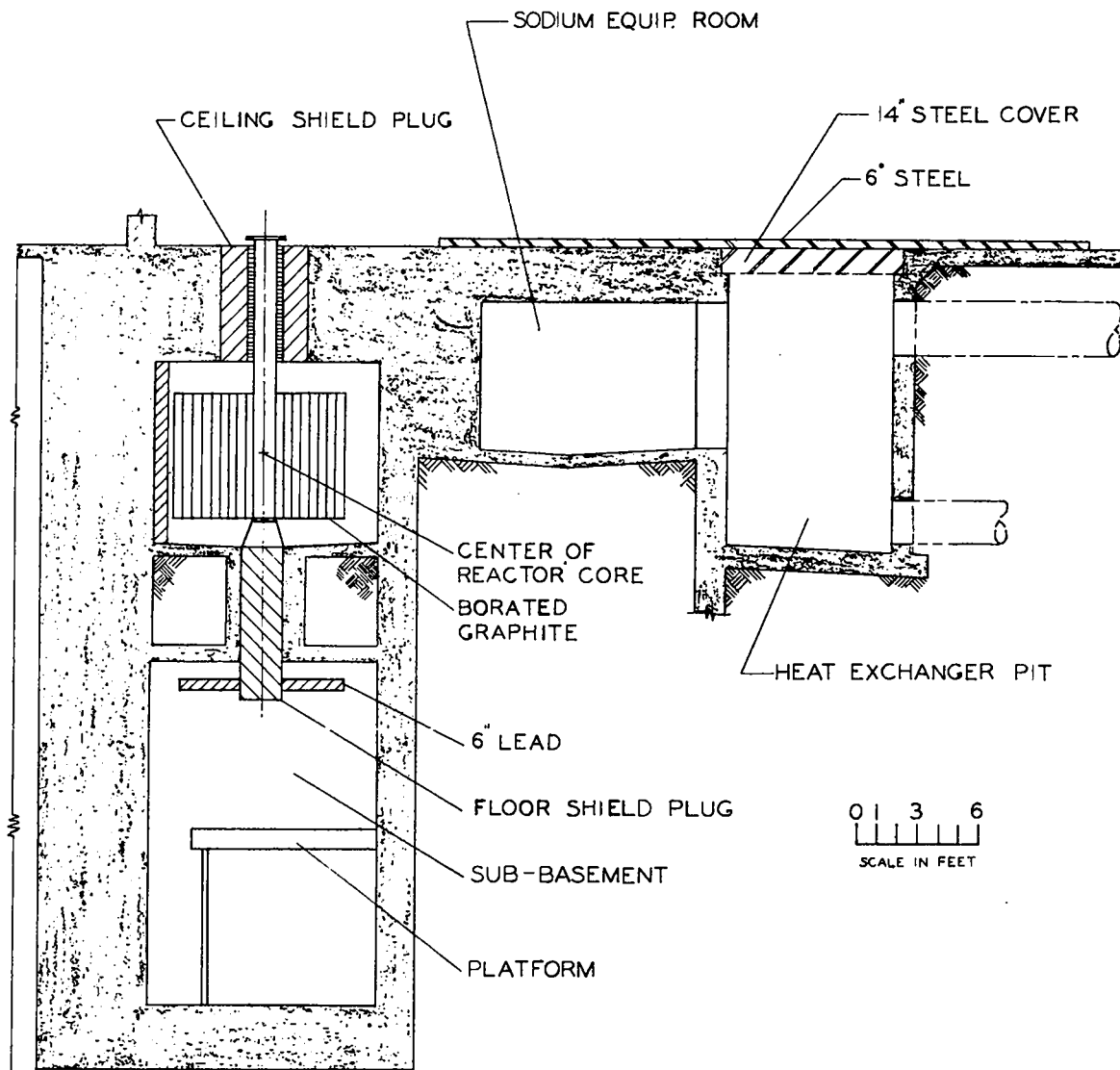
Fig. 2.34 Vertical cross section showing core shielding.

the residual gamma ray and neutron flux to below tolerance values in the control room. A removable neutron shield, probably heavy concrete blocks, will be placed in the entrance to the reactor cell. During operation, access to the area south of the reactor cell and sodium equipment room will be allowed only with the approval of the health physics personnel.

Shielding Below Reactor

The main shield directly below the reactor is provided by 16 in. of iron plus a 7 ft long floor shield plug. The bottom 2 ft of the floor shield plug is filled with lead shot. The remaining volume is filled with magnetite aggregate having a density of ~ 230 lb/ft^3. The floor shield plug is provided with holes through which the shim and control rods are moved. Calculations indicate that access to the sub-basement will not be possible even during low power operation. However, immediately after shutdown, from three-month operation at 1 Mw, the gamma level in the subbasement directly below the reactor is calculated to be 2 mr/hr. Dose rates in the area not shadowed by a 6 in. lead shield on the subbasement ceiling are estimated to be as high as several hundred mr/hr. A radiation survey will be made to check the accuracy of the calculations prior to full power operation. Since the control mechanisms will be located directly below the reactor, no difficulty in maintenance of these components, after shutdown, is anticipated. The control system hydraulic pumps are located at a point where inspection and maintenance is possible during full power operation.

Shielding Above Reactor

As mentioned in Section 2.2 of this report, the fuel capsule handles constitute the upper reflector and part of the radiation shield for the reactor. These parts provide about 9 ft of iron shielding above

the reactor core. The fuel transfer area will be protected by the cell ceiling (5-1/2 ft of concrete) or the ceiling shield plug. The latter consists of a cylinder 47 in. o.d., 18 in. i.d. and 4-1/2 ft long filled with ferrophosphorous concrete, the inner 3-1/2 in. thick annulus being filled with stainless steel shot. Since it is difficult to estimate neutron streaming along the gaps in the graphite shield, the adequacy of the concrete shielding above the graphite region surrounding the reactor has not been determined. Additional shielding can be placed on the transfer area floor around the vessel top if the radiation survey indicates a need for such shielding. Access to this area is required only during fuel charging operations, a procedure undertaken while the reactor is shut down.

Although not shown in Fig. 2.34, the capsule charger housing extends above the transfer area floor. Shielding will be provided around the housing to protect personnel from fission product decay gammas during removal of a fuel capsule from the reactor to a transfer shield pot.

Shielding for Sodium Loop

The total volume of sodium in the LAMPRE I system is ~ 7.5 ft^3. Of this total, 3 ft^3 is contained in the sodium equipment room piping, 2 ft^3 in the piping from the reactor to the sodium equipment room and 1 ft^3 in the heat exchanger. The equilibrium N^{24} activity induced in the sodium is calculated to be 6 mc/cm^3. In estimating the radiation levels in the vicinity of the sodium system the coolant loop was divided into four parts, each part being considered as an independent source. The four sources considered were: sodium equipment room piping, the surge tank, the heat exchanger, and the dump tank.

Radiation levels were calculated for the block storage and boiler room areas, and for the sodium equipment room. Typical values for the gamma ray dose rates above the sodium equipment room (2-1/2 ft normal concrete ceiling) are 7 mr/hr with 6 in. of steel and 40 mr/hr with 2 in.

of lead. Dose rates 1 ft from the 8 in. lead walls at the north and
south ends of the sodium equipment room ~ 50 mr/hr. The shielding for
the sodium loop is shown in Figs. 2.32, 2.33, and 2.34.

The 40 mr/hr dose rate estimated for the boiler room is con-
sidered acceptable since routine boiler servicing requires that
personnel enter the room for only a few minutes during each eight-
hour shift.

3. SITE INFORMATION

3.1 Location of Site

The site at which the reactor is being installed, TA-35, is located relative to the town site and other laboratory sites in Fig. 3.1. Circles of 1/2, 1, 1-1/2, 2, and 3 miles radii with TA-35 as the center are shown in this figure. The three mile zone encloses most of the technical areas and all of the town site with the exception of a small portion of the residential section. No areas open to the public, except a short section of highway, lie within the one mile zone.

Access to the site is limited to persons having a technical area badge. Access to areas within the site that are near the reactor installation is controlled outside the building by fences and gates and inside by the arrangement of lockable doors.

3.2 Information on the Surrounding Areas

Listed in Table 3.1 are the numbers and names of Technical Areas now assigned to the Laboratory. Their location is shown on Fig. 3.1. Los Alamos Scientific Laboratory operating group designations have been indicated in parenthesis.
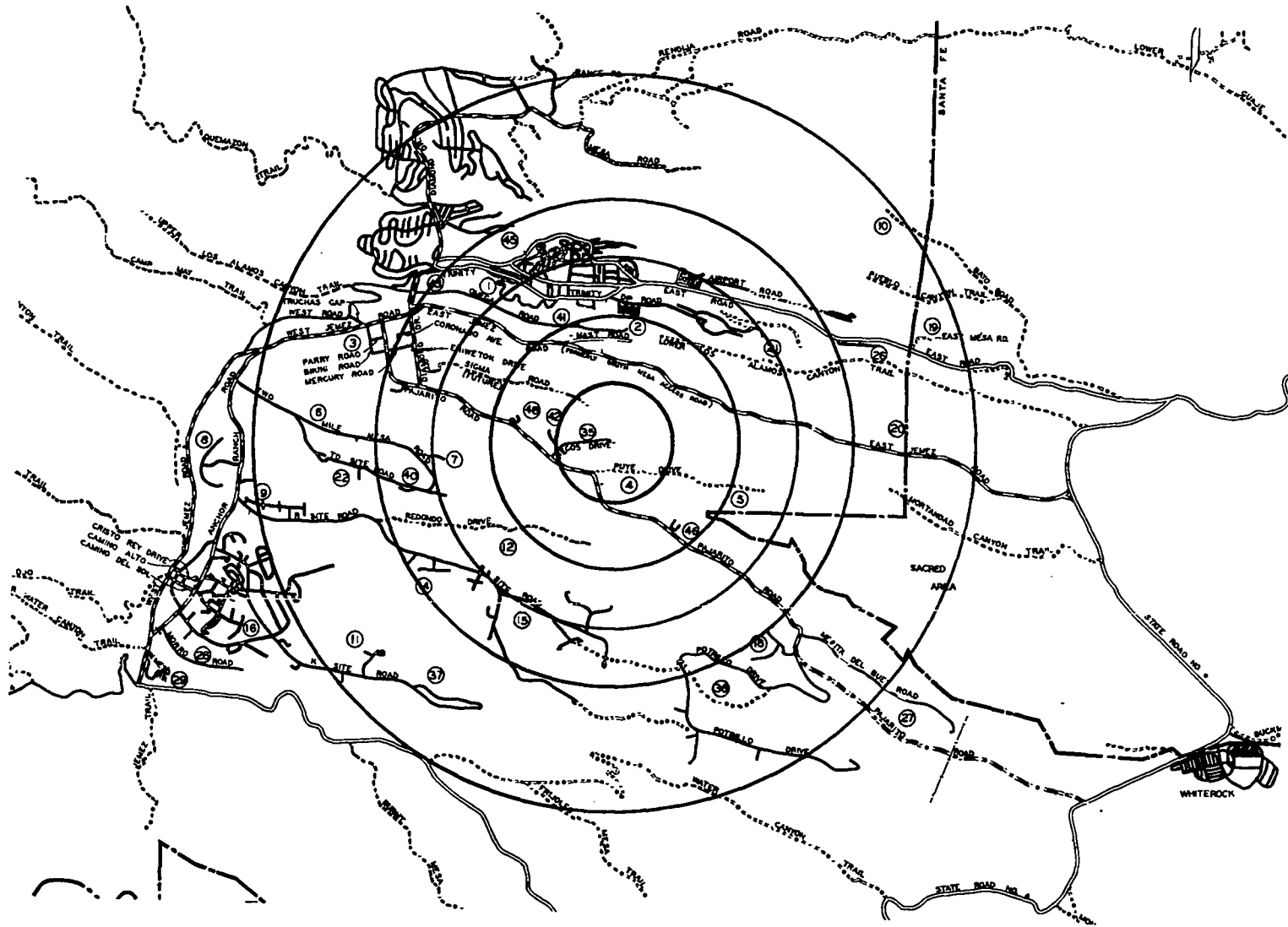
Fig. 3.1 Map of Los Alamos and Laboratory sites.

Table 3.1
LOS ALAMOS SCIENTIFIC LABORATORY SITE LOCATION

TA-1	Former Main Technical Area	TA-20	Sandia Canyon Site (Abandoned)
TA-2	Omega Site (P-2)	TA-21	DP-Site (1) DP-East (CMB-3, 7) (2) DP-West (CMB-4, 8, 11)
TA-3	South Mesa Site (Main Technical Area)	TA-22	TD-Site (GMX-7, CMB-6)
TA-4	Alpha Site (Abandoned)	TA-26	D-Site (ADP-SF)
TA-5	Beta Site (Abandoned)	TA-27	Gamma Site (Abandoned)
TA-6	Two Mile Mesa Lab. (GMX-7)	TA-28	Magazine Area A (GMX-3)
TA-7	Gomez Ranch Site (GMX-7)	TA-29	Magazine Area B (GMX-3)
TA-8	Anchor Site West (J-13, GMX-1); GMX-1 Area also known as GT-Site	TA-35	Ten Site (K-DO, K-1, K-2, K-3, CMB-DO)
TA-9	Anchor Site East (GMX-2)	TA-36	Kappa Site (GMX-7)
TA-10	Bayo Canyon Site (GMX-5, H-1)	TA-37	Magazine Area C - PMA (GMX-3)
TA-11	K-Site (GMX-3)	TA-40	DF-Site (GMX-7)
TA-12	L-Site (Abandoned)	TA-41	W-Site (W-1, W-7)
TA-14	Q-Site (GMX-2)	TA-42	Incinerator Site (H-1)
TA-15	R-Site (GMX-4)	TA-43	Health Research Lab. (H-4, H-5, H-DO Property, D-2)
TA-16	S-Site (Includes TA-13, 24, and 25)	TA-45	WD-Site (H-1, H-7)
TA-18	Pajarito Lab. (N-2, N-4)	TA-46	WA-Site (N-DO, N-1, N-3)
TA-19	East Gate Lab. (H-4)	TA-48	Radiochemistry Site (J-11)

3.3 Population

The number of people expected to be included within the circles on Fig. 3.1 are tabulated below.

Table 3.2
POPULATION WITHIN RADIAL ZONES

Zone (miles)	Installations	Number of People
0 - 0.5	TA-35	110
0.5 - 1	TA-2, TA-42, TA-46, TA-48	245
1 - 1.5	TA-7, TA-21, TA-41	435
	Community Center Shopping District, Residential Areas	3325
1.5 - 2	TA-1, TA-3, TA-14, TA-15, TA-40, TA-43, TA-45	1750
	Residential Areas	3325
2 - 3	Various Technical Areas	500
	Residential Areas	6650

The figures for residential areas were computed by multiplying the total residential population by estimated percentages. The residential population of Los Alamos is about 13,300; it is estimated that about 1000 people commute to Los Alamos and are present during working hours. University of California employees number about 3200 and Zia employees about 1200. Zia personnel include housekeeping people and craftsmen. There are, then:

People in Los Alamos area	14,300
People in technical areas and associated installations	4,400

3.4 Meteorological Data

Wind Velocity and Direction

Table 3.3 lists the surface winds at Los Alamos. The table is based on 35,000 observations over a four year period.

Table 3.3

WIND VELOCITY

	Direction From Which Wind is Blowing (%)								Mean Speed (mph)	Max. Speed (mph)
	N	NE	E	SE	S	SW	W	NW		
January	4	4	5	6	16	28	19	18	6	68
February	8	5	5	6	15	23	19	18	5	72
March	5	4	5	5	11	26	27	18	6	87
April	6	6	5	7	10	24	28	13	6	81
May	3	4	5	4	16	30	27	12	6	66
June	2	4	3	5	16	29	26	15	6	59
July	5	5	4	9	13	25	20	17	6	49
August	5	5	4	9	15	22	24	8	6	50
September	3	7	4	6	9	27	28	16	6	51
October	4	5	4	8	9	27	21	23	6	65
November	6	7	7	11	5	14	20	31	6	60
December	7	6	6	8	8	17	22	25	6	57
Annual	5	5	5	7	12	24	23	18	6	87

Thunderstorm Frequency

The frequencies of thunderstorms listed below are based on observations over a 20 year period.

	October through June	July	August	September
Frequency range	Negligible	8-20	8-20	3-14
Mean number	Negligible	12	15	9

Precipitation Data

The data in Table 3.4 below is based on observations over a 20 year period.

Table 3.4

PRECIPITATION (INCHES)

January	0.85	July	2.70
February	0.69	August	3.91
March	0.85	September	2.31
April	1.06	October	1.38
May	1.40	November	0.68
June	1.42	December	0.85
		Annual	18.10

3.5 Geology

Hydrology of the Los Alamos Area

A study of the hydrology of the Los Alamos area has been made as part of a survey to locate suitable well locations for community and laboratory water supply.* LAMPRE I operation is expected to have no effect on ground water contamination, since no waste products will be released intentionally except gases, and no mechanism has been proposed for accidental introduction of radioactive materials to ground water.

Seismicity of North Central New Mexico**

About 99% of the 575 earthquakes recorded in New Mexico during the last century have originated in a narrow belt of the Mexican High-land section of the Basin and Range province adjoining the southeastern border of Colorado Plateau province. About 94% have originated at the

---

*Theis, C. V., "Geologic Background of Waste and Water Supply Problems at Los Alamos," Paper No. 1, TID-460.

**This information taken from Los Alamos Scientific Laboratory report LAMS-1611(Del.), December 2, 1953.

northern end of this belt in the 75 mile strip along the Rio Grande Valley between Socorro and Albuquerque. In this region, earthquakes have been recorded in 25 different years between 1855 and the present.

Notable features of these Rio Grande Valley earthquakes include:

a. Occurrence in swarms; daily for three weeks in 1935 at Belen; daily for three months in 1893 at Belen and Los Lunas; and daily for six months in 1906 at Socorro.

b. Maximum noctural frequency; 69% at night; 31% during the day.

c. Maximum annual frequency of 82% in the July to December period; only 18% in the January to June period.

d. Fairly large areas affected by several of the shocks; a few have been felt over areas ranging from 20,000 up to 186,000 square miles.

e. Occasional property damage and local panic, but no loss of life.

f. Numerous strong to moderately strong shocks; a few very strong shocks. Using the Rossi-Forel intensity scale, there have been four quakes of intensity VIII plus to IX, six of intensity VIII, 15 of VII, 27 of VI, and 33 of V.

Most of the Rio Grande earthquakes have originated in the Socorro-Belen region; only a few have originated near Albuquerque. Recent shocks originating at Albuquerque include one of intensity VI on December 3, 1930; lesser shocks on January 27 and February 3, 1931; and finally one of intensity VII on February 4, 1931. Few earthquakes have originated in New Mexico north of Albuquerque.

One of New Mexico's greatest earthquakes occurred at Cerrillos on May 28, 1918, at 5:30 a.m. A remarkable feature is that although it was of intensity IX plus at Cerrillos the force faded unusually rapidly so that it was felt over an area of only about 45,000 square miles. However, plaster fell in several buildings at Santa Fe, and people were awakened at Espanola and several places in that vicinity.

Other recent earthquakes and their intensities were: August 12, 1924, a shock of intensity VI near Valmore, northeast of Las Vegas; February 12, 1931, a slight shock (IV?) at Las Vegas; January 28, 1939, a slight shock of III at Chama; March 11, 1948, 21:31 MST, a moderately strong quake, of intensity VI to VI plus, originating in the northwest corner of the Texas Panhandle near Dalhart, was felt over an area of 50,000 square miles in parts of five states. In northeastern New Mexico it was of intensity VI; at Raton, V; at Cimarron, Wagon Mound, and Tucumcari, about IV; apparently it was not felt at Eagle Nest or Las Vegas.

It should be stressed that, although the entire state of New Mexico is generally placed in the next risk zone below California, the most seismic part of New Mexico is the Socorro-Belen zone. Albuquerque is much less seismic, but some of the Socorro and Belen quakes have been felt in Albuquerque.

Seismologists generally believe that a region of high frequency with quakes of intensity less than VIII may be fairly safe because these frequent shocks act as a safety valve and relieve earth stress before it can accumulate in force sufficient to produce a violent shock of intensity IX or X.

It is quite likely that the Socorro-Albuquerque zone will experience many more earthquakes. A swarm, such as the one Belen had in 1935, may be expected any time in this zone. It is unlikely that many of these shocks will be very strong as far north as Los Alamos. The Socorro shock of November 15, 1906, may have attained intensity IV at Los Alamos. The Socorro shock of July 16, 1906, ranked V at Santa Fe, and possibly IV to V at Los Alamos.

Only one quake is recorded for Cerrillos but that one developed intensity IX plus at the epicenter, intensity VII to VIII at Santa Fe, VI to VI plus at Pena Blanca and Espanola, and presumably attained intensity VI at Los Alamos. It must be kept in mind that Los Alamos is only 33 miles from Cerrillos and that for some reason the 1918 quake faded unusually rapidly. A deeper-focus quake at Cerrillos of intensity

IX might not fade so rapidly, in which event Los Alamos might experience a shock of intensity VII.

It is unlikely that any earthquakes originating in either Arizona or Colorado will be perceptible at Los Alamos.

It is possible (but scarcely probable) that shocks originating in the Texas Panhandle will extend as far west as Los Alamos.

3.6 Building

Type of Construction

The reactor is installed in a building which also houses offices and laboratories. Originally the building, of monolithic concrete construction, was used by a radiochemistry group. The group prepared large radioactive sources of high specific intensity and did research on related problems.

The building was designed expressly for the operations of this chemistry group and included two large, well shielded process cells and an elaborate contaminated waste disposal plant. One of these process cells has been converted to a reactor cell. The cell ceiling and three of the walls are 5-1/2 ft thick and made of reinforced normal concrete. The floor has a 3-1/2 ft tamped earth fill between 1-ft top and bottom layers of reinforced concrete. The remaining wall, in which is located the access door, is made of 2 ft of reinforced concrete.

Ventilation

The general layout of the building ventilation system is shown in Fig. 3.2. The office portion has normal window ventilation while the laboratory section is mechanically air conditioned. Preset air pressure differences are maintained between certain areas in the laboratory part of the building. For instance, corridor pressure is higher

MECHANICAL VENTILATION (CONDITIONED AIR)   NORMAL VENTILATION

HOT LABS   COLD LABS

INTAKE ROOM 'G'   AIR EXHAUST ROOM 'G'

BOILER ROOM   ROOM E   LAB B   TOILET (LABS)   SHOP   LUNCH ROOM   LIBRARY

BLOCK STORAGE   DARK ROOM   MEN   WOMEN

LAB C   JANITOR   CLOSET   EAST CORRIDOR (LABS)   WEST CORRIDOR (OFFICE)

TRUCK INTAKE   LAB A   LOBBY   DRAFTING ROOM

BLDG. ENGR.   ROOM D   TOILET (LAB-D)   RECEIVING   ENTRANCE

TOILET   TOILET (LAB-A)   LOADING PLATFORM

P L A N   F I R S T   F L O O R

REACTOR ROOM

CONTROL ROOM 'G'

PARTIAL PLAN BASEMENT

Fig. 3.2 Building layout (room details).

than that of laboratories which open to the corridor. The reactor control room, with an independent supply and exhaust air system, is maintained at a pressure positive with respect to the cell.

The exhaust system of the cell is shown in Fig. 3.3. It is completely independent of the rest of the building. Inlet air for the cell is first used to cool the sodium equipment room then passes into the cell through two damper controlled ducts. One damper adjusts the air flow which cools the graphite neutron shield, the other admits air directly to the cell. Both dampers may be closed for isolation of a sodium fire.

Exhaust air from the cell and from the laboratory areas is put through capillary washers and dry filters before being released to the atmosphere.* The filtering process removes particulate matter larger than 1/2 micron.

Layout

Figure 3.4 is the building layout at TA-35. The arrangement of the main building is shown in Fig. 3.2. More detailed views of the general reactor region are given by Figs. 2.1 and 2.2.

---

*Leary, J. A., et al., "Design and Performance of a Disposal Plant for Radioactive Wastes," Nucleonics 12 No. 7, 64-67 (1954).

TWO STAGE CAPILLARY
AIR WASHER

SEPARATOR

REACTOR CELL

SODIUM
EQUIPMENT ROOM

← EAST

Fig. 3.3 Cell air exhaust system.

TEST PIT

CAUSTIC TREATER
BLDG.

UNDER CONST.

OFFICE & LAB. BLDG.

TEMP. OFFICE

LAMPRE I

FILTER BLDG.

SODIUM TEST BLDG.

SODIUM BLDG.

N

100 50 0 100

SCALE, IN FEET
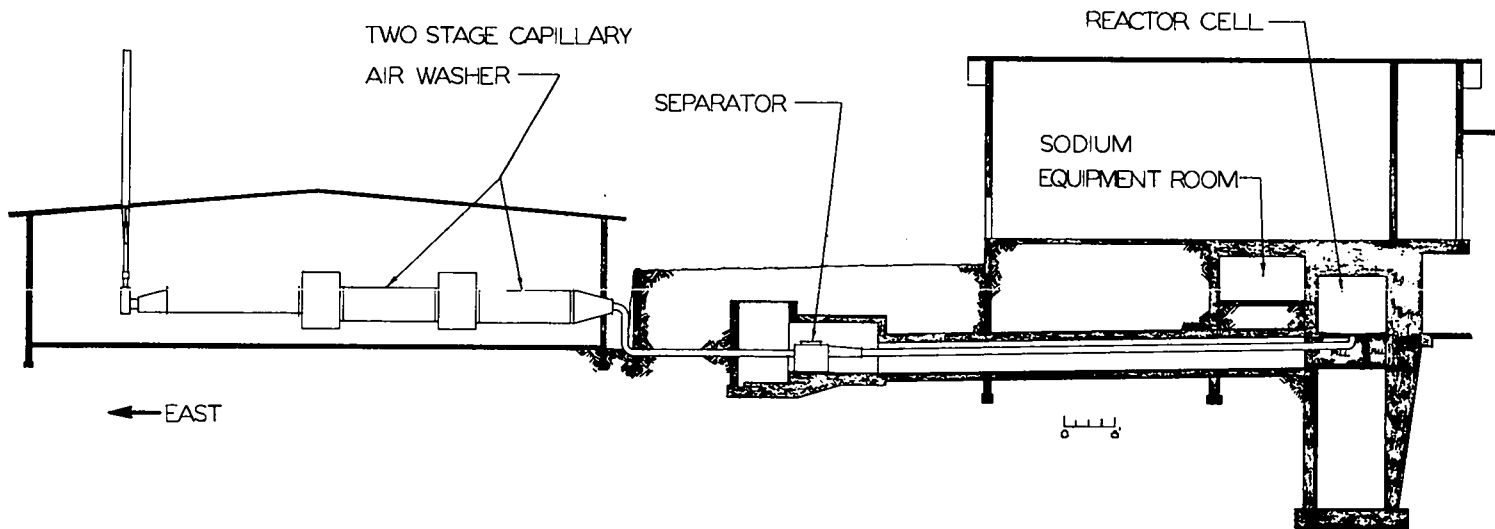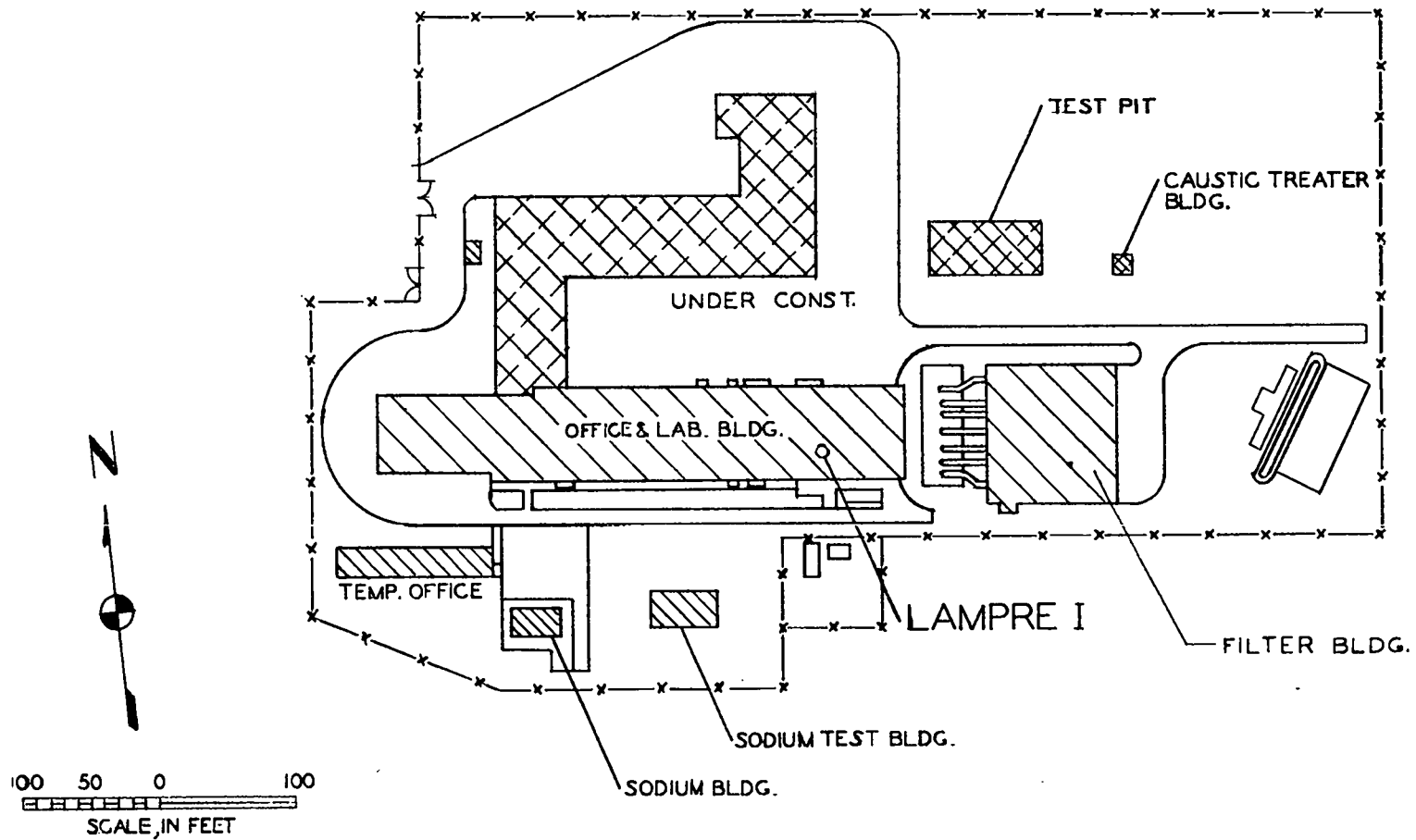
Fig. 3.4 Site layout.

4. HAZARDS

4.1 General

The types of hazard potentially present in LAMPRE I are release of radioactive material, blast damage, and sodium fires. The hazard arising from radioactive fission product release is, of course, present and is aggravated by the presence in the system of toxic plutonium and radioactive sodium. In the reactor the fuel is contained in a molten condition in approximately 145 tantalum capsules. Leakage of one or more of these capsules is considered to be likely but to constitute no hazard. Experiments have demonstrated conclusively that the fuel is compatible with the coolant sodium and is virtually insoluble in it. At the only location in the system where the fuel can be considered likely to collect or drain after release from the capsules, there is a quantity of iron which absorbs fuel to form solid, high-melting alloys and compounds. The geometry is such that the resulting plutonium-iron alloys cannot reach criticality, even if all capsules ruptured.

Capsule leakage or rupture would result also in release of gaseous fission products to the reactor cover gas. If a leaking capsule were withdrawn into the charger housing, plutonium contamination and fission product gas release would occur in this vessel. In either case, the radioactive material is still considered to be fully contained and adequately shielded, so that no hazard exists unless housing rupture also occurs. The gas disposal system is designed to permit the safe removal and purging of fission gases from both reactor and charger vessels.

Leakage or major discharge of sodium from the system is not considered as causing any hazard to the core itself, since there are no penetrations in the reactor vessel below the core region, and the vessel is double walled at this point. Full drainage of the rest of the system will therefore not remove the sodium surrounding the fuel. The entire sodium system is located in a shielded area not tenanted during operation, and whose air supply and exhaust are completely controlled. It is believed that sodium fire in the area would be controlled by the damper system, which would quench the fire as soon as the available oxygen is consumed. There are no water pipes in the area. Since the radioactive sodium would thus be confined in a shielded area, it is felt that there is very little chance of its release to the atmosphere.

The possibility of blast damage caused by vessel rupture from a large nuclear excursion is considered to be vanishingly small. This conclusion, discussed in the next section, is reached from consideration of the inherent properties of the reactor fuel system, and not from the provision of various mechanisms or controls. Vessel rupture from accidental introduction of water into the sodium system is considered to be impossible because of the design of the system and the exclusion of water from the reactor area. Accidental overpressure of the reactor gas system will not cause vessel rupture because of the presence of relief valves and weaker components elsewhere in the system. It is concluded, therefore, that there is no likelihood of explosive vessel rupture, and hence no likelihood of blast damage. Nonexplosive rupture would have the same effect as major sodium leakage, discussed above, unless both inner and outer vessels were ruptured. No mechanism has been proposed which can cause such simultaneous rupture.

The use of sodium as a coolant incurs the risk of a sodium fire. The sudden release of 7.5 ft³ of 500°C sodium to the atmosphere would result in a fire of sizeable proportions. No system for extinguishing such a fire is planned, but the provisions for isolating sodium fires are believed to be adequate to prevent hazard to personnel. The areas in

which the sodium system is located, the reactor cell and sodium equipment room, have an independent ventilating system with valves and dampers which close upon the receipt of a signal from smoke or radiation detectors. Large quantities of sodium leaking from the system would burn until the oxygen in the area was consumed and then combustion would cease. Because of isolation by dampers and valves, no appreciable amount of radioactive sodium smoke would be released into the atmosphere. The risk of termination of the experiment by fire is accepted as an alternative to costly measures which would minimize fire damage.

4.2 Hazards Created by Power Failure or Component Malfunction

Loss of Coolant Pumping

Loss of coolant pumping, whether from power failure or pump malfunction, would automatically shut down the reactor through the low coolant-flow scram and rundown channels. Calculations indicate that core temperature would rise to about 685°C with no coolant flow and a power history of 1 Mw for 9 months. The maximum temperature would occur 7-1/2 hr after shutdown.

Loss of Electrical Power

Loss of electrical power results in a scram through several channels, but primarily it de-energizes the scram valve in the shim hydraulic system. The hazard, if any, is the same as for loss of coolant pumping. There are dual emergency diesel generating units at the site to which most instrumentation, one coolant pump, and the heat exchanger blower automatically transfer in case there is a main power outage.

Malfunction of Heat Exchanger Air System

Malfunction of the heat exchanger air system can result in an abnormally high or low core temperature. If, during 1 Mw operation, the heat exchanger air system malfunctions so that there is no heat removal and all other conditions remain unchanged, the system equilibrium temperature is about 580°C, which is permissible.

A malfunction which causes overcooling might lower system temperature below the fuel freezing point. While freezing the fuel is not in itself hazardous, it could result in capsule rupture because of fuel expansion when it freezes. Conditions under which freezing fuel might rupture a capsule and the number of melt-freeze cycles which result in rupture are under investigation.

Malfunction of Cell Air System

Malfunction of the cell air system causes no immediate hazard. Loss of cooling air flow through the graphite neutron shield would raise shield temperature, but no deterioration of the graphite would occur unless operation at high power were continued for some time. Loss of cooling air through the sodium equipment room would slowly raise the ambient temperature in that room and eventually result in the deterioration of components and electrical wiring.

Malfunction of Shim or Control Rod Actuation

Malfunction of shim or control rod actuation is, by itself, not hazardous. Although the reactivity that can be added by the shim is large, it is planned that criticality will be achieved only by control rod movement after the shim is up and positioned mechanically against a stop. Normal control rod reactivity addition rates will be about 5 ¢/sec. Malfunction of the hydraulic pressure regulator might increase this rate

to 10 ¢/sec. The maximum capacity of the pump which drives the shim cylinder is such that were the pump connected directly to the cylinder, with no throttling restrictions in the oil lines, the maximum reactivity insertion rates which could result would not exceed $2.25/sec. In general, hydraulic and electrical components of the actuation system are fail-safe and their malfunction results in the shim or control rod being either inoperable or dropping.

A sticking shim could, however, be a definite hazard. Sticking could occur if the shim itself or its pusher rods were somehow bound or wedged against surrounding structure. Other sources of sticking might be the piston in the hydraulic cylinder or a plug in an hydraulic line.

In order to minimize the sticking possibility, great care is being taken with shim and push rod alignment, clearances are being made relatively large, and installation of the hydraulic system is being carefully supervised. A rigorous test of the system prior to nuclear operation is planned. An hydraulic accumulator in the shim hydraulic system will be employed to maintain a pressure reserve to force the shim down in the event that the scram valve sticks closed.

Malfunction of Fuel Charger

The only credible malfunction of the fuel charger producing a dangerous situation is that of a fuel element somehow being disengaged from the lifting mechanism and falling into the core. An estimate of the size of the power excursion which this malfunction might cause was made by means of reactor kinetic equations which were simplified by neglecting the effects of delayed neutrons.

This calculational method was tested by applying it to the core of Godiva whose power excursion characteristics have been experimentally studied.

The prompt temperature coefficient is assumed to furnish a shutoff mechanism which counteracts the ramp reactivity insertion by an amount

proportional to the energy released as the power excursion progresses. This calculated procedure was applied to the following hypothetical situation: The reactor is barely subcritical and a central fuel element, about to be inserted, is dropped by the capsule charger and falls into the core, unimpeded by friction.

The above situation supposes an interlock to be inoperative, a completely uninformed operator, and an equipment malfunction.

A central fuel pin is estimated to be worth about $4, or approximately 70 ¢/in. of inserted length. The fuel assembly would fall 10 ft before the fuel pin entered the core, and the maximum velocity as the pin approached the core could not exceed the corresponding free fall velocity of about 27 ft/sec. This could produce a ramp reactivity insertion rate of nearly $230/sec. The nuclear burst, which can be shown to be oscillatory, would reach a peak power level of

$$P_{max} \cong 8 \times 10^8 \text{ watts}$$

The ramp reactivity insertion would persist for about 0.018 sec, and a series of bursts, separated in time by $\sim 10^{-3}$ sec, would occur while reactivity was being added. The energy release per burst is estimated to be

$$E_{burst} \cong 2.7 \times 10^4 \text{ watt-sec}$$

and the total energy release would be

$$E_{tot} \cong 4.5 \times 10^5 \text{ watt-sec}$$

The fuel temperature would rise about 135°C. No mechanical shock to the system should occur as a result of this excursion; it is estimated that reactivity insertion rates greater than $5000/sec would be necessary to produce shocks, as long as the expected prompt shutdown coefficient was effective.

4.3 Hazards Created by In-Reactor Experiments

No in-reactor experiments are contemplated.

4.4 Hazards Created by Acts of God, War, Sabotage, and External Explosions

The installation of the reactor proper in a heavy walled cell in a basement location makes it extremely resistant to the violence of the elements and to external explosions. It will be seen from the discussion on seismicity that the occurrence of an earthquake of intensity sufficient to damage such a cell is extremely remote.

Windstorm, lightning, and earthquakes of foreseeable severity might cause superficial damage to external facilities such as the air heat dump and ventilating system, but not to the reactor in the cell or even with any likelihood to the sodium system in a neighboring basement room. Flooding of the area is a virtual impossibility because of the building's mesa-top location.

Because the site is located within a guarded security area, there is little possibility of danger from sabotage. This fact, together with the location far from the country's borders, makes danger from war's effects small.

5. ADMINISTRATION AND PERSONNEL

5.1 Organization

The division which is building and will operate the reactor is made up of three groups; one having nuclear physics as its main interest, one whose primary effort is in the field of chemistry and materials, and a third which is concerned with engineering. Personnel responsible for design and fabrication came from all three groups and were aided by various Los Alamos Scientific Laboratory groups outside the division. Some tasks performed outside the division are, for example, tantalum capsule development, fuel alloy fabrication and analysis, and nondestructive testing of components.

Of the total of some 40 scientists and engineers in the division, about 15 have been directly concerned previously with the operation of one or more reactors. Two reactors, LAPRE I and II, have been operated at the site.

5.2 Operators

The operators for cold critical and the early phases of power operation will be staff members from the division. When the characteristics and behavior of the reactor are determined, technicians will be trained as operators. A staff member supervisor having detailed knowledge of the reactor and of established procedures will be in charge at all times.

5.3 Staff Training

Prior to the hot critical experiments a school will be conducted
for personnel who will be concerned with reactor operations. Besides
familiarization in some detail with the entire installation, written
procedures will be thoroughly studied.

5.4 Safety Regulations

Safety regulations, operational procedures, and check lists have
not yet been written, but will be formulated prior to the loading of
any fuel into the core. Proposed regulations and procedures will be
reviewed by a committee whose members are experienced in critical
assembly work and in reactor startups.

5.5 Security Regulations

Operations, from a security standpoint, will be conducted in
conformance with existing regulations and within the framework of Atomic
Energy Commission security policy. The reactor site is surrounded by
a security fence and the gates are manned by the Atomic Energy Commission
protective force.

Appendix A

LAMPRE CRITICAL EXPERIMENTS

In support of the LAMPRE program, two critical experiments were
performed at the N Division (Pajarito Site) remotely controlled critical
assembly facility. LCX I (LAMPRE Critical Experiment No. 1)* mocked up
an early LAMPRE I design. Since, in the development of the final LAMPRE I
design, extensive modification was made of the core and other components,
the need arose for additional critical experiments. These experiments
(LCX II) were performed using the machine depicted in Fig. A.1.

The LCX II core consists of approximately 24 sandwiches each of
which contain four 5.94 in. o.d. disks of the following materials:

Material	Thickness (in.)
Pu (clad with 0.005 in. Ni)	0.122
Al (perforated to make number of Al atoms per cm^3 equal to atomic density of Na at 560°C)	0.075
Ta	0.022
S.S.	0.014

As seen in Fig. A.1 the core is reflected on all sides by iron,
which was more readily available in the required shapes than the stainless

---

*Barkmann, H. G., et al., "Preliminary Critical Experiments on a Mock-Up
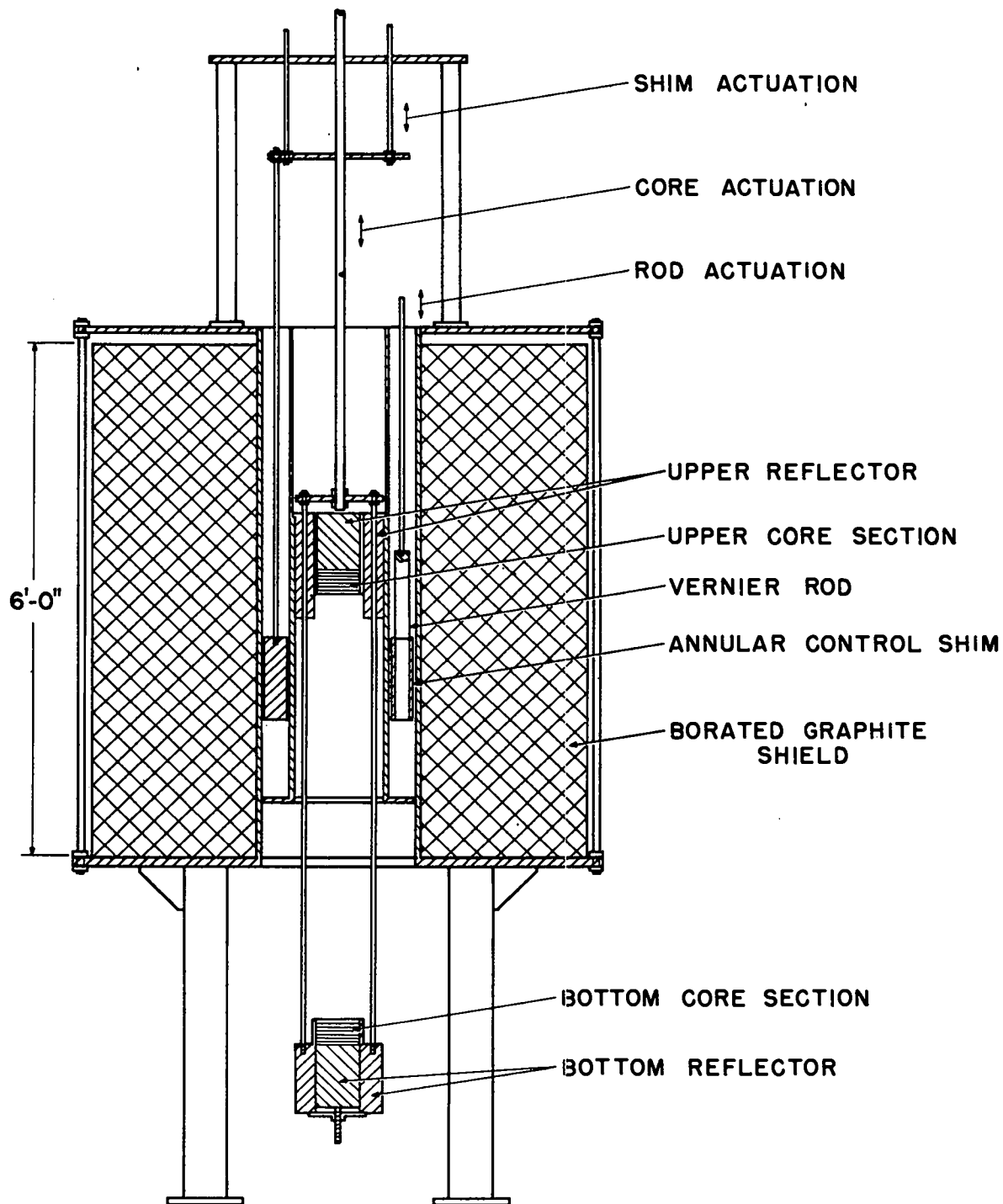of the Los Alamos Molten Plutonium Reactor," LA-2142, June 1957.

Fig. A.1 Schematic of LCX II.

steel selected for use in LAMPRE I. The side iron reflector consists of a 3 in. thick fixed reflector situated adjacent to the core, and a 3 in. thick, 12 in. long, movable reflector surrounding the fixed reflector. This movable reflector serves as the reactivity control shim. Critical masses measured over the 12 in. length of shim travel are shown in Fig. A.2. It is seen the shim worth is 1050 g, or about $12.4 on the basis of the measured mass-dollar relationship:

$$\frac{\Delta m}{m} \; / \; \$1.00 = 0.41\%/\$1.00 \cong 1.18\cancel{c}/g \text{ fuel alloy}$$

As a consequence of this measurement of shim worth, both the thickness and length of the LAMPRE I shim were increased (over the LCX II dimensions) in order to obtain the desired amount of shut down Δk. Similarly, the worth of the LCX II vernier (control) rod, an independently actuated small section of the shim, had a measured worth of 30¢. The control rods in LAMPRE I are larger than those in LCX II, and are made of nickel to further increase their effectiveness.

The shield in LCX II consists of the same type graphite cylinders as will be used in LAMPRE I; however, only 18 in. of the nominal LAMPRE I 3-1/2 ft shield thickness is used in LCX II, since it appeared this amount would serve to evaluate the shield contribution to reactivity. This contribution was measured to be $8.

Other experiments performed on LCX II include:

a. An examination of the effect of plenums situated at the ends of the core.

b. A measurement of the critical mass of the core containing only the nickel clad plutonium disks, and no diluent disks.

c. A comparison of the effectiveness of stainless steel, nickel, and copper as control rod materials. (A relative effectiveness of 1 : 1.62 : 1.68 was observed for equal volumes of stainless steel, nickel, and copper.)

d. An investigation of the effect of increasing the core plutonium density. (A 1% increase in volume-averaged plutonium density decreased the critical mass by ~ 1%.)
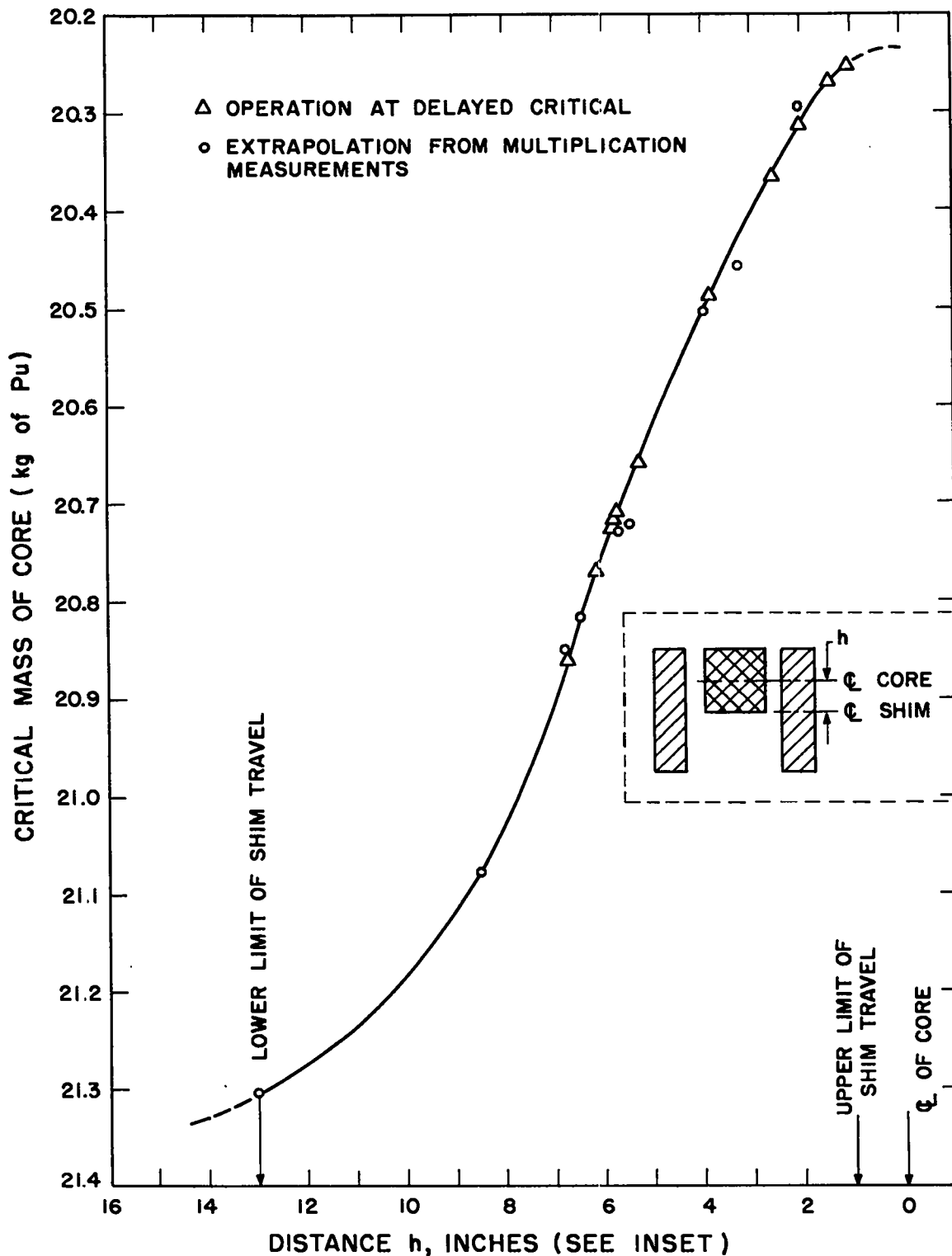
Fig. A.2 Critical mass vs shim insertion, LCX II.

e. The examination of several oscillator rod designs.

f. The testing of the transfer function analyzer equipment which will be used on LAMPRE I.

Appendix B

FUEL ELEMENT BOWING

B.1 Introduction

Data from LCX II lead one to expect a power density in the LAMPRE
core which is well approximated by the expression

$$P(r,z) = P_0 \cos\left(\frac{r}{3.06}\right) \cos\left(\frac{z-0.5\ h}{3.34}\right) \qquad (B.1)$$

where r,z and h are in inches. Here P_0 is the power density at the center
of the core, h is the core height, and the origin of the cylindrical coor-
dinate system is taken at the center of the bottom of the core. If we let
$\theta(r,z)$ represent the temperature rise in the coolant above that entering
the bottom of the core

$$\theta(r,z) = \theta(0,z) \cos\left(\frac{r}{3.06}\right) \qquad (B.2)$$

This leads to a radial temperature gradient

$$\theta'(r,z) = \frac{-\theta(0,z)}{3.06} \sin\left(\frac{r}{3.06}\right) \qquad (B.3)$$

Taking $\theta(0,h) = 147^\circ C$ ($\theta_m = 113^\circ C$ = mean rise through core) as represent-
ative of nominal LAMPRE I operating conditions, one obtains the values
given in Table B.1.

Table B.1

NOMINAL CORE EXIT CONDITIONS $(\theta_m = 113^\circ C)$

r (in.)	0	1	2	3
$\theta(r,h)$ °C	147	139	117	82
$\theta'(r,h)$ °C/in.	0	- 15.4	- 29.2	- 39.8

The radial temperature gradients of Table B.1 will be superimposed upon the local temperature variations in the molten fuel, tantalum capsules, and coolant stream. Specifically, any particular tantalum capsule will be hottest nearest the core centerline, and will therefore bow inward with a curvature C and radius of curvature R_c given by

$$C = \frac{1}{R_c} = \alpha \theta' \qquad (B.4)$$

where α is the thermal expansion coefficient of the metal.*

From Table B.1 it will be noted that θ' is roughly proportional to radius. Hence capsule curvature and deflections toward the core center line are also about proportional to radius, leading to approximately uniform density variation over the cross section (at a given value of z) as bowing occurs.

The tantalum capsules are taken to be simply supported at their lower ends, where their conical tips fit into mating holes in the bottom locator plate. Their tops are rigidly attached to long 17-4 PH stainless steel handles which are themselves subjected to radial temperature gradients over part of their lengths. Fig. 2.12 shows an entire fuel element. The round part of the handle is in contact with a flowing sodium coolant, in which the radial gradient at the core exit may be assumed to exist. The hexagonal part of a handle is bathed by stagnant sodium, so it may

---

*Roark, R. J., Formulas for Stress and Strain (Mc-Graw Hill Book Company, Inc., New York, 1954), third edition.

be assumed to be essentially free of radial temperature gradient and bowing. When assembled at room temperature, the handles are expected to fit snugly against each other at the spline section, just above the core. However, the spline metal (17-4 PH stainless steel) has a lower temperature coefficient of expansion than does the 18-8 stainless steel container which surrounds the fuel element array, so that at operating temperature some 0.020 in. differential expansion occurs across the entire core. If we assume the cumulative clearance across the core diameter (at the splines) at room temperature to be 0.005 in., the expected clearance at operating temperature will be 0.025 in. across the core or about 0.0016 in. per gap.

The nominal clearance per gap at the lower ends of the hexagonal parts of the handles is 0.017 in., some ten times that at the spline section. Since the long handles will not be perfectly straight, actual gaps existing at either spline or hexagonal sections will be subject to large variations from nominal values. The lower ends of the hex section have about ten times the nominal separation of the splines, and they are only about three times as far from the pivot points (tantalum capsule tips). Hence the splines are more likely to provide the constraint of warped fuel element assemblies than are the lower hexagonal sections.

Maximum bowing reactivity rate (¢/Mw) is produced if each and every fuel element is free of constraint except at its lower end (conical tantalum capsule tip) and upper end (top locking section). In the calculations reported below, the splines are assumed to be initially thus free of constraint and in their nominal positions. This assumption leads to maximum rate, but largest total bowing reactivity would result if one assumed all splines to be initially pressing outward against the core container. In the latter case the total reactivity due to bowing would be perhaps twice as large as calculated below, but the rate (¢/Mw) would be lower.

Starting with the splines free of constraints, radial temperature gradients far less than those of nominal operating conditions of Table B.1 are sufficient to displace the spline sections to the extent that all

splines will be in contact. For temperature gradients above those required for spline constraints to act, bowing effects are much smaller. Under these conditions, actual bowing becomes a complicated function of section moduli and elastic constants in the entire fuel element assembly. If one considers the inward bowing that would occur in a simple fuel capsule simply supported at both its lower tip and at the spline section, the inward bowing will be overestimated, since the bowing of the handle will certainly tend to transmit through the spline section an effect at least partially opposing the inward bowing so calculated.

B.2 Results

Estimates of bowing have been made using LAMPRE I constants under the two assumptions outlined in the preceding paragraph. In addition, the following assumptions have been made: (1) Vertical variation in power density has been neglected so that coolant temperature is assumed to rise linearly with height from bottom (inlet) to top (outlet) of the core. This means that in Eq. B.2

$$\theta(0,z) = \frac{z}{h} \theta(0,h), \quad 0 \leq z \leq h \tag{B.5}$$

(2) Radial temperature gradient is assumed to follow Eq. B.3 within the core. The fuel element handles up to the top of the round section are assumed to be subjected to the same radial gradient as that existing at core outlet plane. (3) The long hexagonal sections of the fuel handles are considered to be subject to no radial gradient and to remain straight extensions of the round handle sections. (4) Results are expressed in terms of average coolant temperature θ_a, the coolant temperature rise (above entrance temperature) averaged over the entire core--that is, half the temperature rise θ_m of the mixed outlet coolant stream. For example the average coolant temperature θ_a for the nominal operating conditions of Table B.1 would be $\theta_a = \theta_m/2 = 113^\circ C/2 = 56.5^\circ C$. (5) Dimensions (measured from lower end of tantalum capsule) and materials data

used in the calculations are as given in Table B.2. (6) Reactivity
worths are based on (a) LCX II value of 1.18 ¢/g combined with (b) S-4
calculations giving $(\Delta M_c/\Delta\rho) = -1.91 \times 10^3$ g per g/cm³ fuel alloy density
(i.e. -610 g or +720¢ for -1% $\Delta R/R$ at constant core height).

Table B.2

DIMENSIONS AND MATERIALS OF FUEL ELEMENTS

Range (in.)	Part	Material	Expansion Coefficient α
0 - 6	core	Ta	6.5×10^{-6}/°C
6 - 9.75	core to spline	S.S. + Ta	9.1×10^{-6}/°C
9.75 - 32	round handle	17-4 PH(S.S.)	11.7×10^{-6}/°C
32 - 123	hex handle	17-4 PH(S.S.)	11.7×10^{-6}/°C

A summary of the results is given in Table B.3. The positive
power coefficients listed have been broken down into (1) a slightly
delayed component due to tantalum capsules bowing in the core and (2) a
delayed component due to bowing of the handles. The first component,
effective at all values of θ_a, has the value +43 ¢/Mw. The second com-
ponent is present only up to $\theta_a = 6$°C, and has the value +643 ¢/Mw.

Table B.3

SUMMARY OF BOWING-EFFECTS ESTIMATES

θ_a(°C)	P(Mw)	Displacements at R = 3 in. ΔR (mils) in interval $\Delta\theta_a$(°C) Spline ΔR	Effective Core ΔR	and $\Delta R/\Delta\theta$	Reactivity Effects Δk (¢) at θ_a	$\Delta k/\Delta\theta_a$ (¢/°C)	Full Flow Power Effects ($\Delta k/\Delta P$ in ¢/Mw) Slightly Delayed	Delayed
0	0				0			
		-10	-3.06	-0.51		+12.2	+43	+643
6	0.10				+73.5			
		0	-1.60	-0.032		+0.77	+43	0
56	1.00				+112.0			

It is estimated that there will be a prompt power coefficient associated with fuel expansion amounting to about -556 ¢/Mw (based on estimates that $\Delta k/\Delta \Theta_f$ = -3.21¢ per $^\circ$C of average fuel temperature rise and that the average fuel temperature rise, Θ_f, is equal to 3.1 Θ_a for nominal operating conditions). The capsule bowing coefficient is necessarily slightly delayed as compared to the prompt fuel coefficient, as the capsule bowing is driven by fuel temperature rise effects; the magnitude of this delay is about 0.1 sec. The handle bowing power coefficient is still further delayed by a time estimated to be of the order of two or three seconds--because of sodium transit time effects coupled with thermal capacity of the handles.

There are other sources of negative power coefficient having delay times as short or shorter than the delayed handle bowing coefficient. Among these are density changes of the coolant in and above the core and of the fuel element handles (acting as reflecting material). Calculations lead to estimated values of -88 ¢/Mw for these delayed effects before the splines make contact (Θ_a = 6°C), and -134 ¢/Mw after splines make contact.

B.3 Discussion

A summary of the reactor power coefficients discussed above is presented in Table B.4. It will be seen that the net prompt coefficient has a large negative value at all power levels, whereas if one includes delayed effects (several seconds time constant) the overall power coefficient may be slightly positive at low power. It must be remembered, however, that we have assumed the worst possible situation--namely, that all fuel elements are completely free of constraints over their entire length of about 10 ft.

Table B.4

SUMMARY OF REACTIVITY EFFECTS

Range of θ_a ($^\circ$C)	0 - 6	6 - 56
Power at full flow (Mw)	0 - 0.10	0.10 - 1.0
Power reactivity coefficients ($\cancel{c}$/Mw)		
Fuel expansion (prompt)	-556	-556
Other negative effects (delayed)	- 88	-134
Total negative	-644	-690
Capsule bowing (slightly delayed)	+ 43	+ 43
Handle bowing (delayed)	+643	0
Total positive	+686	+ 43
Net total power coefficient	+ 42	-647
Net prompt power coefficient	-556	-556

It is likely that there will be sufficient deviation from straightness of the fuel assemblies to cause a fair number of them to be in contact at the spline section, where nominal clearances are only about 1.6 mils. If only 7% of them are so constrained, the resulting overall power coefficient would become negative at low power as well as at high power. Also, about half of the 643 $\cancel{c}$/Mw contributed to the power coefficient by the handles is due to the long straight hexagonal sections acting as extensions of the round sections where the bowing occurs. This contribution will vanish to the extent that these hexagonal handles are constrained by warpage.

In any case, in the power range where the net coefficient is positive the total magnitude of reactivity caused by bowing (about 73$\cancel{c}$ gross, of which all but 4 or 5$\cancel{c}$ is nullified by negative reactivity effects) and its time constant (several seconds) should present no appreciable control problem. Further, for all powers above about 10% of nominal operating power the net power coefficient has a large negative value; no control problem is anticipated.

It should be pointed out, in conclusion, that the above analysis applies only to full sodium flow conditions. Consider, for example, the conditions at θ_a = 6°C at reduced flow. Since the temperature rise within the fuel $(\theta_f - \theta_a)$ is proportional to power level (now reduced in proportion to the flow) the fuel is now cooler than for θ_a = 6°C at full flow. Whereas for full flow it was estimated that θ_f = 3.1 θ_a, we get instead θ_f = θ_a in the limit of very slow flow. The prompt negative power coefficient due to fuel expansion is therefore reduced a factor 3.1 relative to all other power coefficients; the latter are, of course, inversely proportional to the flow. The bowing reactivity at θ = 6°C remains at +73¢, while the compensating negative reactivity is reduced from -69¢ (full flow value) to -29¢ (slow-flow value). It should be recalled, too, that the 2 or 3 second time constant associated with handle bowing increases in inverse proportion to the flow.